UNIVERSITY OF CALIFORNIA, SAN DIEGO

MCL-1 is Essential for Myocardial Homeostasis and Autophagy

A dissertation submitted in partial satisfaction of the
requirements for the degree Doctor of Philosophy

in

Biomedical Sciences with Specialization in Anthropogeny

by

Robert Lee Thomas III

Committee in charge:

Professor Åsa Gustafsson, Chair
Professor Joan Heller Brown
Professor Laurence Brunton, Emeritus
Professor Anne Murphy
Professor David Roth

2014

The dissertation of Robert Lee Thomas III is approved, and it is acceptable in quality and form for publication on microfilm and electronically:

_____

_____

_____

_____

_____

Chair

University of California, San Diego

2014

DEDICATION

This work is dedicated to mentors past and present whose advice and support made this project possible. In particular, this page is for my mother, who somehow convinced her three year old son that learning to read was worth the effort.

EPIGRAPH

Though a little one, the master-word looms large in meaning. It is the open sesame to every portal, the great equalizer in the world, the true philosopher's stone which transmutes all the base metal of humanity into gold. The stupid man among you it will make bright, the bright man brilliant, and the brilliant student steady … And the master-word is *Work*, a little one, as I have said, but fraught with momentous consequences if you can but write it on the tables of your heart and bind it upon your forehead.

-William Osler

TABLE OF CONTENTS

LIST OF ABBREVIATIONS AND SYMBOLS

aa	amino acid
ATP	Adenosine Triphosphate
BCL-2	B-cell CLL/lymphoma 2
BH	Bcl-2 homology
BNIP3	BCL2/adenovirus E1B 19kDa interacting protein 3
BSA	Bovine serum albumin
C-term	C-terminus
COIP	Co-immunoprecipitation
CsA	Cyclosporine A
CypD	Cyclophilin D
EF	Ejection Fraction
ETC	Electron Transport Chain
FS	Fractional Shortening
HA	Hemagglutinin
I/R	Ischemia/Reperfusion
KO	Knockout
LVDd	Left Ventricular Diastolic Dimension
MCL-1	Myeloid Cell Leukemia-1
MEF	Mouse embryonic fibroblast
MOMP	Mitochondrial outer membrane permeabilization
mPTP	Mitochondrial permeability transition pore

N-term	N-terminus
OMM	Outer mitochondrial membrane
OXPHOS	Oxidative phosphorylation
PARP	Poly-ADP-ribose-polymerase
RCR	Respiratory Control Ratio
SKM	Skeletal muscle
TAC	Trans-aortic constriction
TUNEL	Terminal deoxynucleotidyl transferase UTP nick end labeling
VDAC	Voltage Dependent Anion Channel
WT	Wild-type
Ψm	Mitochondrial membrane potential

LIST OF FIGURES AND TABLES

ACKNOWLEDGEMENTS

I would like to thank my advisor Åsa Gustafsson who taught me how to pursue science thoughtfully, professionally, and independently. I also thank members of the Gustafsson lab, past and present, whose support and friendship shaped so much of my graduate experience. Thanks specifically to Larry Brunton, whose friendship and guidance helped me with several important decisions. I also appreciate the efforts of four students who worked with me: Jarvis Owens, Andrew La' Pelusa, Sarah Shires, and Jennifer Kuo. Finally, I would like to acknowledge the UCSD MSTP program, Dr. Paul Insel and Dr. Francisco Villarreal, who gave me my start at UCSD.

Chapter 1, in part, is a reprint of the material as it appears in Thomas *et al.*, Circ J, 2013 and Thomas *et al.*, Autophagy 2013. Chapter 2-5, in part, are reprints of the material as it appears in Thomas et al., Genes Dev, 2013. Chapter 6, in part, is a reprint of the material as it appears in Thomas *et al.*, Circ J, 2013, Thomas *et al.*, Autophagy 2013, and Thomas et al., Genes Dev, 2013. The dissertation author was the primary investigator and author of these papers.

The *Ppif*$^{-/-}$ mice were provided by Dr. Jeffrey D. Molkentin (Cincinnati Children's Hospital Medical Center). This work was supported by NIH grants R01HL087023 and R01HL101217 (A.B.G.), NIH institutional training grant 2T32HL007444-26A1 (K.U.K.), and predoctoral fellowship 12PRE11810030 from the American Heart Association's Western States Affiliate (R.L.T.).

VITA

Education

2006 Bachelor of Science, Chemistry
Santa Clara University

2010-2012 Teaching Assistant, Department of Pharmacology,
University of California, San Diego

2014 Doctor of Philosophy, Biomedical Sciences Program
University of California, San Diego

Publications

Thomas RL, Gustafsson AB. MCL1 is critical for mitochondrial function and autophagy in the heart. Autophagy. 2013 Nov 1;9(11):1902-3.

Thomas RL, Gustafsson AB. Mitochondrial autophagy--an essential quality control mechanism for myocardial homeostasis. Circ J. 2013;77(10):2449-54.

Thomas RL, Roberts DJ, Kubli DA, Lee Y, Quinsay MN, Owens JB, Fischer KM, Sussman MA, Miyamoto S, Gustafsson ÅB. Loss of MCL-1 leads to impaired autophagy and rapid development of heart failure. Genes Dev. 2013 Jun 15;27(12):1365-77.

Yamazaki KG, Ihm SH, Thomas RL, Roth D, Villarreal F. Cell adhesion molecule mediation of myocardial inflammatory responses associated with ventricular pacing. Am J Physiol Heart Circ Physiol. 2012 Apr 1;302(7):H1387-93.

Thomas RL, Kubli DA, Gustafsson AB. Bnip3-mediated defects in oxidative phosphorylation promote mitophagy. Autophagy. 2011 Jul;7(7):775-7.

Rikka S, Quinsay MN, Thomas RL, Kubli DA, Zhang X, Murphy AN, Gustafsson ÅB. Bnip3 impairs mitochondrial bioenergetics and stimulates mitochondrial turnover. Cell Death Differ. 2011 Apr;18(4):721-31.

Quinsay MN, Thomas RL, Lee Y, Gustafsson AB. Bnip3-mediated mitochondrial autophagy is independent of the mitochondrial permeability transition pore. Autophagy. 2010 6(7):855-62.

Brian H. Johnson, Enaanake Allagoa, Robert L. Thomas, Gregory Stettler, Marianne Wallis, Justin H. Peel, Thorsteinn Adalsteinsson, Brian J. McNelis and Richard P. Barber, Jr. Influence of functionalized Fullerene structure on polymer photovoltaic degradation, Solar Energy Materials & Solar Cells 2010 94: 537-541.

Romero-Perez D, Agrawal A, Jacobsen J, Yan Y, Thomas R, Cohen S, Villarreal F. Effects of novel semiselective matrix metalloproteinase inhibitors on ex vivo cardiac structure-function. J Cardiovasc Pharmacol. 2009 53(6): 452-61.

Abstracts

Robert L Thomas, Youngil Lee, David Roberts, Rita Hanna, Xiaoxue Zhang, Shigeki Miyamoto, Mark A Sussman, and Åsa B Gustafsson. Cardiac Specific Deletion of Mcl-1 Leads to Impaired Autophagy and Rapid Development of Heart Failure. Circulation. 2012; 126: A19297

Robert L. Thomas, Youngil Lee, Chengqun Huang, Xiaoxue Zhang, Kimberlee Fischer, Aleksander Andreyev, Anne N. Murphy, Mark A. Sussman, and Åsa B. Gustafsson. Abstract 498: Loss of Mcl-1 in the Heart Leads to Rapid Mitochondrial Dysfunction and Development of Heart Failure. Abstract presented at 2011 BCVS Conference, New Orleans

Youngil Lee, Chengqun Huang, Robert L. Thomas, Melissa N. Quinsay, Shivaji Rikka, Jennifer M. Ramil, Kimberly Fisher, Mark A. Sussman, and Åsa B. Gustafsson. Mcl-1 is Essential for Mitochondrial Function and Cardiac Specific Deletion leads to Rapid Development of Heart failure. Abstract presented at 2010 BCVS Conference, Palm Springs

Awards

American Heart Association Predoctoral Fellowship (2012-2014)
UCSD BMS Retreat: Best Research Talk Award (2011)
The McGraw-Hill Companies Medical Publishing Lange Student Award (2008)
Sigma Xi Honors Society (2006)
Phi Lambda Upsilon Honors Society (2006)
The American Institute of Chemists Foundation Award (2006)
The Orella Prize (2006)
Carl H. Hayn Physics Prize (2005)
American Chemical Society Award in Analytical Chemistry (2005)
American Chemical Society Polyed Award (2004)
CRC Freshman Chemistry Achievement Award (2003)

ABSTRACT OF THE DISSERTATION

MCL-1 is Essential for Myocardial Homeostasis and Autophagy

by

Robert Lee Thomas III

Doctor of Philosophy in Biomedical Sciences

University of California, San Diego 2014

Professor Åsa Gustafsson, Chair

Myeloid cell leukemia-1 (MCL-1) is an anti-apoptotic BCL-2 protein that is upregulated in several human cancers. MCL-1 is also highly expressed in myocardium, but its function in myocytes has not been investigated. To study this function, I generated inducible, cardiomyocyte-specific *Mcl-1* knockout mice and found that loss of MCL-1 in the adult heart led to rapid cardiomyopathy, cardiac hypertrophy, fibrosis with loss of myocytes, and early mortality.

Although MCL-1 is known to inhibit apoptosis, this process was not activated in MCL-1-deficient hearts. Instead, ultrastructural analysis revealed disorganized sarcomeres and swollen mitochondria in myocytes. I found that

loss of MCL-1 led to mitochondrial rupture, LDH release, and cardiac inflammation that indicate myocardial necrosis. Mitochondria isolated from MCL-1-deficient hearts also exhibited reduced respiration, impaired oxidative phosphorylation enzyme activity, and reduced Ca^{2+}-mediated swelling. Taken together, these data are consistent with mitochondrial damage and opening of the mitochondrial permeability transition pore (mPTP). Double knockout mice lacking MCL-1 and cyclophilin D, an essential regulator of the mPTP, exhibited delayed progression to heart failure and extended survival.

Autophagy is normally enhanced in response to myocardial stress, but induction of autophagy was impaired in MCL-1-deficient hearts. Accordingly, I found that ablation of MCL-1 led to accumulation of autophagic substrates in cardiac tissue. In addition, the loss of MCL-1 compromised mitochondrial turnover in myocardium by disrupting PINK1/Parkin-mediated mitophagy. Finally, my studies show that MCL-1 and Parkin do not directly interact in the heart.

These data demonstrate that MCL-1 is essential for myocardial homeostasis and induction of autophagy in cardiac myocytes. My dissertation also raises concerns about potential cardiotoxicity for chemotherapeutics that target MCL-1.

Chapter 1: Introduction

A. MCL-1 and the BCL-2 protein family

Myeloid Cell Leukemia-1 (MCL-1) is an anti-apoptotic member of the BCL-2 protein family, which regulates mitochondrial integrity and the intrinsic pathway of apoptosis (Figure 1). BCL-2, the prototype member of this group, was initially identified as a proto-oncogene in B-cell lymphoma, and its overexpression prolongs cell survival by antagonizing apoptosis (Tsujimoto, *et al.*, 1985; Chen-Levy *et al.*, 1989; Vaux *et al.*, 1988; McDonnell *et al.*, 1989). Subsequent studies identified additional anti-apoptotic proteins such as BCL-X_L and MCL-1 (Boise *et al.*, 1993; Kozopas *et al.*, 1993) and pore forming pro-apoptotic proteins such as BAX and BAK (Oltvai *et al.*, 1993; Kiefer *et al.*, 1995). Under basal conditions, anti-apoptotic proteins promote cell survival by binding to and inhibiting BAX and BAK. BH3-only proteins such as BIM, NOXA, and BNIP3 can bind to the anti-apoptotic proteins' BH domains, displacing BAX and BAK and freeing them for activation. Upon activation, BAX and BAK oligomerize on the outer mitochondrial membrane. The resulting mitochondrial outer membrane permeabilization (MOMP) releases pro-apoptotic factors such as cytochrome *c* and AIF. These factors activate caspases, leading to nuclear fragmentation, apoptotic body formation, and cell clearance by phagocytes (Figure 2) (Gustafsson & Gottlieb, 2007; Czerski and Nuñez, 2004; Volkmann, *et al.*, 2013). During overwhelming cell stress, BAX

and BAK may also promote the opening of a high-conductance channel in the mitochondrial membrane known as the mitochondrial permeability transition pore (mPTP) (Whelan *et al.*, 2012). Pore opening is regulated by matrix protein cyclophilin D (CypD) and allows rapid equilibration of ions and water between the cytosol and mitochondrial matrix. The resulting osmotic stress and dissipation of mitochondrial membrane potential lead to necrosis, a poorly regulated process characterized by mitochondrial rupture, plasma membrane disruption, and inflammation (Figure 2).

MCL-1, BCL-2, and BCL-X_L are often co-expressed in the same tissue, but knockout studies have revealed that they have distinct physiological roles. For instance, BCL-2 knockout mice are viable but display growth retardation, renal failure, and apoptosis of lymphocytes (Veis *et al.*, 1993). BCL-X_L is required for brain development, and BCL-X_L-deficient mice do not survive past embryonic day 13.5 (Motoyama *et al.*, 1995). MCL-1 is also essential for embryonic development, and global deletion results in lethality before embryonic day 4 (Rinkenberger *et al.*, 2000). Despite functional overlap with BCL-2 and BCL-X_L, MCL-1 is distinguished by its short half-life and lack of a BH4 domain (Krajewski *et al.*, 1995; Zhou *et al.*, 1997). PEST sequences in the non-homologous N-terminal region facilitate rapid proteosomal degradation of MCL-1 in response to cellular stress. N-terminal caspase-cleavage sites also facilitate rapid MCL-1 degradation, allowing apoptosis to proceed (Figure 1) (Thomas *et al.*, 2010).

In the heart, several studies have established BCL-2 and BCL-X_L as important pro-survival molecules, and elevated levels of these proteins protect against myocardial ischemia/reperfusion injury (Chen *et al.*, 2001; Imahashi *et al.*, 2004; Huang *et al.*, 2003). BCL-2 also protects against p53-mediated apoptosis in cardiac myocytes (Kirshenbaum & de Moissac, 1997) and increases the calcium threshold for permeability transition pore opening in heart mitochondria (Zhu *et al.*, 2001). Although MCL-1 is highly expressed in the heart (Wu *et al.*, 1997), its role in this tissue has not previously been characterized.

B. BCL-2 proteins and autophagy

In addition to their role in cell survival, BCL-2 family proteins regulate autophagy. Autophagy is an evolutionarily conserved cellular recycling process that sequesters cytotoxic protein aggregates, senescent organelles, and other cellular debris in autophagic vesicles and delivers them to lysosomes for destruction (Gustafsson & Gottlieb, 2008). During the process, cellular contents are tagged with p62, the nascent phagophore envelopes these substrates, and cytosolic LC3I is converted to autophagosome-bound LC3II via conjugation with phosphatidylethanolamine. The mature, double-membrane autophagosome then fuses with a lysosome to form the final autophagolysosome (Figure 3) (Levine & Kroemer, 2008). As the process continues, autophagy degrades p62 and releases amino and fatty acids for

biosynthesis and energy production. p62 and LC3 are well characterized autophagy markers, but the balance between their synthesis and degradation requires specialized flux experiments to accurately characterize cellular autophagic activity (Iwai-Kanai *et al.*, 2008; Terada *et al.*, 2010).

Autophagy is a tightly regulated process, and the mammalian target of rapamycin (mTOR) integrates intracellular and extracellular signals to match autophagic activity with metabolic needs (Figure 4). Hormonal signals and amino acids that signal nutrient abundance increase mTOR-mediated repression, while stressors like starvation and hypoxia reduce mTOR-inhibitory effects (Boya *et al.*, 2013). In addition, BCL-2 family proteins interact with core autophagic machinery such as BECLIN-1 to repress autophagy, and disruption of this interaction is essential for autophagic initiation (Pattingre *et al.*, 2005; Maiuri *et al.*, 2007). MCL-1 also interacts with BECLIN-1 (Germain *et al.*, 2011; Elgendy *et al.*, 2011), but this interaction has not been characterized in the heart.

C. Autophagy and mitophagy in the heart

Basal autophagy is essential for myocardial homeostasis, and mouse models with disrupted autophagy develop heart failure in the absence of other stress. For instance, cardiac specific deletion of ATG5, a critical autophagy protein, leads to rapid cardiac failure and mitochondrial disorganization in adult mice (Nakai *et al.*, 2007). Similarly, my recent work demonstrates that loss of

MCL-1 in the heart leads to impaired autophagy and rapidly culminates in accumulation of dysfunctional mitochondria and heart failure (Thomas *et al.*, 2013). In clinical patients, Danon disease results from a LAMP-2 deficiency that impairs fusion between autophagosomes and lysosomes and causes a lethal cardiomyopathy (Nishino *et al.*, 2000). In addition, autophagy is responsible for clearing mitochondrial DNA (mtDNA) that has been released from ruptured mitochondria. mtDNA that escapes from autophagy can activate the Toll-like receptor 9-mediated inflammatory response. Interestingly, disruption of this process can lead to myocarditis and dilated cardiomyopathy (Oka *et al.*, 2012). In contrast, pharmacologic activation of autophagy can be cardioprotective (Sciarretta *et al.,* 2012). In kidney allograft patients, for instance, treatment with rapamycin/sirolimus inhibits mTOR and reduces cardiac hypertrophy (Raichlin *et al.*, 2008).

Although early work described autophagy as a non-selective, bulk-degradation response during nutrient deficient conditions, recent studies have demonstrated that autophagy can selectively target specific organelles including mitochondria (Quinsay *et al.*, 2010), endoplasmic reticulum (Hanna *et al.*, 2012), peroxisomes (Hutchins *et al.*, 1999), and ribosomes (Kraft *et al.*, 2008). In order to maintain densely packed mitochondrial networks and meet metabolic demands, cardiomyocytes utilize selective mitochondrial autophagy, or mitophagy (Carreira *et al.*, 2010; Shin *et al.*, 2011). Damaged or senescent mitochondria are labeled and isolated based on reduced membrane potential,

enclosed in autophagosomes, and delivered to lysosomes for degradation (Twig *et al.*, 2008). Efficient clearance of dysfunctional mitochondria prevents activation of cell death pathways, protects against reactive oxygen species (ROS) production, and preserves efficient production of ATP by the electron transport chain (ETC) (Kubli and Gustafsson, 2012).

Mitophagy is regulated at several levels including mitochondrial morphology and protein ubiquitination. Mitochondrial fission (DRP-1, FIS1) and fusion proteins (MFN1, MFN2, OPA1) shape mitochondrial networks, and selective fission and fusion events determine which mitochondria can be targeted for autophagy (Figure 5) (Dorn, 2013; Zungu *et al.*, 2011). For example, network elongation during starvation precludes mitochondrial destruction by mitophagy (Gomes *et al.*, 2011). Myocardial autophagy is also regulated by Parkin, an E3 ubiquitin ligase that is mutated in autosomal recessive Parkinson's disease (Kitada *et al.*, 1998). Parkin is localized to the cytosol, but translocates to mitochondria with reduced membrane potential where it ubiquitinates protein targets (Narendra *et al.*, 2010). The adaptor protein p62 then binds ubiquitinated mitochondrial proteins and LC3 on autophagosomes, recruiting autophagic membranes for mitochondrial clearance (Figure 6). (Pankiv *et al.*, 2007; Geisler *et al.*, 2010). At present, little is known about the specific protein targets Parkin ubiquitinates on mitochondria. Recent studies have implicated voltage dependent anion channels (VDACs), outer mitochondrial membrane proteins involved in ion

exchange, and MFN2 (Sun *et al.*, 2012; Chen & Dorn, 2013). PINK1 is a serine/threonine kinase that recruits Parkin to depolarized mitochondria. In mitochondria with an intact membrane potential, PINK1 is imported and degraded by mitochondrial proteases (Jin and Youle, 2013). In mitochondria with reduced membrane potential, PINK1 breakdown is inhibited, causing it to accumulate on the outer mitochondrial membrane and recruit Parkin through direct interaction, Parkin phosphorylation, or phosphorylation of mitochondrial targets (Figure 6) (Narendra *et al.*, 2010; Matsuda *et al.*, 2010; Xiong *et al.*, 2009; Kim *et al.*, 2008).

D. Autophagy and cardiac stress

Autophagy and mitophagy are important adaptive stress responses that are rapidly upregulated by cardiac injury (Gustafsson and Gottlieb, 2008). By clearing damaged cellular components and providing amino and fatty acids to support energy production, autophagy helps sustain cardiac myocyte viability. Chronic ischemia, I/R injury, and heart failure are associated with extensive mitochondrial damage. Damaged mitochondria can produce excessive ROS, release pro-apoptotic factors, and trigger necrosis through permeability transition pore opening (Elrod and Molkentin, 2013). In depolarized mitochondria, the F_1F_0-ATPase may also run in reverse, consuming ATP when cellular stores are already low (Grover *et al.*, 2004). Upregulating mitophagy eliminates damaged mitochondria before they cause further harm to the cell.

While mitochondria are occasionally found in autophagosomes in control mice by electron microscopy, up to 10% of the autophagosomes in the border zone of a myocardial infarction contain mitochondria eight hours after the injury (Hoshino *et al.*, 2012). In addition, Parkin-mediated mitophagy is important for clearance of damaged mitochondria and myocardial recovery after infarction. Parkin-deficient hearts rapidly accumulate dysfunctional mitochondria which contribute to cardiac dysfunction and reduced survival (Kubli *et al.*, 2013).

However, autophagy is not always beneficial. In the setting of increased myocardial demand such as pressure overload, enhanced autophagy contributes to pathologic remodeling, contractile dysfunction, and cardiac atrophy (Zhu, *et al.*, 2007). Similarly, Matsui *et al.* demonstrated that AMPK-independent autophagy can exacerbate cardiac damage during the reperfusion phase of I/R injury (Matsui *et al.*, 2007). In summary, cellular context determines whether autophagy promotes survival or cell death. As such, several regulatory pathways precisely modulate autophagic flux to meet cellular needs.

E. MCL-1 and clinical care

Heart disease is the leading cause of mortality in the United States. Based on the Framingham and NHANES studies, this burden is exacerbated by several common comorbidities, including obesity, diabetes, hypercholesterolemia, and hypertension (D'Agostino *et al.*, 2008; Go *et al.*,

2013). Consequently, cardiac disease substantially increases health care costs and utilization in the United States (Go *et al.,* 2013). While existing therapies significantly improve outcomes, little progress has been made in preventing myocyte death and fibrosis after ischemic insult. Relative stagnation in cardiac care, increasingly prevalent risk factors, and an aging population highlight a critical need for novel therapeutic approaches. Proteins that regulate mitochondrial integrity and function such as MCL-1 present a new avenue for potential cardiac intervention.

In addition to its role in the myocardium, MCL-1 appears prominently in current cancer literature. Aberrant expression of anti-apoptotic BCL-2 family members is a defining feature of many cancers, and upregulation of these proteins is strongly associated with resistance to current therapies (Kang & Reynolds, 2009). MCL-1 overexpression is especially common among malignancies, and the protein is associated with relapse and resistance to chemotherapeutics including other BCL-2 family antagonists (Beroukhim *et al.*, 2010, Wuillème-Toumi *et al.*, 2005, Lin *et al.*, 2007). Since BCL-2 family inhibitors, such as ABT-737, can actually select for cancer cells that overexpress MCL-1, MCL-1 antagonists have been developed to overcome this resistance (Yecies *et al.*, 2010, Nguyen *et al.*, 2007, Wei *et al.*, 2010). New therapeutics continue to target mechanisms involving MCL-1 to improve treatment outcomes for cancer patients, but their efficacy and toxicity remain poorly characterized (Wei *et al.*, 2012).

F. Rationale (hypothesis and specific aims)

Anti-apoptotic effects of MCL-1 have been extensively characterized in malignancies. Conversely, little is known about the function of MCL-1 in normal cells, including cardiac myocytes. Although myocytes typically comprise less than a third of cells in the human heart, they occupy almost 80% of cardiac volume (Vliegen *et al.*, 1991). Cardiac myocytes are also the functional units of contraction, and their survival after cardiac injury determines clinical prognosis. Cardiovascular therapy particularly emphasizes myocyte salvage because these cells are terminally differentiated and difficult to replace (Mani, 2008).

In this study, I generated inducible, myocyte-specific *Mcl-1* knockout mice to investigate the hypothesis that MCL-1 is essential for mitochondrial integrity and cardiac function in the adult heart. I discovered that ablation of MCL-1 in adult myocytes led to mitochondrial dysfunction, impaired autophagy, and rapid development of severe heart failure. These findings indicate that MCL-1 is critical for cardiac homeostasis and have broad clinical implications for the design of potential chemotherapeutic antagonists of MCL-
During these studies, I have addressed three major aims:

1. To characterize the functional role of MCL-1 in the myocardium
2. To investigate the role of apoptosis, the mitochondrial permeability transition pore, and necrotic cell death in MCL-1 deficient hearts
3. To examine the role of MCL-1 in cardiac autophagy and mitophagy

Acknowledgements

Chapter 1, in part, is a reprint of the material as it appears in Thomas *et al.*, Circ J, 2013 and Thomas *et al.*, Autophagy 2013. The dissertation author was the primary investigator and author of these papers.

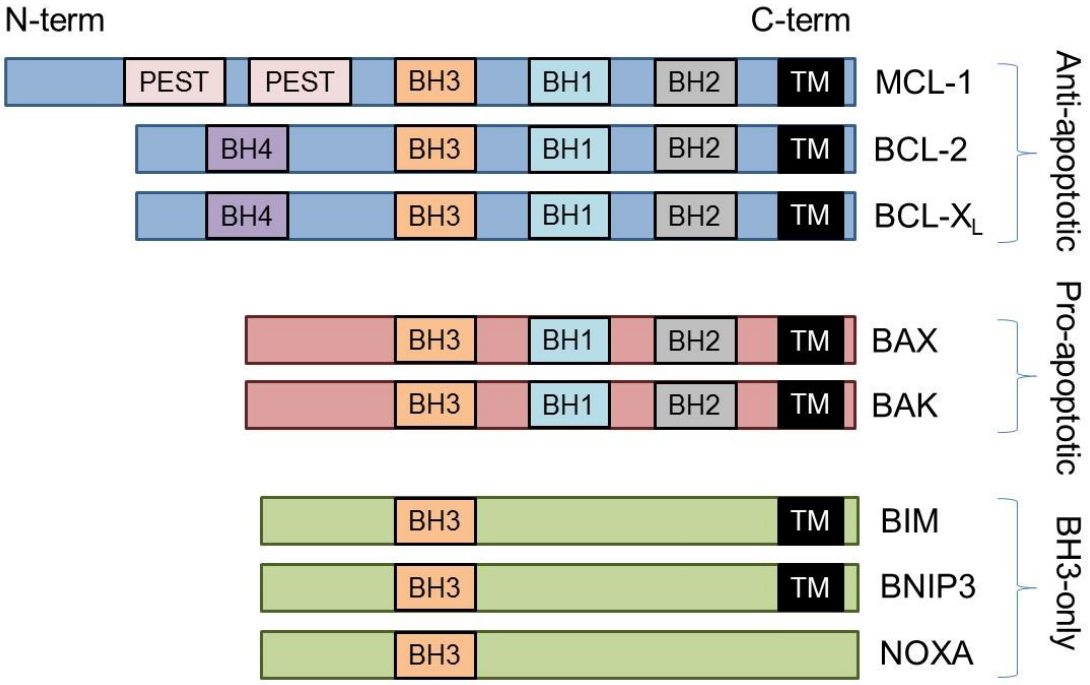

Figure 1: Protein homology of BCL-2 family proteins. Proteins in this family feature characteristic BCL-2 homology (BH) domains that facilitate interactions between them. Anti-apoptotic proteins are shown in blue, pro-apoptotic proteins are shown in red, and BH3-only proteins are shown in green. Lack of a BH4 domain and an extended N-terminal (N-term) regulatory region distinguish MCL-1 from other anti-apoptotic proteins. Transmembrane (TM) domains are present at the C-terminus (C-term) in most BCL-2 proteins.

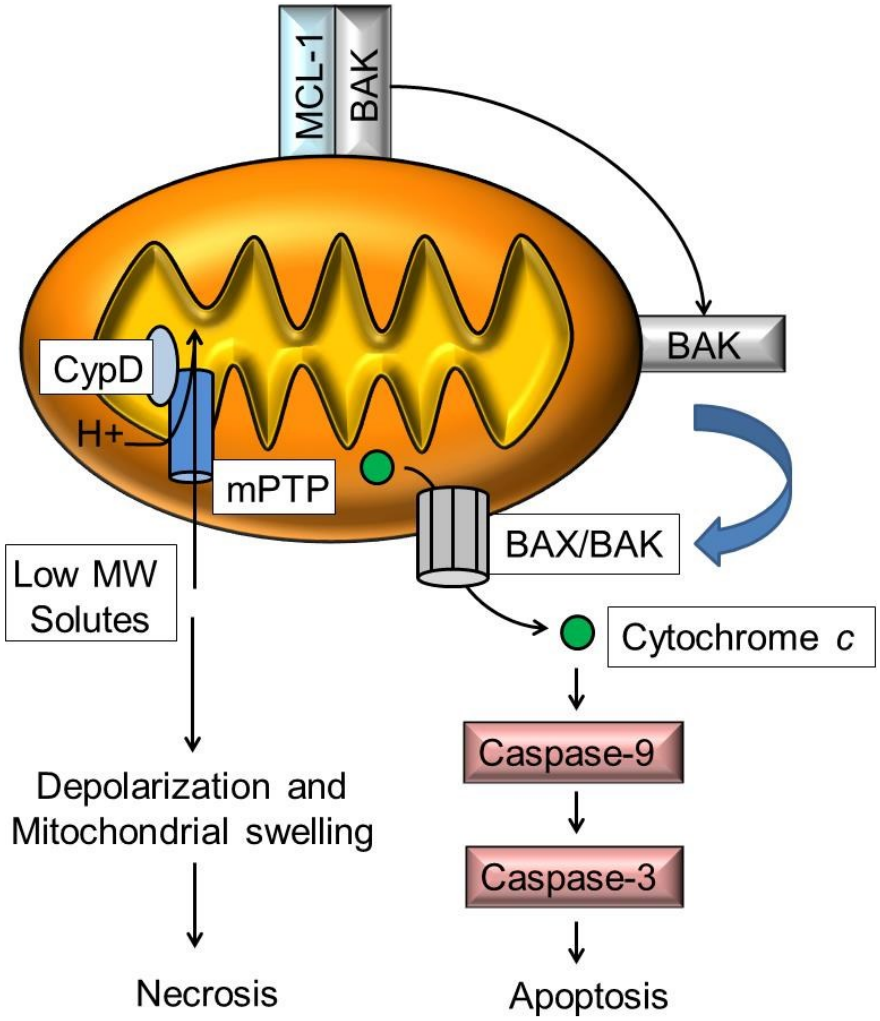

Figure 2: MCL-1 and mitochondrial regulation of cell death pathways. MCL-1 resides at mitochondria, which produce ATP and integrate cell death pathways. Activation of the intrinsic pathway of apoptosis via BAX/BAK releases pro-apoptotic factors such as cytochrome *c*, while necrosis is associated with mitochondrial permeability transition pore opening.

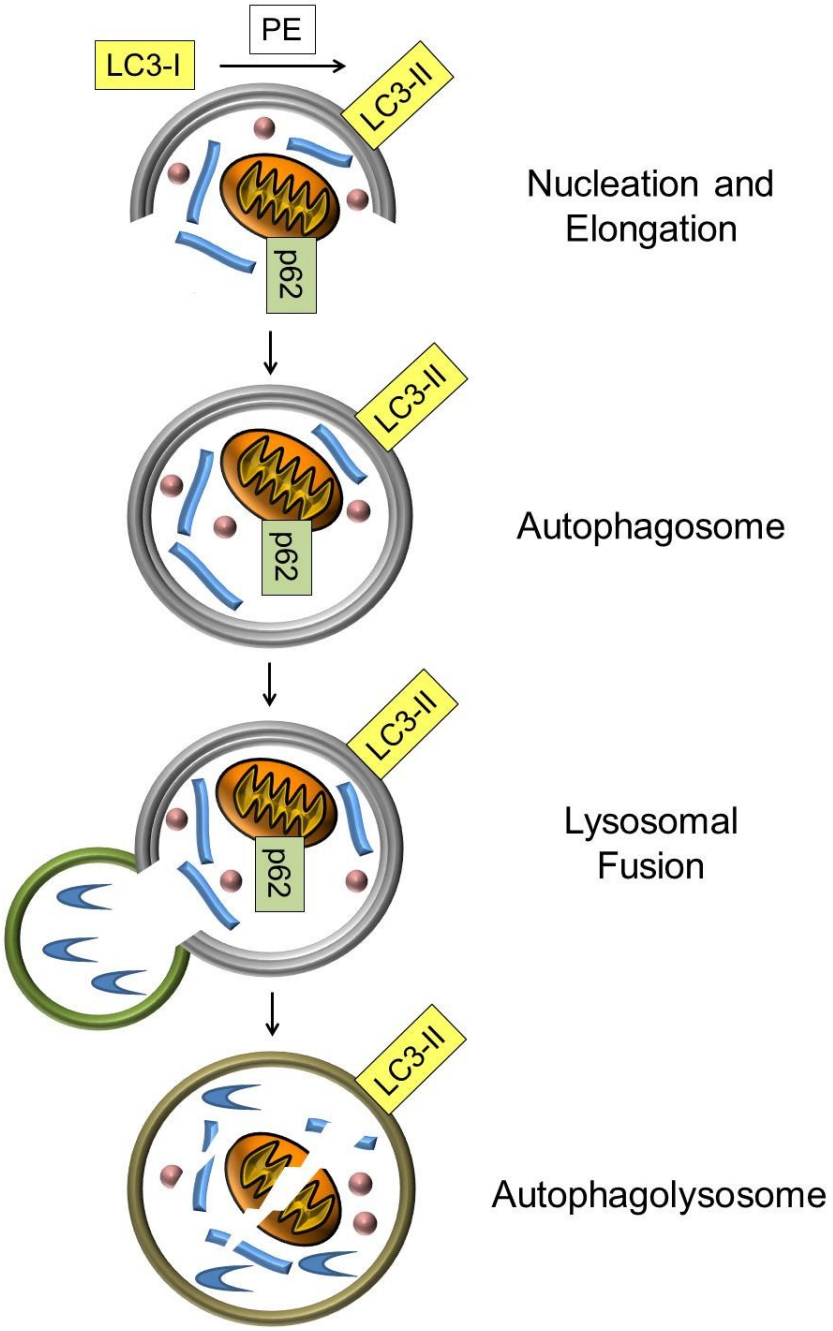

Figure 3: Overview of autophagy. Cellular components are targeted for degradation using p62 and enveloped in a double membrane autophagosome. During autophagosome formation, conjugation with phosphatidylethanolamine (PE) converts cytosolic LC3-I to membrane bound LC3-II. Fusion with the lysosome leads to degradation of autophagosome contents, releasing fatty and amino acids for biosynthesis and energy production.

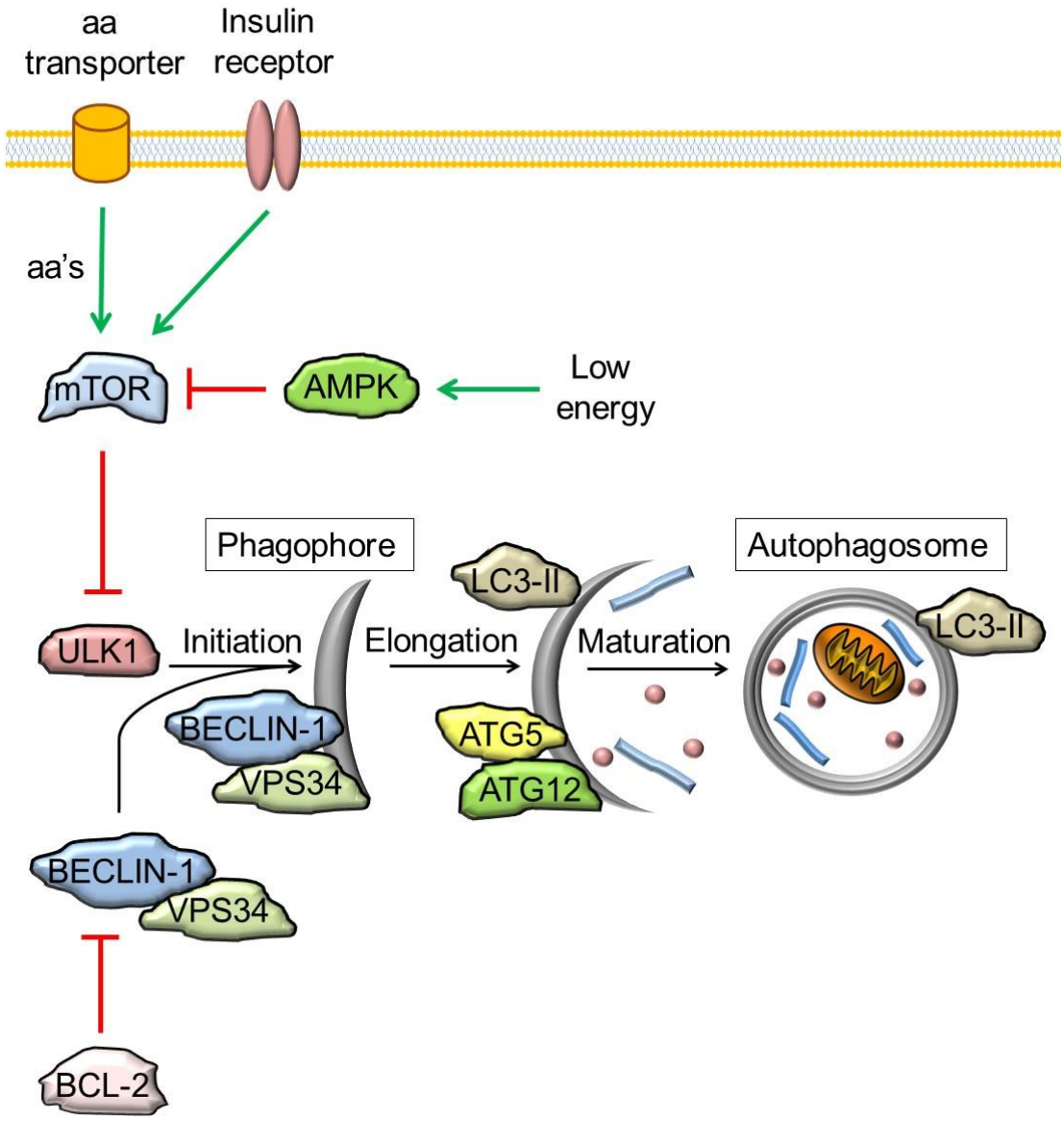

Figure 4: Regulation of autophagy proteins. mTOR integrates signals from the endocrine system, nutrient availability (aa = amino acid), and intracellular stress to regulate initiation of autophagy. Once mTOR is inhibited, ULK1 and BECLIN-1/VPS34 complexes initiate phagophore formation. Elongation of the autophagosome membrane is carried out by the ATG5/12 and LC3 conjugation systems. The mature autophagosome is a double membrane structure tagged with LC3-II.

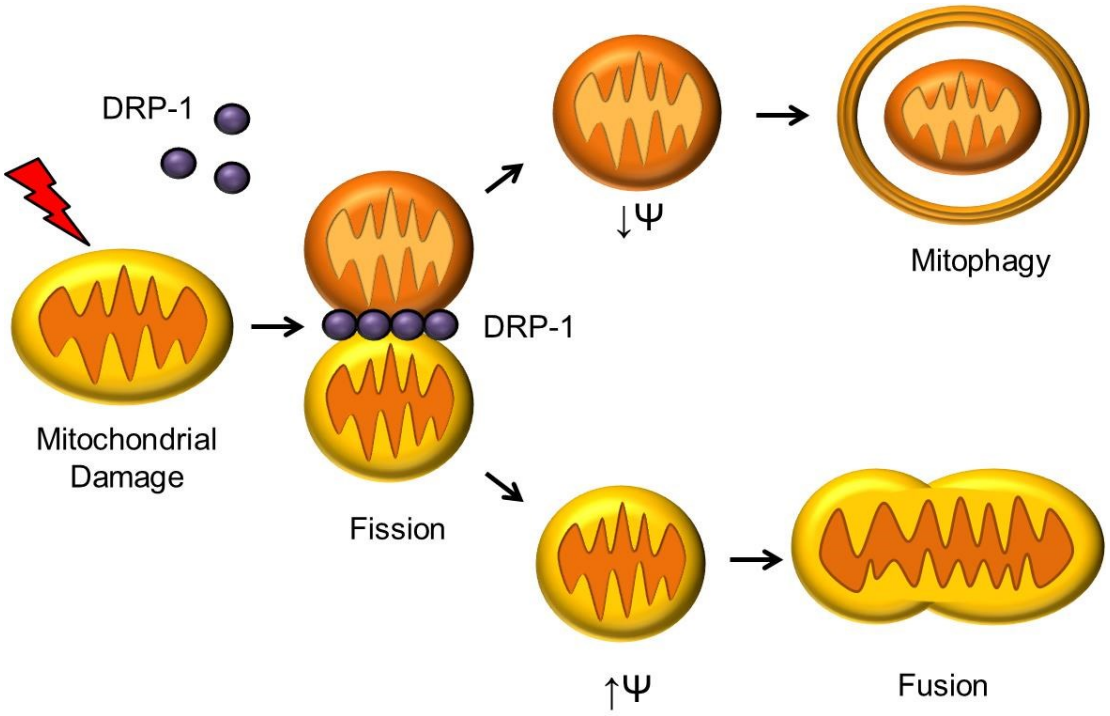

Figure 5: Mitochondrial fission precedes mitophagy. DRP-1 translocates to damaged mitochondria, leading to fission that selectively isolates dysfunctional mitochondrial fragments. Mitochondria with low membrane potential (↓Ψ) undergo mitophagy while functional mitochondria fuse and persist.

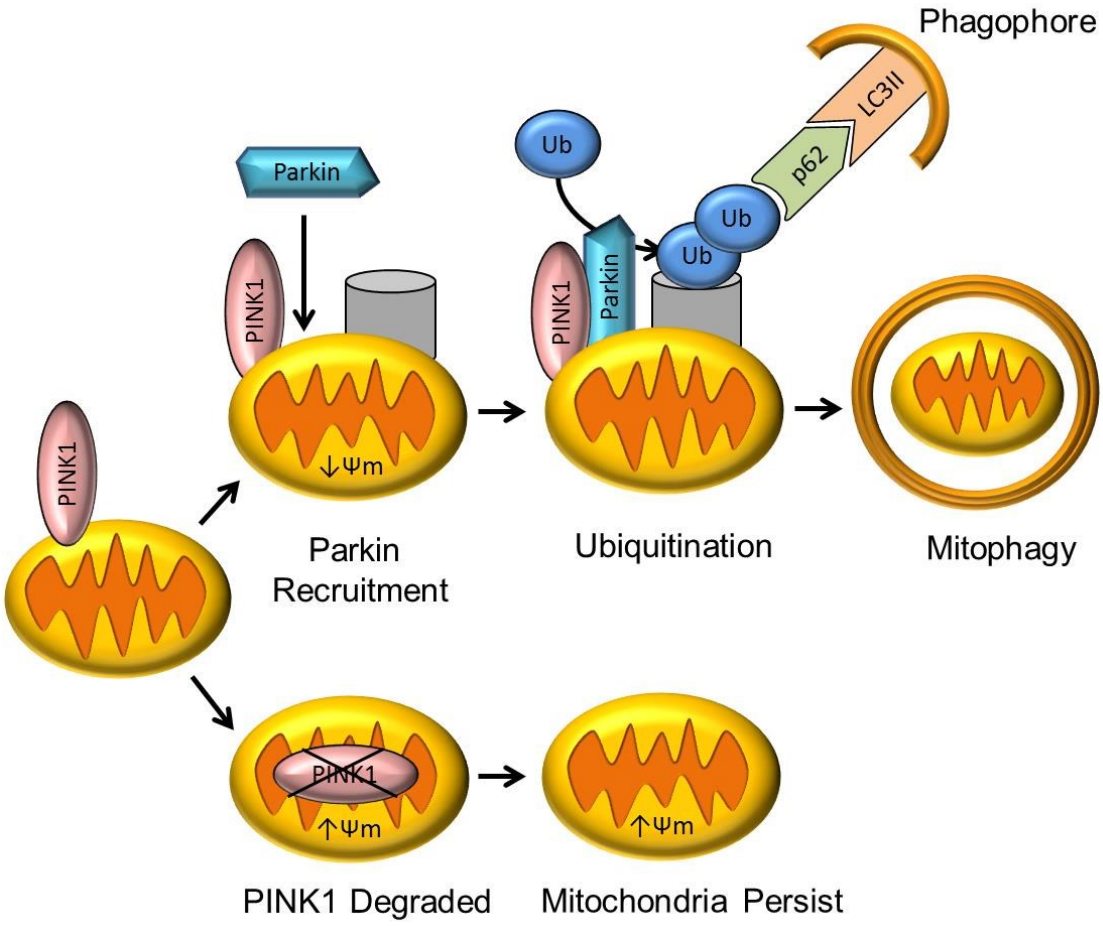

Figure 6: The PINK1/Parkin pathway regulates mitophagy. PINK1 is targeted to mitochondria. In mitochondria with high membrane potential (Ψm), PINK1 is imported and degraded. In damaged mitochondria with reduced Ψm, PINK1 recruits Parkin, which ubiquitinates mitochondrial proteins to recruit autophagosomes.

Chapter 2: Materials and methods

Mouse surgeries and cardiac-restricted ablation of the *Mcl-1* gene

I carried out all animal experiments in accordance with institutional guidelines and approval by the Institutional Animal Care and Use Committee of the University of California, San Diego. We subjected adult mice to myocardial infarction by permanently ligating the left anterior descending coronary artery (LAD) as described previously (Kubli *et al.*, 2013). Briefly, we anesthetized 12-16-week-old C57Bl/6J mice with isoflurane. We intubated and ventilated (Harvard Apparatus) the animals. We then ligated the LAD with an 8-0 silk suture and immediately closed the chest with sutures and tissue adhesive.

I crossed mice harboring a homozygous conditional null mutation in the *Mcl-1* gene (*Mcl-1*$^{flox/flox}$) (Opferman *et al.*, 2003) with transgenic α*MHC-MerCreMer* mice (Sohal *et al.*, 2001) that express Cre recombinase under the transcriptional control of the cardiomyocyte-specific α-myosin heavy chain (αMHC) promoter to generate conditional cardiomyocyte-specific *Mcl-1* knockout mice. I then crossed *Mcl-1*$^{flox/flox}$*;MerCreMer+* mice with cyclophilin D null mice (*Ppif*$^{-/-}$*)* (Baines *et al.*, 2005) to generate *Ppif*$^{-/-}$*Mcl-1*$^{flox/flox}$*;MerCreMer+* double knockout mice. All mice were on a C57BL/6J background and I used Cre- littermates as controls. To selectively delete *Mcl-1* in cardiomyocytes, I injected 8-10 week old mice with 80 mg/kg of tamoxifen for five days (Koitabashi *et al.*, 2009). I found that this dose resulted in the

most rapid and effective knockdown of the *Mcl-1* gene without causing cardiotoxicity.

Echocardiography

I carried out echocardiography as described previously using a VisualSonics Vevo 770 with an RMV707B 15-45-MHz imaging transducer (Kubli *et al.*, 2013). I anesthetized mice with 0.5-1.5% isoflurane in 95% O_2, 5% CO_2 and placed them on a recirculating water warming pad. I acquired all scans under light anesthesia with heart rates > 500 bpm to avoid anesthetic depression of heart rate and cardiac function (Yang *et al.*, 1999).

qPCR for hypertrophy markers

We isolated RNA from cardiac tissue using a thiocyanate-phenol-chloroform extraction protocol based on the method of Chomcyznski and Sacchi (1987). Briefly, we homogenized cardiac tissue samples in TRIzol reagent (Ambion), separated organic and aqueous layers by centrifugation, precipitated RNA from the aqueous phase, and synthesized cDNA via reverse transcriptase reaction using 1 µg of RNA and Oligo-dT primers (Thermo Scientific). We then carried out qPCR using standard TaqMan primers and TaqMan Universal Mastermix II (Applied Biosystems) on a 7500 Fast Real-Time PCR system (Applied Biosystems). We calculated fold difference according to the comparative C_T ($2^{-\Delta\Delta C_T}$) method using GAPDH as a control (Schmittgen & Livak, 2008).

Histological analysis and immunofluorescence

I arrested hearts in diastole during tissue collection with 200 mM cold KCl, fixed them in 4% paraformaldehyde, dehydrated them in 70% ethanol, and embedded them in paraffin. I then stained sections with H&E or Masson's Trichrome. To determine the size of cardiomyocytes, we labeled transverse sections with fluorescein isothiocyanate–labeled (FITC-labeled) wheat germ agglutinin (WGA) (Sigma-Aldrich), counterstained nuclei with DAPI (Vector Laboratories), and determined cross-sectional area of myocytes in the LV wall using Image Pro Plus software as described previously (Xiang *et al.*, 2011). We stained sections for DNA fragmentation *in situ* as previously described (Quinsay, *et al.,* 2010) using terminal deoxynucleotidyl transferase dUTP nick end labeling (TUNEL) with fluorescein labeled nucleotides (Roche Applied Science). To detect activated caspase-3, we incubated heart sections with an antibody specific for cleaved caspase-3 (Cell Signaling Technology) and counterstained nuclei with Hoechst 33342. We used sections from 3-4 hearts in each group for staining and analyzed at least five different fields/sections in each experiment.

LDH and caspase-3 activity assay

To determine LDH activity, we cleared blood samples by centrifugation at 3,000 x g for 10 min at 4°C. We quantified LDH activity via colorimetric assay by measuring the reduction of a tetrazolium salt to formazan (Biovision). We determined caspase-3 activity in whole heart homogenates using a

fluorescent caspase-3 activity assay (EMD Biosciences). We used HL-60 cells treated with 0.5 μg/mL actinomycin D for 24 hours as a positive control. We measured fluorescence using a Molecular Devices SpectraMax M3 spectrophotometer.

Western blot analysis

I homogenized hearts in Triton X-100 lysis buffer (50 mM Tris-HCl, 150 mM NaCl, 1 mM EGTA, 1 mM EDTA, 1% Triton X-100 plus cOmplete Protease Inhibitor cocktail (Roche)), and cleared lysates by centrifugation at 20,000 x g at 4°C for 20 min. I ran samples on Invitrogen NuPAGE Bis-Tris Gels and transferred proteins to nitrocellulose membranes. I incubated membranes with the indicated antibodies and imaged them with a BioRad ChemiDoc XRS+ imager. Antibodies were directed against MCL-1 (Rockland #600-401-394, 1:1000), BCL-2 (BD Biosciences, 1:1000), BCL-X_L (Santa Cruz #sc-8392. 1:100), BAK (Millipore Upstate #06-536, 1:500), BAX (Cell Signaling #2772, 1:1000), LC3 (Cell Signaling #4108, 1:1000), p62 (ARP #03-GP62-C, 1:1000), cleaved caspase-3 (Cell Signaling #9664, 1:1000), GAPDH (Cell Signaling #2118, 1:1000), actin (Sigma #A4700, 1:1000), tubulin (Sigma #T6074, 1:1000), ubiquitin (Santa Cruz, sc-8017 1:100), AIF (Cell signaling #5318, 1:1000), BNIP3 (Sigma B7931, 1:1000), p84 (Genetex GTX70220, 1:1000), Complex III subunit Core 2 (Invitrogen 459220, 1:1000), TIM23 (BD Biosciences 611222, 1:1000), PINK1 (Cayman 10006283, 1:500), BIM (Cell

Signaling 2819, 1:500), NOXA (Novus NB600-1159, 1:200), GFP (Clontech 632380 1:1000) and ATG5 (Abgent AP1812a, 1:1000)

Co-immunoprecipitation

I carried out co-immunoprecipitation experiments as previously described (Hanna *et al.*, 2012). Briefly, I co-transfected mouse embryonic fibroblasts with myc-tagged MCL-1 and YFP-tagged Parkin using FuGENE 6 transfection reagent according to the manufacturer's protocol (Promega E2691). After 24 hours, I harvested cells in Triton X-100 lysis buffer (50 mM Tris-HCl, 150 mM NaCl, 1 mM EGTA, 1 mM EDTA, 1% Triton X-100 plus cOmplete Protease Inhibitor cocktail (Roche)) and pre-cleared lysates with protein G PLUS-agarose (Santa Cruz Biotechnology #SC-2002) for 1 hour. I incubated lysates with anti-myc antibody (Sigma #M4439) overnight, captured immunocomplexes with protein G PLUS-agarose beads, eluted proteins in 2X LDS sample buffer, and analyzed samples by Western blot.

Electron microscopy

We performed transmission electron microscopy on heart sections as previously described (Quinsay *et al.*, 2010). The hearts were fixed in 2.5% glutaraldehyde in 0.1M cacodylate buffer, post-fixed in 1% osmium tetroxide, treated with 0.5% tannic acid and 1% sodium sulfate, cleared in 2-hydroxypropyl methacrylate and embedded in LX112 (Ladd Research, Williston, VT). We mounted sections on copper slot grids coated with parlodion

and stained them with uranyl acetate and lead citrate for examination on a Philips CM100 electron microscope (FEI, Hillsbrough OR).

Cellular fractionation

I isolated mitochondria from mouse cardiac tissue according to the methods described in Sayen *et al.,* 2003. Briefly, I collected hearts from terminally anesthetized mice, minced them in homogenization buffer (250 mM Sucrose, 5mM KH_2PO_4, 2 mM $MgCl_2$, 10mM MOPS, 1mM EGTA, 0.1% fatty acid free bovine serum albumin (BSA)) and homogenized them by polytron at 11,000 RPM. I broke up homogenates using a teflon drill and centrifuged them at 600 x g and 4°C for 5 minutes. I collected the supernatant and centrifuged it at 3000 x g and 4°C for 10 min. The resulting pellet contained mitochondria while the remaining supernatant constituted the cytosolic fraction. I washed mitochondria in homogenization buffer, and re-centrifuged them twice at 3000g and 4°C for 10 min. For Western blot, I lysed the resulting mitochondrial pellet in Triton-X 100 lysis buffer, and quantified protein concentration by Bradford assay.

Mitochondrial swelling assay, oxygen consumption and Complex I/II activity

We isolated cardiac mitochondria from tamoxifen treated *Mcl-1$^{f/f}$*, *Mcl-1$^{f/f}$Cre+, Ppif$^{-/-}$Mcl-1$^{f/f}$*, *and Ppif$^{-/-}$Mcl-1$^{f/f}$Cre+* mice at one week and carried out mitochondrial swelling assays as described previously (Quinsay ***et al.***, 2010). Briefly, we suspended sixty micrograms of mitochondria in 100 µl of

homogenization buffer (250 mM sucrose, 5 mM KH_2PO_4, 2 mM $MgCl_2$, 10 mM MOPS (pH 7.4), 1 mM EGTA and 0.1% fatty acid free BSA) and added them to a 96-well plate. We monitored mitochondrial swelling by measuring absorbance on a plate reader (Molecular Devices SpectraMax M3) at 520nm. The procedures used for mitochondrial respiration have been described previously (Kubli *et al.*, 2013). We recorded mitochondrial oxygen consumption at 30°C using a Clark-type oxygen electrode (Hansatech Oxygraph) in 600 µl of respiration buffer (140 mM KCl, 1 mM EGTA, 10 mM MOPS (pH 7.4), 10 mM $MgCl_2$, 5 mM KH_2PO_4, and 0.2% fatty acid-free BSA). We measured complex I dependent respiration using 200 µg of mitochondria with 5 mM of pyruvate and 5 mM of malate as a substrate and complex II dependent respiration with 5 mM succinate as a substrate. We recorded ADP-stimulated respiration rate (*state 3*) after the addition of 2 mM ADP, oligomycin-insensitive respiration rate (*state 4*) after the addition of 2 µM oligomycin, and the maximal respiration rate after uncoupling the mitochondria with 2 µM FCCP. We expressed rates as nA $O \cdot min^{-1} \cdot mg^{-1}$ protein. As a measure of mitochondrial integrity, we also calculated the respiratory control ratio (RCR) (*state 3* divided by *state 4 in the presence of oligomycin)*. The data reported represent three to four independent mitochondrial preparations comprising two hearts each.

In separate experiments, we measured the enzymatic activity of oxidative phosphorylation (OXPHOS) complexes I and II as previously

described (Frazier & Thorburn, 2012). To assess complex I activity, we resuspended mitochondria in buffer (50 mM KH_2PO_4, 5 mM $MgCl_2$, 50 µM NADH, 1 mM KCN, 10 µM Antimycin A, and 0.1% docecyl maltoside) and recorded oxidation of NADH at 340 nm in a spectrophotometer (Molecular Devices) upon addition of 50 uM CoQ1. To assess Complex II activity, we resuspended mitochondria in buffer (50 mM KH_2PO_4, 5 mM $MgCl_2$, 50 µM CoQ1, 80 µM DCIP, 1 mM KCN, 10 µM Antimycin A, and 0.1% docecyl maltoside) and recorded reduction of DCIP at 600 nm upon addition of 10 mM succinate. We then calculated enzymatic activities using absorption coefficients of 6.22 mM/1cm for NADH and 21 mM/1cm for DCIP.

***In vivo* autophagy experiments**

I administered tamoxifen by intraperitoneal injection to *Mcl-1*$^{flox/flox}$;*MerCreMer*+ and *Mcl-1*$^{flox/flox}$;*MerCreMer*- littermates for five days. One week after the first injection (day 7), I injected these mice with 60 mg/kg chloroquine (Sigma) or vehicle to block autophagic flux. Six hours later, I harvested hearts for Western blotting experiments as described above. In separate experiments, I evaluated autophagy in *Mcl-1*$^{flox/flox}$;*MerCreMer*+ and *Mcl-1*$^{flox/flox}$;*MerCreMer*- mice in response to exercise. One week after initiating tamoxifen administration, I subjected mice to two 10 minute swimming sessions in a 37°C water bath separated by a two hour resting period in between. On day 8, the two swimming periods were extended to 20 minutes.

On day 9, the mice were subjected to swimming for up to 120 minutes followed by immediate euthanasia and tissue collection.

Isolation of neonatal rat cardiomyocytes

We isolated myocytes from 1-2 day old Sprague-Daley rat pups using an isolation system from Worthington based on the method of Toraason *et al.* (1988). After overnight trypsinization and collagenase dissociation, we plated cells on 1% gelatin coated tissue culture plates using 4:1 media (80% DMEM, 20% M199, 100 μM BrdU, 1X Antibiotic-Antimycotic (Invitrogen), 10% fetal bovine serum) as previously described (Xiang *et al.*, 2011).

Analysis of autophagy in neonatal rat cardiomyocytes

Twenty four hours after plating, I infected neonatal rat cardiomyocytes with adenoviruses encoding β-gal or MCL-1 (100 MOI) in 2% heat-inactivated serum in DMEM for 3 h. For imaging of autophagosomes, I co-infected cells with GFP-LC3. After 3-4 h, cells were rinsed and cultured in serum free 4:1 media for 24 h. For the experiment, I incubated cells in DMEM with or without glucose for six hours before imaging GFP-LC3 positive autophagosomes or measuring endogenous LC3 processing by Western blot. We captured high resolution fluorescence micrographs using a Carl Zeiss AxioObserver Z1 fitted with a motorized Z-stage and an Apotome for optical sectioning. We acquired Z-stacks in ApoTome mode using a high-resolution AxioCam MRm digital camera, a 63X Plan-Apochromat (Oil-immersion) objective and Zeiss AxioVision 4.8 software (Carl Zeiss). For western, I harvested cells in RIPA

lysis buffer (50 mM Tris-HCl, 150 mM NaCl, 0.5% sodium deoxycholate, 1% Triton X-100 plus cOmplete Protease Inhibitor cocktail (Roche)). I prepared samples with NuPAGE LDS Sample Buffer (Invitrogen #NP0008), ran them on Invitrogen NuPAGE 12% Bis-Tris gels, and transferred proteins to nitrocellulose membranes. I incubated these membranes with LC3 antibody (Cell signaling #4108, 1:1000) and goat anti-rabbit HRP (Invitrogen Molecular Probes, #G21234, 1:3333), added Pierce ECL chemiluminescent substrate (Thermo Scientific #32209), and imaged the resulting bands with a BioRad ChemiDoc XRS+ imager and Quantity One Software.

Cell death in neonatal rat cardiomyocytes

Twenty hours after plating, I infected neonatal rat cardiac myocytes with an adenovirus encoding β-gal or MCL-1 (100 MOI) in 2% heat-inactivated serum in DMEM for 3 h. After 3-4 hours, I rinsed cells and cultured them in serum free 4:1 media for 24 h. The next day, I treated the cells with doxorubicin (0.5 μM) for 24 h. We measured apoptosis by quantifying nucleosomes using an ELISA-based cell death assay (Roche #1774425) as previously described (Del Re *et al.*, 2007). We also stained live cells with YO-PRO-1 (1 μM) and Hoechst (10 μg/mL) as described previously (Hamacher-Brady *et al.,* 2007) and imaged them using a Carl Zeiss AxioObserver Z1 with a high-resolution AxioCam MRm digital camera, a 10X EC Plan-Neofluar objective, and Zeiss AxioVision 4.8 software (Carl Zeiss).

Statistical analyses

I expressed all values as mean ± standard error of mean (SEM). I performed statistical analyses using Student's t-test. I assessed survival using the Kaplan-Meier method and log-rank test. Throughout these experiments, I considered $p<0.05$ significant.

Acknowledgements

Chapter 2, in part, is a reprint of the material as it appears in Thomas et al., Genes Dev, 2013. The dissertation author was the primary investigator and author of this paper.

Chapter 3: Characterization of cardiac-specific MCL-1 knockout mice

Introduction

Early histologic characterization demonstrated that MCL-1 is highly expressed in normal myocardium (Krajewski *et al.*, 1995). Several publications have characterized the anti-apoptotic functions of MCL-1 in malignancies (Thomas *et al.*, 2010), but the functional role of MCL-1 in the heart has not been investigated. Recent literature also identified two isoforms of MCL-1, but relatively little is known about the function of each isoform (Huang and Yang-Yen, 2010). MCL-1 contains a mitochondrial targeting signal in the first 33 residues of its N-terminal region. Cells import a fraction of expressed MCL-1 into mitochondria with an intact membrane potential. N-terminal processing by mitochondrial proteases then generates a smaller cleavage product that is localized to the mitochondrial matrix (Huang & Yang-Yen, 2010). The larger, uncleaved isoform of MCL-1 resides at the outer mitochondrial membrane and protects against apoptosis; the smaller isoform appears to facilitate mitochondrial fusion, respiration, and protein assembly (Figure 7) (Perciavalle *et al.*, 2012).

In this chapter, I discuss experiments that provided rationale for generating a cardiac-specific MCL-1 knockout mouse. I confirmed that MCL-1 is expressed in myocardium and identified both isoforms of MCL-1 in murine tissues, including cardiac tissue from mice subjected to myocardial infarction.

Using a tamoxifen-driven lox-Cre system, I then selectively disrupted the gene that encodes *Mcl-1* in adult mouse hearts and characterized their rapid progression to pathologic hypertrophy, heart failure, and early mortality.

A. MCL-1 is altered by cardiac stress and promotes myocyte survival

My initial characterization confirmed that MCL-1 is highly expressed in the adult mouse heart relative to other tissues such as skeletal muscle and brain (Figure 8). Both isoforms of MCL-1 are clearly expressed in different tissues, including myocardium. Western blot analysis of mitochondrial and cytosolic fractions and fluorescent co-localization experiments also confirmed that MCL-1 primarily localizes to mitochondria (Figure 9A,B). To determine how stress affects MCL-1 isoforms in the myocardium, I analyzed MCL-1 protein levels in border zone tissue from control and infarcted hearts at different time points. The border zone surrounding an infarct contains salvageable myoctes, and their survival influences recovery of cardiac function and prognosis. After inducing myocardial infarction in adult mice, I found that the outer mitochondrial membrane (OMM) form is rapidly degraded in the border zone (t = 4 hours), whereas the matrix form is unchanged (Figure 10A,B). The OMM isoform is exposed to the cytosol, where it is subject to ubiquitination and caspase cleavage that explain its rapid elimination (Weng *et al.*, 2005, Zhong *et al.*, 2005). Meanwhile, the matrix isoform appears to be protected from such degradation. Strikingly, OMM levels of MCL-1 are

restored in border zone tissue 24 hours after the infarct, suggesting that surviving cardiac tissue prioritizes MCL-1 expression. In addition, the matrix form of MCL-1 is significantly increased at 24 hours, indicating that MCL-1 may play an adaptive role in mitochondrial preservation during the cardiac stress response. Finally, I overexpressed MCL-1 in rat neonatal cardiac myocytes to determine whether the protein protects against doxorubicin, a pro-apoptotic chemotherapeutic with known clinical cardiac toxicity (Chatterjee *et al.*, 2010). Using YO-PRO-1 staining to measure membrane permeabilization and a nucleosome ELISA assay to detect nuclear fragmentation, I found that overexpression of MCL-1 reduced apoptotic cell death (Figure 11A,B). These results demonstrate that MCL-1 is an important pro-survival protein in myocytes.

B. Loss of MCL-1 leads to rapid contractile dysfunction, cardiac hypertrophy, and early mortality

To further investigate the functional role of MCL-1 in the myocardium, I employed inducible, myocyte-specific *Mcl-1* knockout mice. These animals were generated by crossing *Mcl-1*$^{flox/flox}$ mice with transgenic mice expressing *MerCreMer* under the control of the α-*myosin heavy chain* promoter to permit tamoxifen-inducible deletion of the *Mcl-1* allele in the adult heart (Figure 12). The *Mcl-1*$^{flox/flox}$;*MerCreMer*+ (*Mcl-1*$^{f/f}$*Cre*+) mice were born at the expected Mendelian frequency and were indistinguishable in appearance from control

Mcl-1$^{flox/flox}$;*MerCreMer-* (*Mcl-1*$^{f/f}$) littermates. To delete MCL-1 in cardiac myocytes, I administered tamoxifen for five days to eight to ten week old mice (Figure 13A). Tamoxifen treatment reduced MCL-1 staining in cardiac tissue sections from *Mcl-1*$^{f/f}$*Cre*+ mice (Figure 13B). Western blotting of heart lysates confirmed a reduction in MCL-1 protein levels in hearts of *Mcl-1*$^{f/f}$*Cre*+ mice without affecting MCL-1 levels in skeletal muscle (Figure 13C).

After treating *Mcl-1*$^{f/f}$ and *Mcl-1*$^{f/f}$*Cre*+ mice with tamoxifen, I monitored cardiac function at weekly time points using transmural echocardiography. Echocardiographic analysis of tamoxifen-treated *Mcl-1*$^{f/f}$*Cre*+ mice revealed surprisingly severe contractile dysfunction and left ventricular dilatation as early as one week after initiating tamoxifen injection (EF=74.59±1.53%, FS=42.60±1.36%, LVdD=3.54±0.14mm for *Mcl-1*$^{f/f}$ mice vs. EF=47.54±6.27%*, FS=24.31±3.68%**, LVdD=4.11±0.15mm*** for *Mcl-1*$^{f/f}$*Cre*+; *,**,***p<0.05) (Figure 14A,B). Cardiac dysfunction in *Mcl-1*$^{f/f}$*Cre*+ mice persisted out to four weeks, corresponding with a significant increase in left ventricular diastolic diameter. Cardiac functional deficiencies and dilatation amongst *Mcl-1*$^{f/f}$*Cre*+ mice culminated in early mortality. Strikingly, all *Mcl-1*$^{f/f}$*Cre*+ mice died within 29 days after the initiation of tamoxifen treatment (median survival = 16 days) (Figure 15). Cardiac function was not impaired in tamoxifen treated *Mcl-1*$^{WT/WT}$*MerCreMer*+ mice, confirming that the cardiac dysfunction was not due to off-target Cre recombinase activity (Table 1).

Gene deletion in a homozygous knockout typically produces a more severe phenotype than partial ablation in a heterozygote. Heterozygotes reveal whether smaller reductions in protein expression are sufficient to induce pathology, and can provide important insights into the mechanism of disease. To compare the severity of complete MCL-1 ablation in cardiac myocytes with the effects of partial ablation, I injected mice that were heterozygous for the floxed MCL-1 allele (*Mcl-1*$^{f/+}$ and *Mcl-1*$^{f/+}$*Cre*+) with tamoxifen and tracked their cardiac function by echocardiography. After tamoxifen treatment, heart tissue from MCL-1 heterozygous knockouts exhibited an intermediate level of MCL-1 by Western blot compared to control and homozygous knockout hearts (Figure 16). Similarly to homozygous knockouts, MCL-1 heterozygous knockouts exhibited severely impaired cardiac function at one week compared to Cre- controls (EF=80.31±0.09%, FS=48.68±2.23% for *Mcl-1*$^{f/+}$ vs. EF=47.85±4.92%*, FS=24.08±2.79%* for *Mcl-1*$^{f/+}$*Cre*+, $p<0.05$), but they improved significantly by week two (EF=67.29±3.83, FS=37.28±2.69 for *Mcl-1*$^{f/+}$*Cre*+, $p<0.05$ compared to week one heterozygotes and week two homozygotes). By the fourth week after tamoxifen treatment, *Mcl-1*$^{f/+}$*Cre*+ mice were functionally indistinguishable from Cre- littermates (Figure 17). This recovery after partial ablation contrasts strongly with the irrecoverable, lethal heart failure evident in *Mcl-1*$^{f/f}$*Cre*+ mice.

Following functional characterization, I examined organ and tissue samples from *Mcl-1*$^{f/f}$*Cre*+ mice and Cre- controls to determine whether MCL-

1 deficient hearts exhibit other pathologic signs of heart failure. *Mcl-1*$^{f/f}$*Cre*+ hearts were enlarged by gross morphology (Figure 18A), and ventricle-to-body and lung-to-body weight ratios were significantly increased compared to *Mcl-1*$^{f/f}$ hearts two weeks after tamoxifen administration (Figure 18B). Increased ventricle weight indicates cardiac hypertrophy, while atrial enlargement and increased lung weight are signs of cardiac insufficiency and pulmonary edema. Additional evidence of cardiac hypertrophy included significantly increased myocyte fiber size (Figure 19A,B) and increased expression of ventricular hypertrophy markers atrial natriuretic factor (ANF) and brain natriuretic peptide (BNP*)* (Figure 20A) in *Mcl-1*$^{f/f}$*Cre*+ hearts. In addition, expression of α–myosin heavy chain (α-MHC) decreased while expression of β–myosin heavy chain (β-MHC) increased upon loss of MCL-1 (Figure 20B). This switch from adult to fetal MHC isoforms indicates reactivation of fetal gene programs that are associated with pathological cardiac hypertrophy (Gupta, 2007).

C. MCL-1 deficiency leads to cardiac fibrosis and loss of myocytes

Tissue sections from MCL-1 deficient hearts revealed signs of extensive cardiac injury. Histological analysis revealed increased left ventricular chamber dimensions and severe ventricular wall thinning in *Mcl-1*$^{f/f}$*Cre*+ hearts two weeks after tamoxifen treatment (Figure 21A). Left atrial thrombus was also evident in the *Mcl-1*$^{f/f}$*Cre*+ heart shown, demonstrating

impaired hemodynamics (Figure 21B). H&E stained cross sections revealed that loss of MCL-1 leads to myofibrillar disarray and myocyte degeneration (Figure 22). Masson's trichrome staining of heart sections from *Mcl-1*$^{f/f}$*Cre*+ hearts demonstrated extensive interstitial fibrosis and loss of myocytes throughout the left ventricle (Figure 23A,B) while qPCR showed increased transcription of collagen mRNA (Figure 23C). MCL-1 deficiency thus leads to rapid, extensive myocardial tissue damage, loss of myocytes, and irreversible, lethal cardiomyopathy.

Conclusion:

I have demonstrated that MCL-1 is essential for normal cardiac function. The protein localizes to cardiac mitochondria, responds rapidly and specifically to cardiac injury, and protects myocytes against cell death. MCL-1 ablation leads to contractile dysfunction, loss of myocytes, cardiac fibrosis, and rapid heart failure in the absence of other stress. MCL-1 knockout mice exhibit key clinical features of heart failure, including hypertrophy, cardiac insufficiency, ventricular dilatation with wall thinning, and early mortality. The observed ventricular dilatation exacerbates the pathology by increasing wall stress, cardiac afterload and myocardial oxygen consumption (MVO2). Dilatation also combines with low cardiac output to promote thrombus formation (Lip & Gibbs *et al.*, 1999). Strikingly, the intact *Mcl-1* allele in heterozygous knockouts preserves MCL-1 expression and allows the heart to

recover functionally. These results suggest that maintaining MCL-1 in the setting of cardiac stress facilitates cardiac recovery. Ultimately, the results presented above led to studies addressing the cause of myocyte death and cardiac dysfunction that will be discussed in the next chapter.

Acknowledgements

Chapter 3, in part, is a reprint of the material as it appears in Thomas et al., Genes Dev, 2013. The dissertation author was the primary investigator and author of this paper.

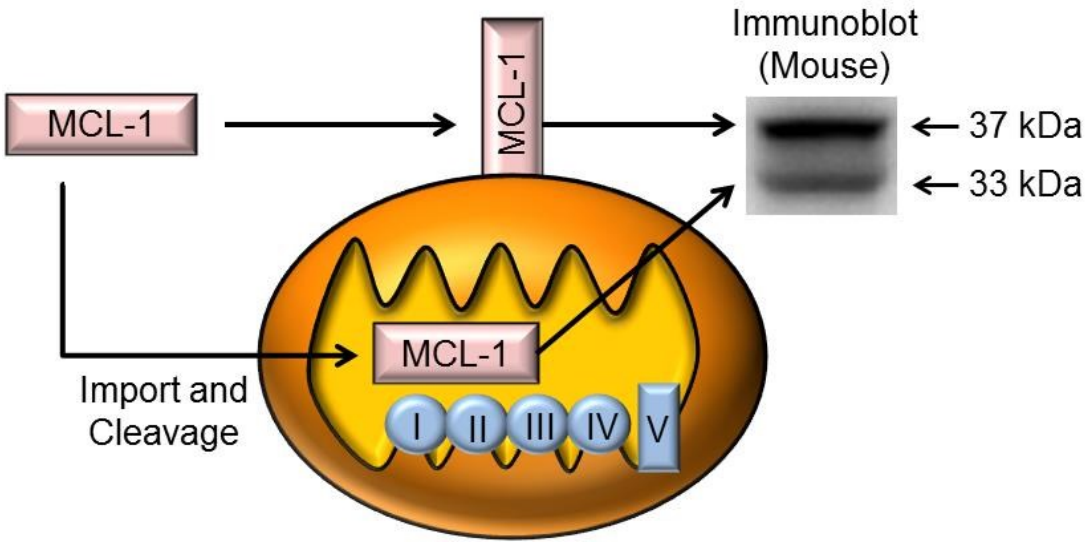

Figure 7: Outer mitochondrial membrane (OMM) and matrix isoforms of MCL-1. MCL-1 is processed at mitochondria to generate OMM and matrix isoforms. Cleavage of N-terminal residues in the mitochondrial matrix produces a smaller MCL-1 isoform on Western blot that appears to facilitate assembly of proteins in the electron transport chain (blue).

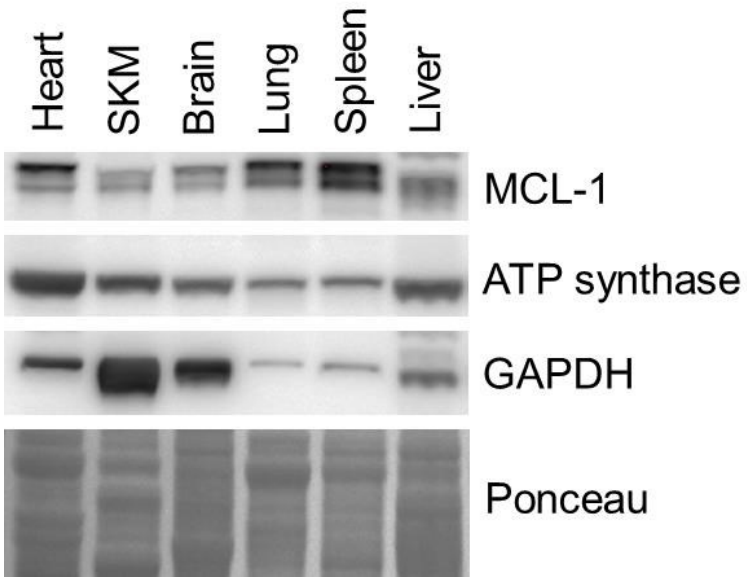

Figure 8: MCL-1 expression in murine tissues. Representative Western blot shows MCL-1 is highly expressed in myocardium relative to tissues such as skeletal muscle (SKM) and brain. The MCL-1 isoform doublet is also clearly detectable in different tissues. Extensive post-translational modification of MCL-1 may contribute to small diffences in gel migration.

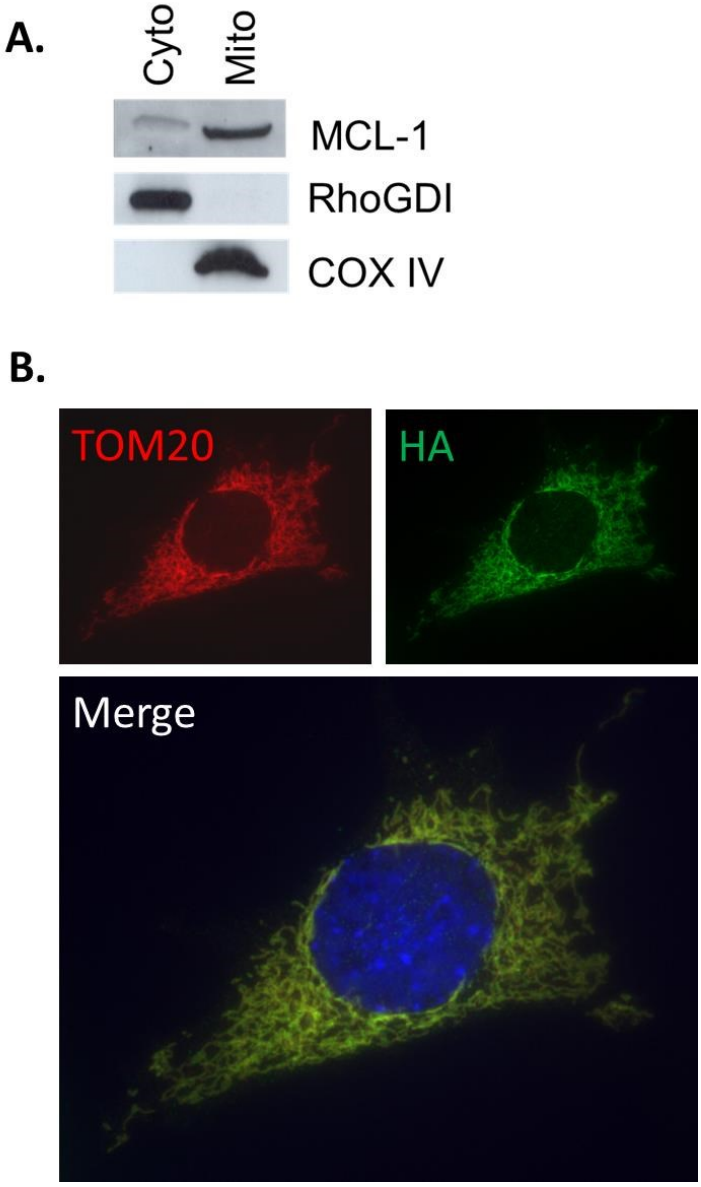

Figure 9: MCL-1 localizes to mitochondria **A.** Fractionation of cardiac lysate shows that the majority of MCL-1 resides in the mitochondrial fraction **B.** Fluorescent microscopy reveals that HA-tagged wild-type MCL-1 (green) overexpressed in mouse embryonic fibroblasts colocalizes with networked mitochondria stained for TOM20 (red).

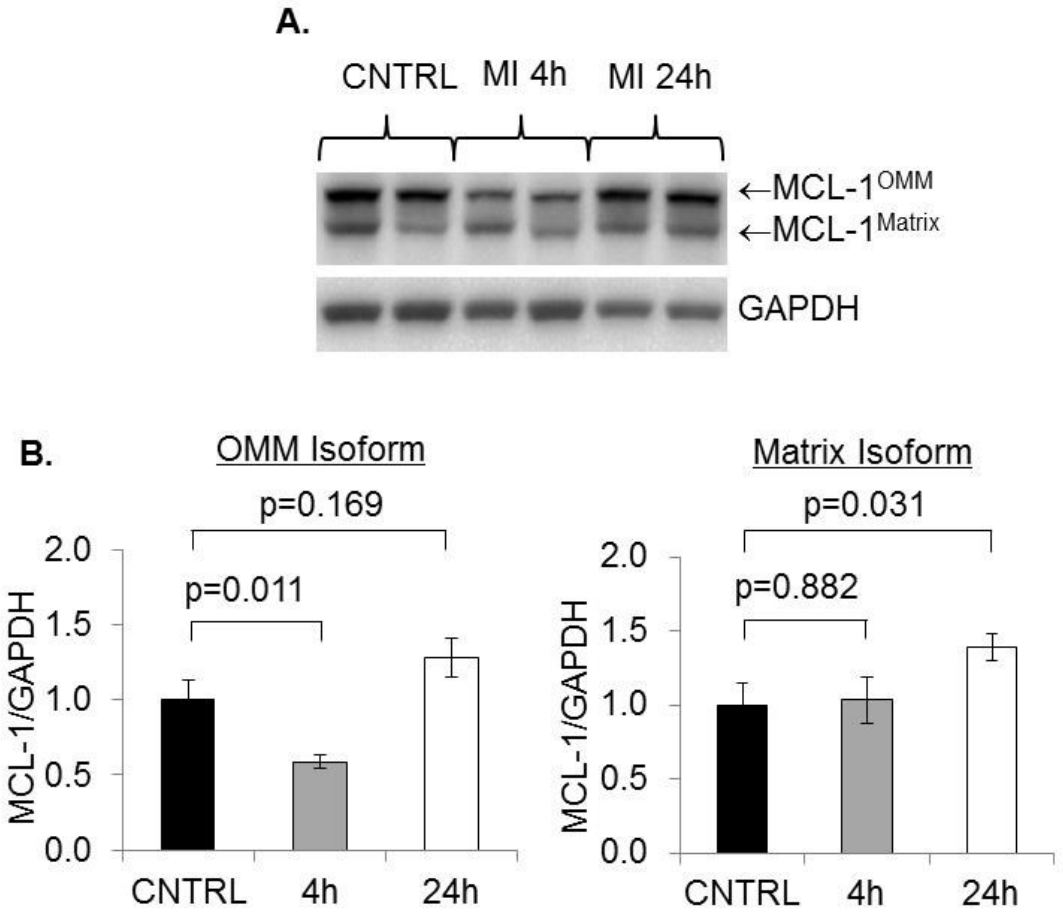

Figure 10: Myocardial infarction alters MCL-1 isoform expression. **A.** Representative Western blot analysis of MCL-1 in control hearts and in the border zone of the infarct. **B.** Quantitation of outer mitochondrial membrane (OMM) and matrix MCL-1 isoforms (n = 5–6).

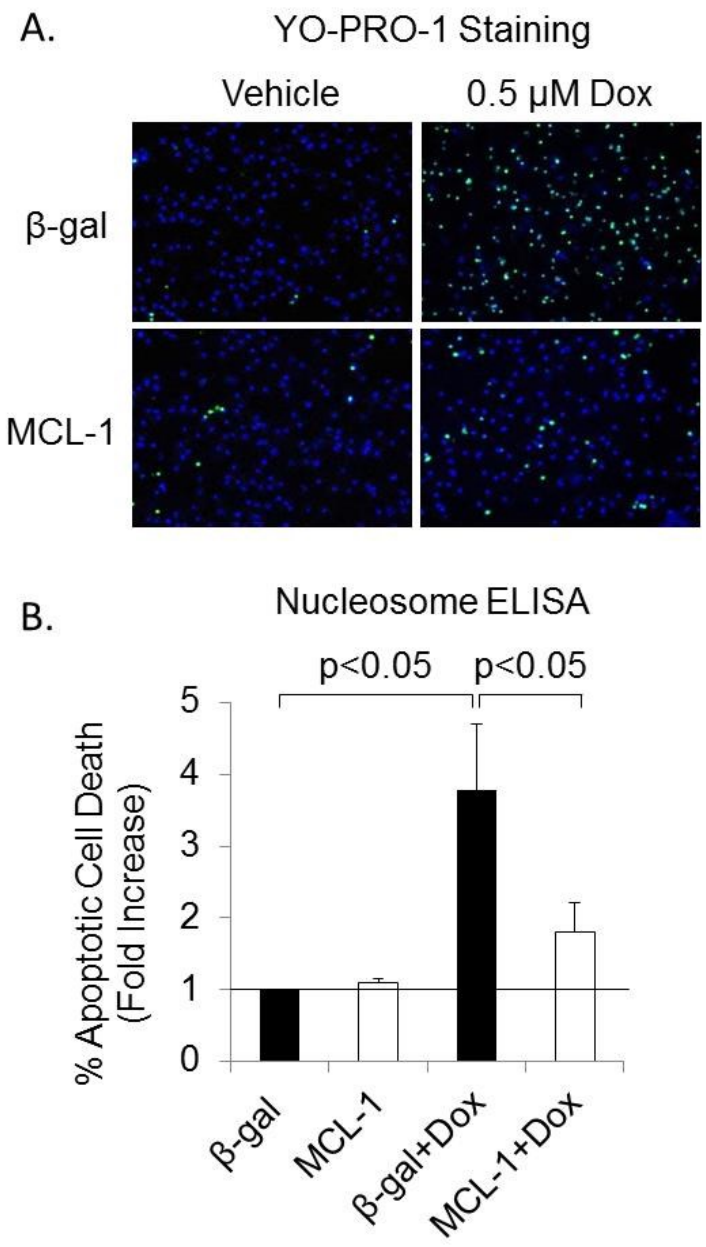

Figure 11: MCL-1 overexpression reduces doxorubicin-mediated cell death in myocytes. Neonatal rat cardiac myocytes were infected with an adenovirus encoding β-gal or MCL-1 (100 MOI) and then treated with doxorubicin (0.5 μM) for 24 hours. **A.** Representative live cell images show fewer permeabilized YO-PRO-1-positive cells (green) when MCL-1 is overexpressed. **B.**. Quantification of apoptosis using nucleosome ELISA shows increased apoptosis in β-gal-overexpressing myocytes. In contrast, cells overexpressing MCL-1 are protected against doxorubicin-mediated cell death (n = 4).

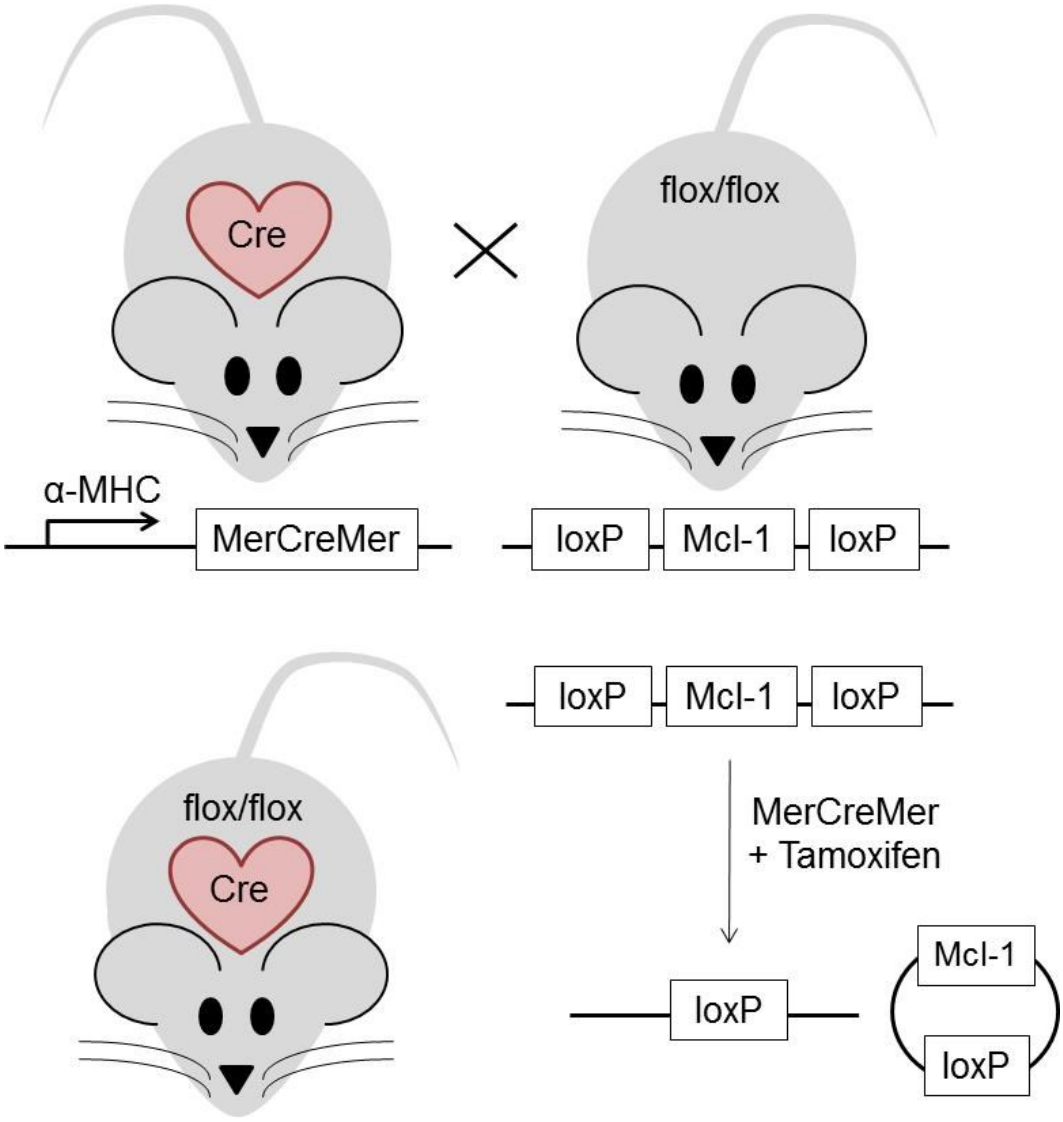

Figure 12: Generation of cardiac specific *Mcl-1* knockout mice. The use of the α-myosin heavy chain promoter restricts MerCreMer fusion protein expression to cardiac myocytes. Tamoxifen treatment induces nuclear translocation of the MerCreMer complex, loxP recombination, and *Mcl-1* deletion.

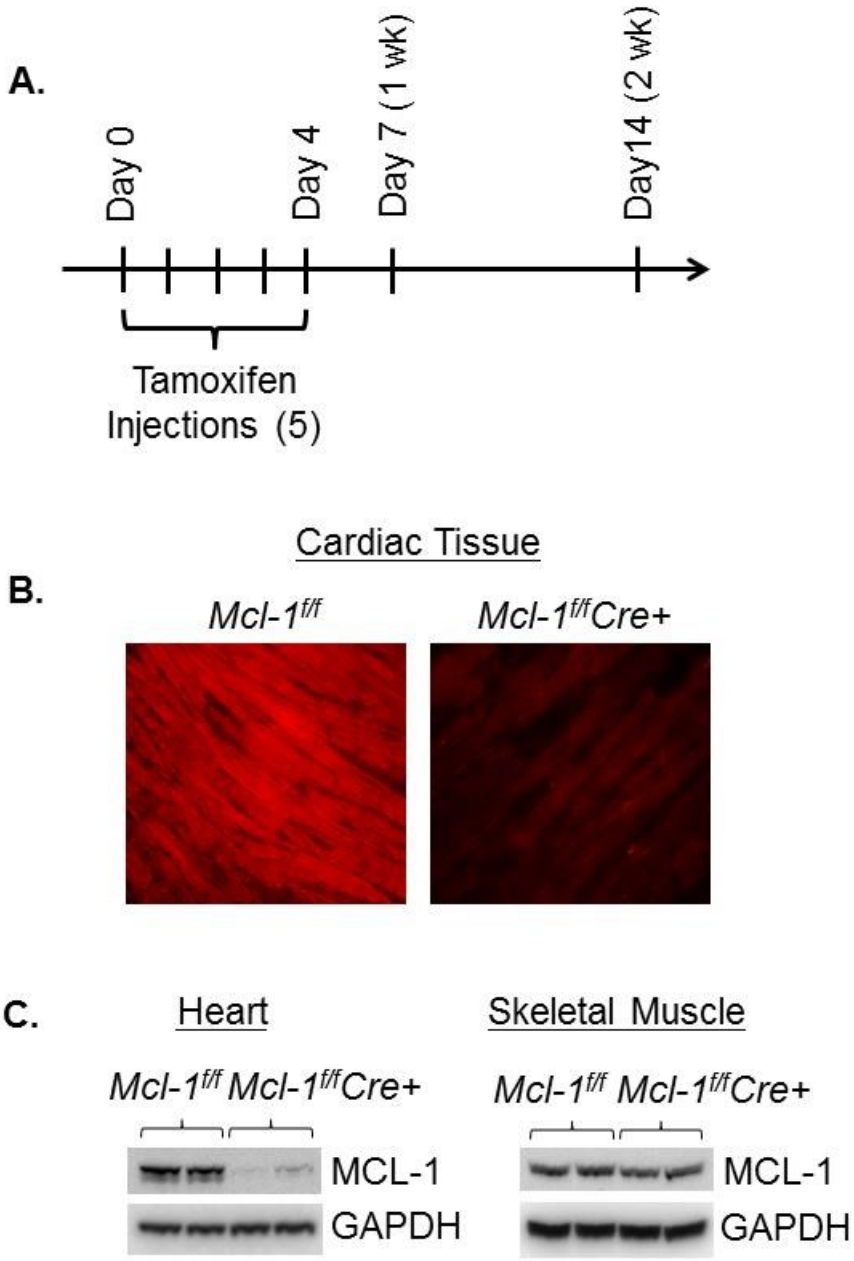

Figure 13: Cardiac specific ablation of MCL-1. **A.** Tamoxifen treatment schedule. **B.** MCL-1 ablation in myocardial tissue sections reduces MCL-1 staining by immunohistochemistry. **C.** Western blot analysis for MCL-1 in heart and skeletal muscle two weeks after initiating tamoxifen treatment demonstrates tissue specific MCL-1 ablation in myocardium from Cre+ mice.

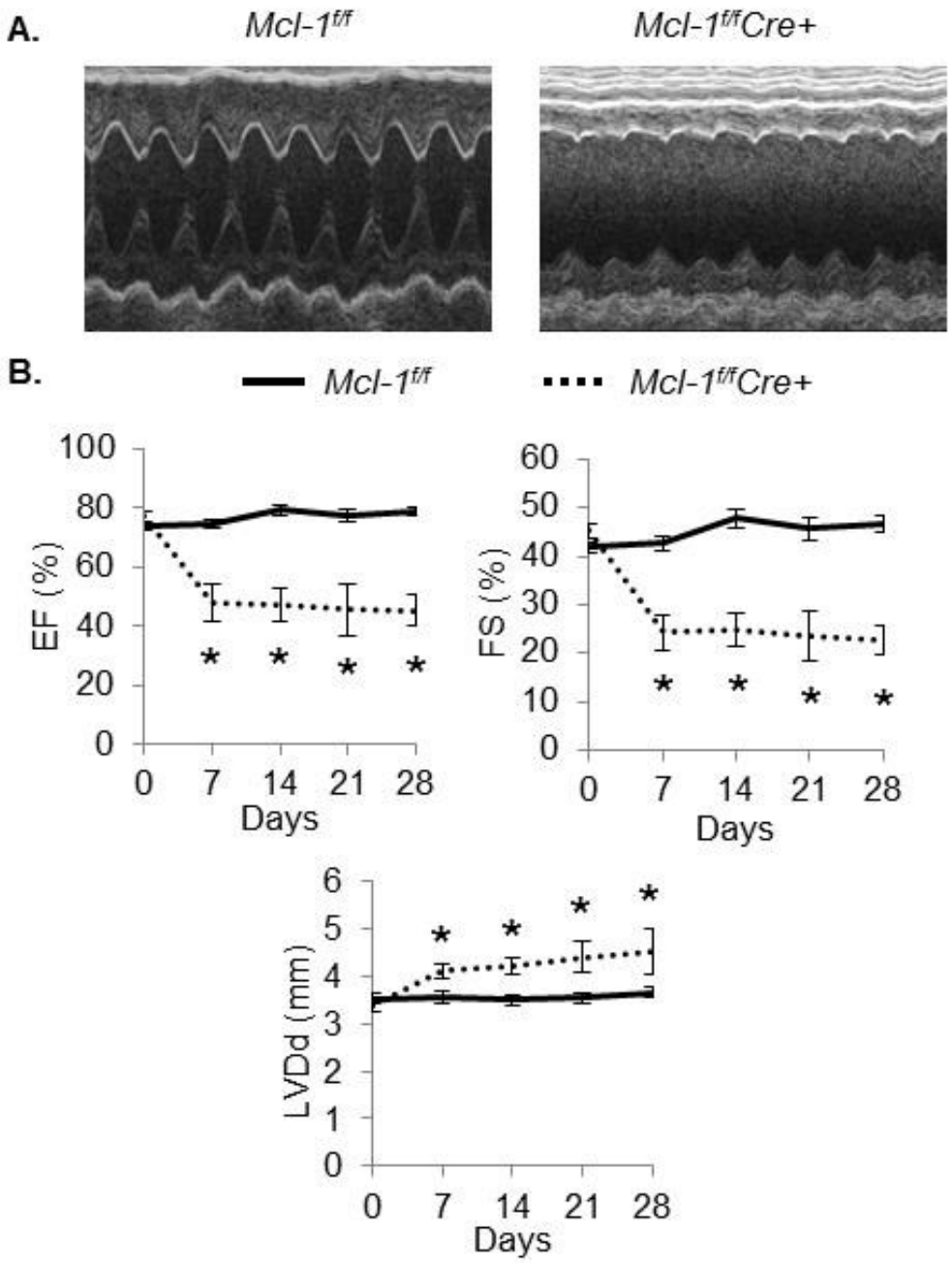

Figure 14: Echocardiography for *Mcl-1$^{f/f}$* and *Mcl-1$^{f/f}$Cre+* mice. **A.** Representative M-Mode echocardiograms at two weeks showed reduced contractile function in *Mcl-1$^{f/f}$Cre+* hearts **B.** Echocardiographic analysis revealed reduced ejection fraction (EF) and fractional shortening (FS) as well as enlarged left ventricular diastolic dimension (LVDd) in *Mcl-1$^{f/f}$Cre+* mice (n = 5–14, *p<0.05).

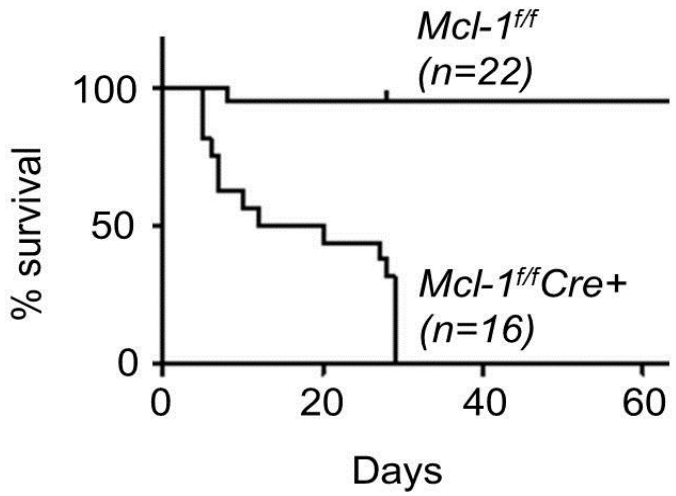

Figure 15: Kaplan-Meyer analysis for *Mcl-1$^{f/f}$* and *Mcl-1$^{f/f}$Cre+* mice. Survival is significantly reduced in *Mcl-1$^{f/f}$Cre+* mice compared to *Mcl-1$^{f/f}$* controls ($p<0.05$). Median survival for *Mcl-1$^{f/f}$Cre+* mice = 16 days after initiating tamoxifen treatment.

Table 1: Echocardiography data for *Mcl-1*$^{WT/WT}$*Cre*+ control mice. Activation of Cre by tamoxifen does not lead to cardiac impairment in the absence of floxed *Mcl-1* alleles.

	Week 0	Week 2	Week 4
EF (%)	79.59 ± 2.02	77.09 ± 4.69	79.83 ± 4.21
FS (%)	47.47 ± 1.91	46.16 ± 3.95	48.35 ± 3.74
LVDd (mm)	3.50 ± 0.14	3.88 ± 0.41	3.71 ± 0.31

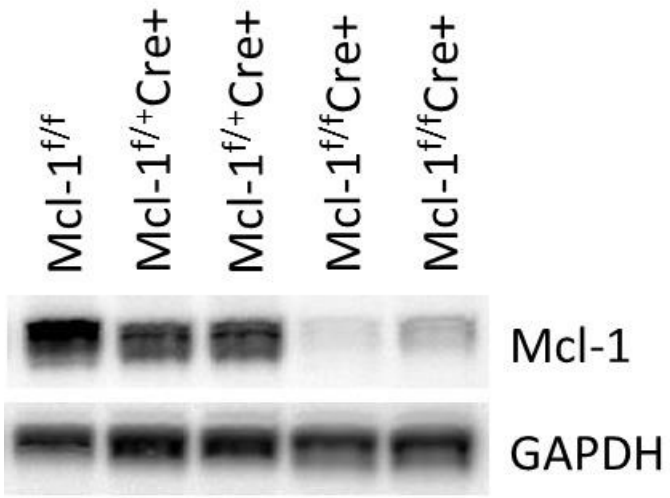

Figure 16: Western blot for heterozygous MCL-1 ablation. Intermediate MCL-1 levels persist in heterozygote floxed MCL-1 heart tissue despite extended tamoxifen treatment (10 doses) over two weeks.

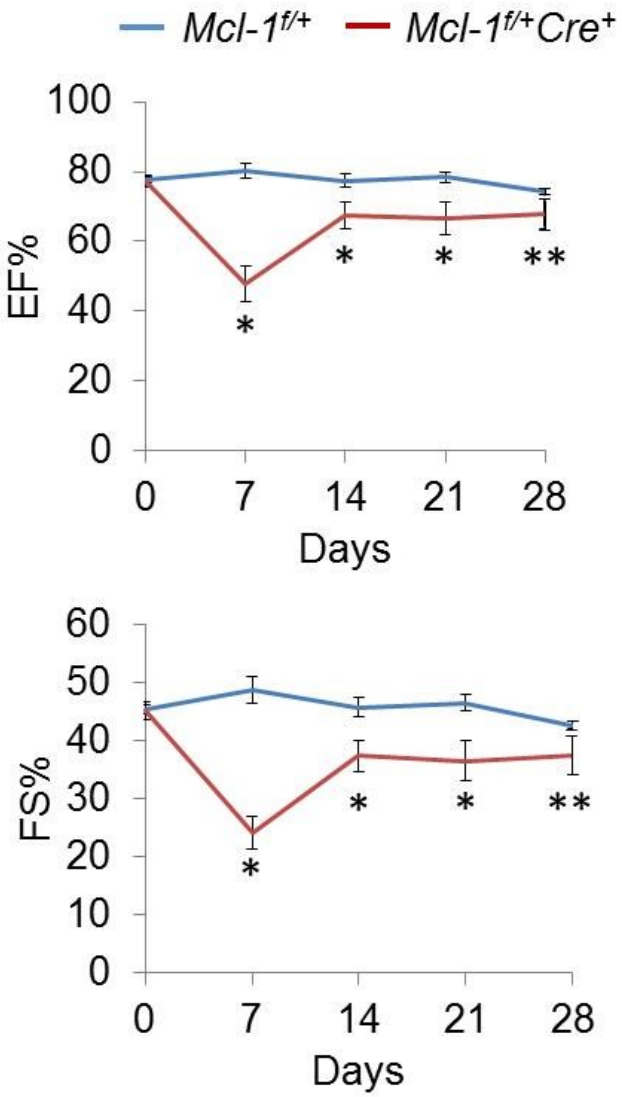

Figure 17: Echocardiography in *Mcl-1*$^{f/+}$ and *Mcl-1*$^{f/+}$*Cre*+ heterozygous mice. Partial ablation of MCL-1 in heterozygotes leads to temporary cardiac impairment followed by functional recovery. Heterozygotes in this experiment received the standard 5-dose tamoxifen treatment (n = 4-10, *p<0.05, **p>0.05).

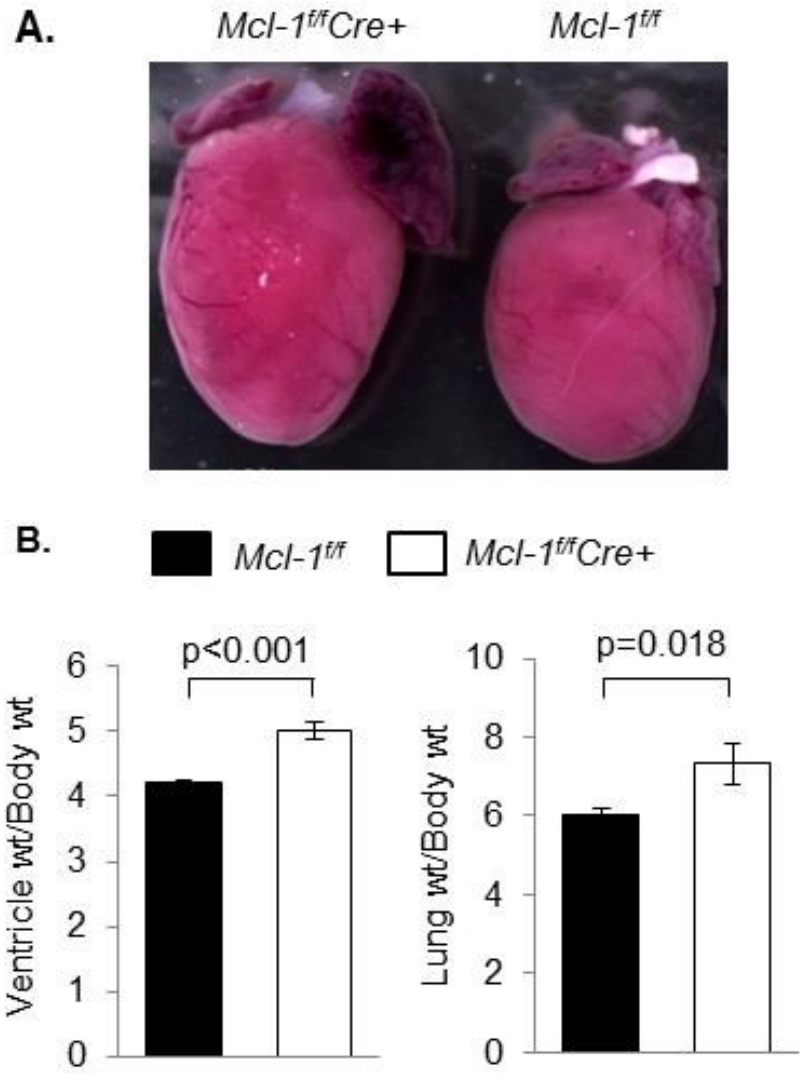

Figure 18: Ablation of MCL-1 leads to cardiac hypertrophy and pulmonary edema. **A.** *Mcl-1$^{f/f}$Cre+* hearts are enlarged on gross morphology one week after initiating tamoxifen treatment. **B.** Ventricle weight and lung weight to body weight ratios from *Mcl-1$^{f/f}$* and *Mcl-1$^{f/f}$Cre+* mice two weeks after tamoxifen treatment (n = 15–17).

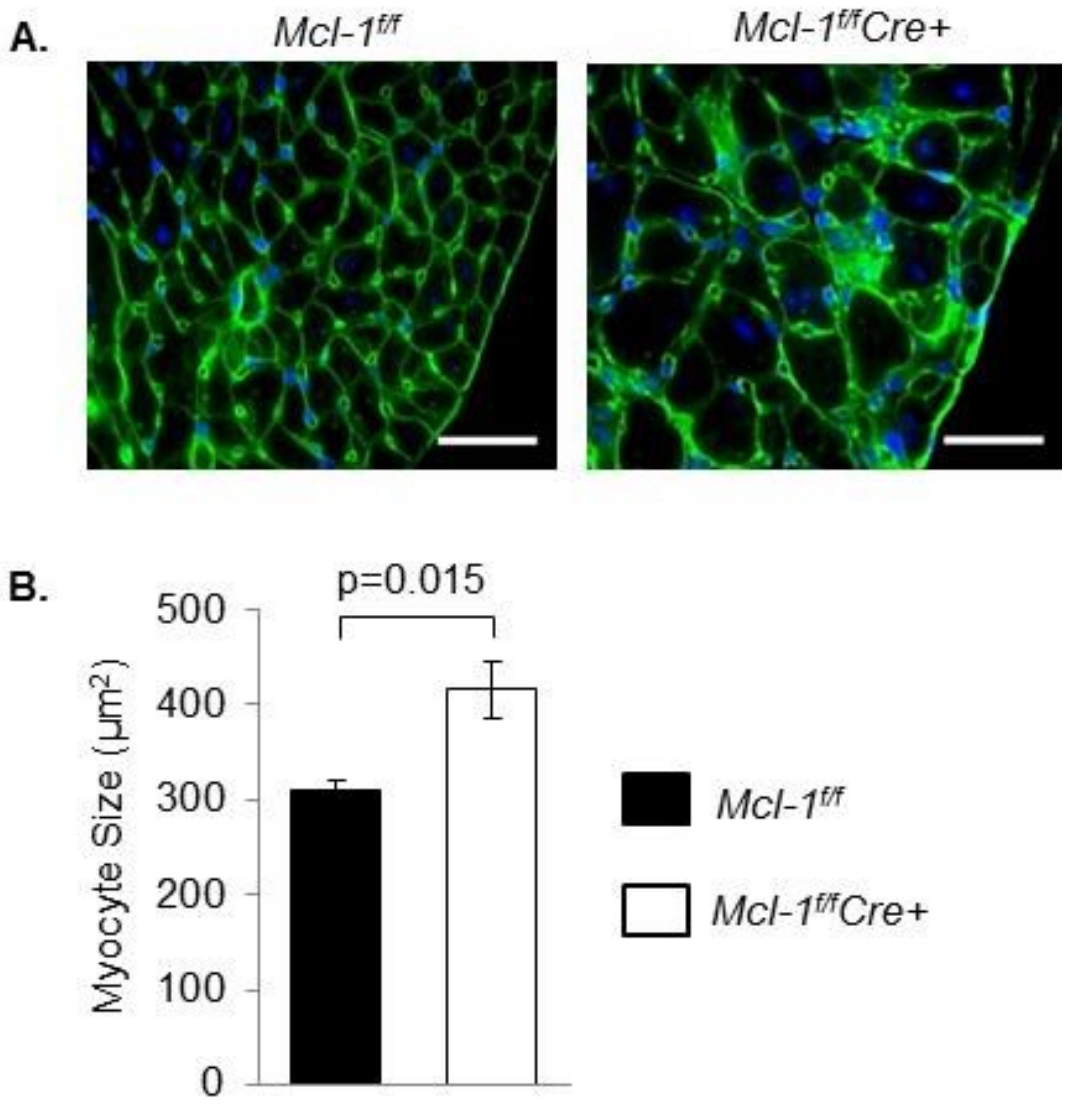

Figure 19: Myocyte cross-sectional area in *Mcl-1$^{f/f}$* and *Mcl-1$^{f/f}$Cre+* hearts **A.** Representative images of wheat germ agglutinin (WGA) staining two weeks after initiating tamoxifen treatment. (scale bar = 35 μm). **B.** Quantitation of myocyte cross-sectional area (n = 4) two weeks after tamoxifen treatment.

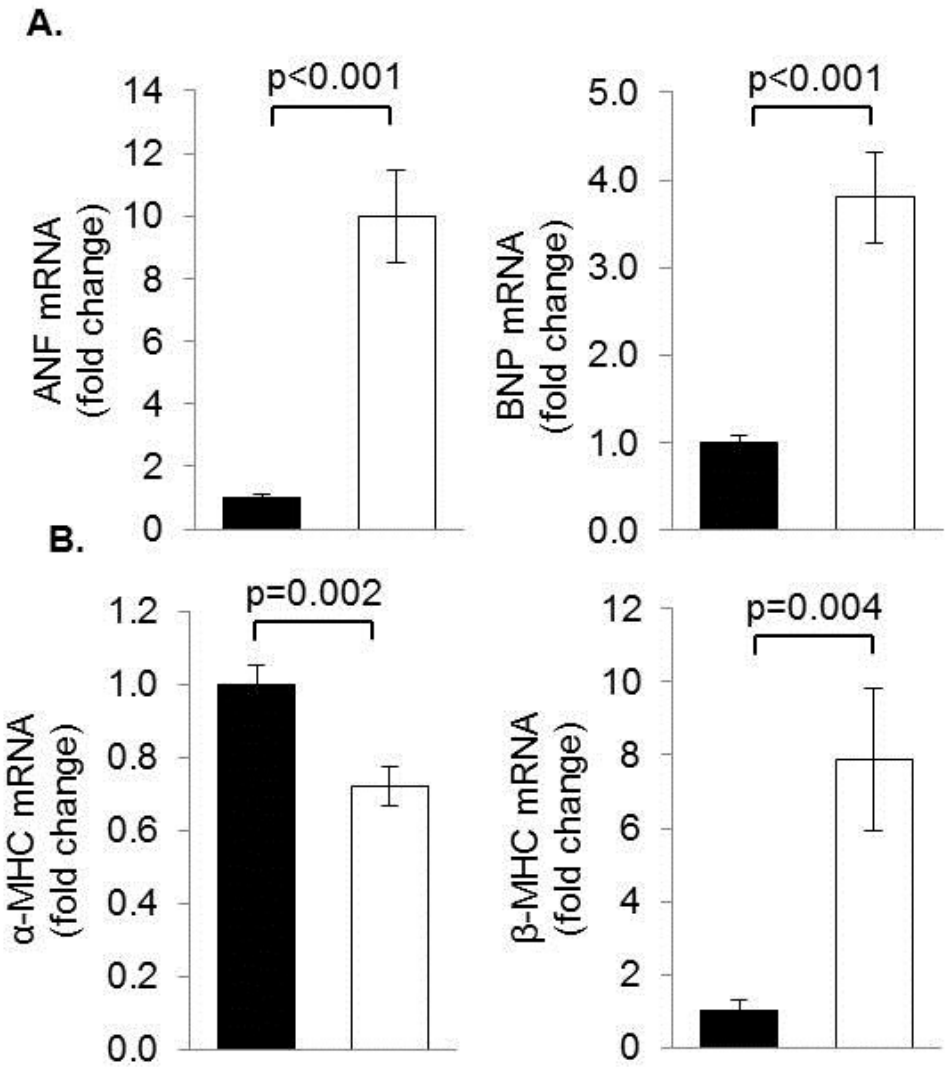

Figure 20: Analysis of hypertrophy markers by qPCR at two weeks. **A.** ANF and BNP mRNA are significantly elevated in *Mcl-1$^{f/f}$Cre+* hearts (n = 9–10). **B.** MHC isotype switching occurs in *Mcl-1$^{f/f}$Cre+* hearts two weeks after initiating tamoxifen treatment (n = 9–10).

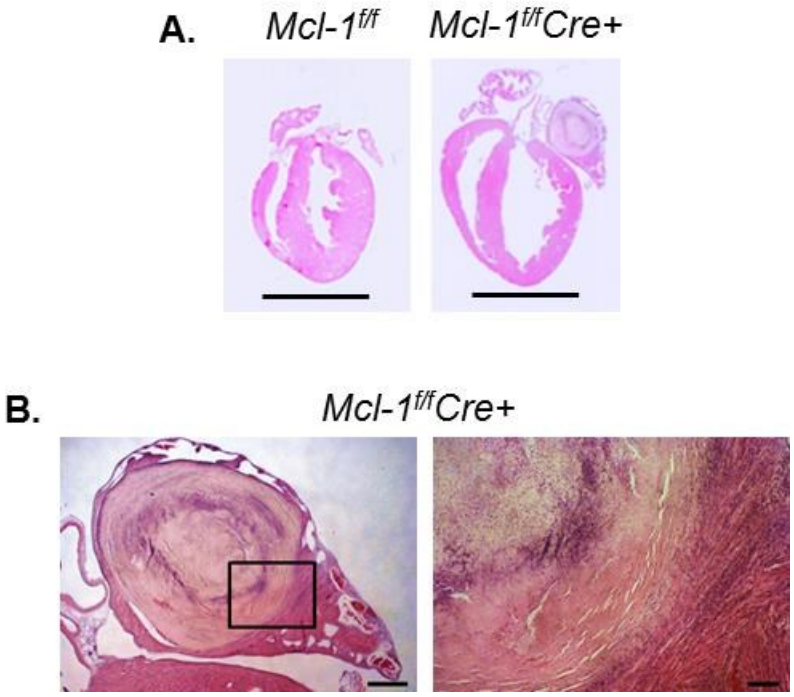

Figure 21: Ablation of MCL-1 leads to ventricular dilatation, atrial thrombosis, and myocyte disorganization. **A.** H&E staining shows thinning of the left ventricular wall in *Mcl-1$^{f/f}$Cre+* hearts two weeks after initiating tamoxifen treatment (scale bar = 5 mm). **B.** Left atrial thrombus in the *Mcl-1$^{f/f}$Cre+* heart (scale bars: left = 500 mm; right = 100 mm).

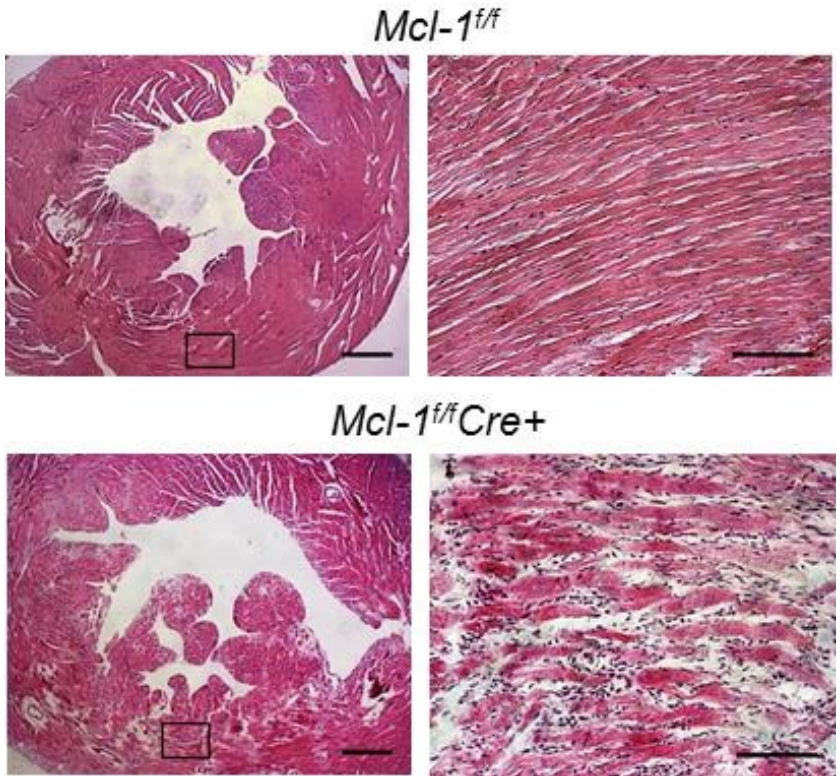

Figure 22: H&E staining in *Mcl-1$^{f/f}$* and *Mcl-1$^{f/f}$Cre+* hearts. Representative sections show marked myocyte disorganization and degeneration in *Mcl-1$^{f/f}$Cre+* hearts two weeks after initiating tamoxifen treatment (scale bars: left = 500 mm, right = 100 mm).

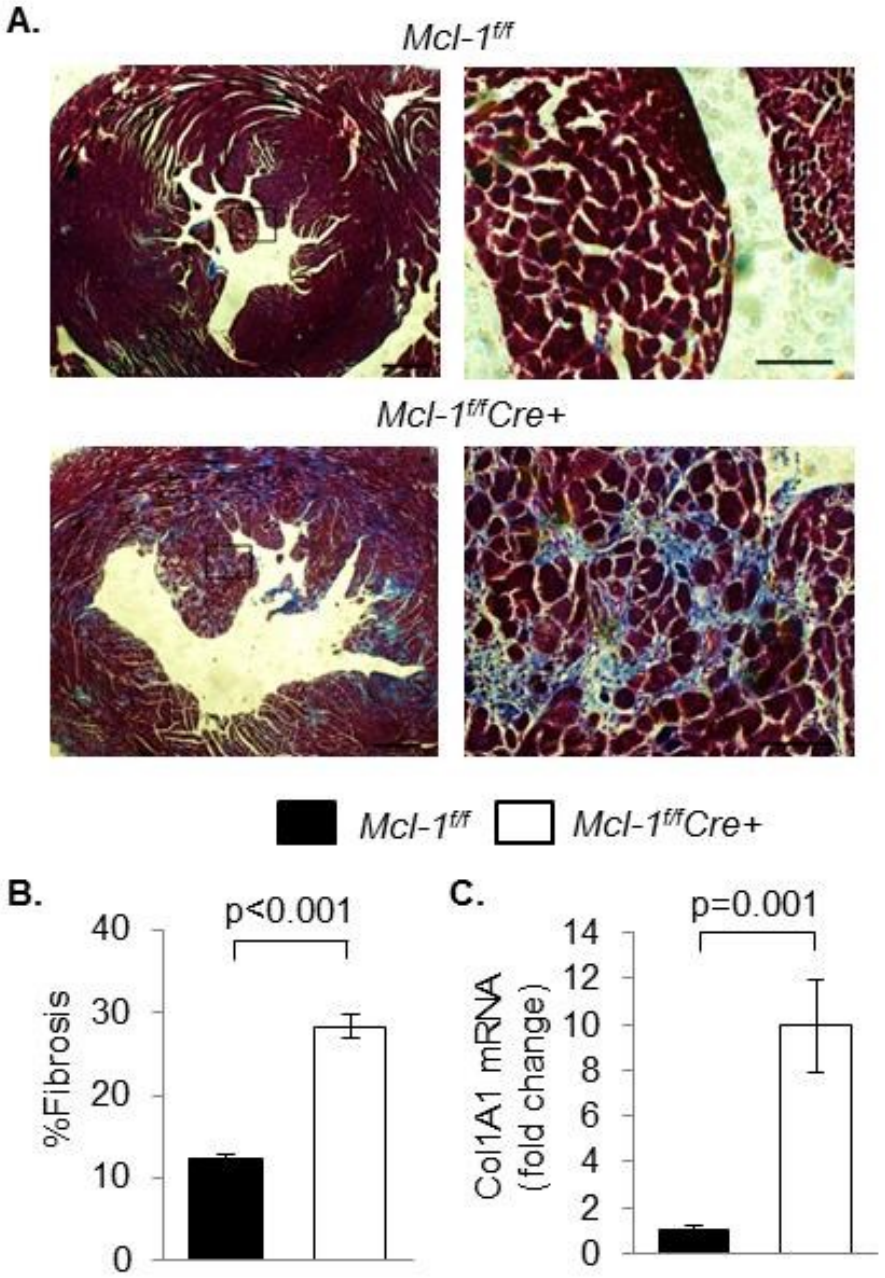

Figure 23: Fibrosis in MCL-1 deficient hearts. **A.** Representative sections stained with Masson's trichrome reveal extensive fibrosis in the left ventricle (LV) of *Mcl-1$^{f/f}$Cre+* hearts two weeks after initiating tamoxifen treatment (scale bars: left = 500 mm, right = 100 mm). **B.** Quantitation of fibrosis (n = 3) at two weeks. **C.** qPCR analysis of Col1A1 mRNA levels at two weeks (n = 9–10).

Chapter 4: The role of apoptosis and necrosis in MCL-1 deficiency

Introduction

Loss of anti-apoptotic proteins such as BCL-2 typically leads to increased apoptosis (Veis *et al.*, 1993). Similarly, the loss of MCL-1 has been shown to increase apoptosis in lymphoid cells (Opferman *et al.*, 2003). The relationship between MCL-1 and apoptosis in other cell types, however, varies remarkably. Rinkenberger, et. al found no increase in apoptosis in *Mcl-1* null embryos (Rinkenberger *et al.*, 2000). More recently, Germain *et al.* (2011) demonstrated that MCL-1 ablation activates very little apoptosis in cortical neurons. In fact, these studies found that apoptosis in the setting of MCL-1 deficiency often requires a second apoptotic stimulus.

In this chapter, I present data that addresses the mechanism of myocyte death in MCL-1 deficient hearts. I investigated activation of apoptosis and necrosis because both pathways have been implicated in the loss of myocytes during cardiac injury and heart failure (Foo *et al.,* 2005, Baines *et al.*, 2005, Nakayama, *et al.*, 2007). In MCL-1 deficient hearts, I found no evidence of increased apoptosis, but I observed several characteristic signs of cardiac necrosis including mitochondrial swelling, release of lactate dehydrogenase from ruptured myocytes, and extensive tissue inflammation. Necrosis is associated with mitochondrial permeability transition pore (mPTP) opening, which can be antagonized by deleting cyclophilin D (Baines *et al.*,

2005). To evaluate the role of mPTP opening in MCL-1 deficient cardiac myocytes, I generated *Ppif*$^{-/-}$*Mcl-1*$^{flox/flox}$*Cre*+ double knockout mice. I found that cyclophilin D ablation does not rescue the *Mcl-1* knockout phenotype but delays progression of heart failure and prolongs survival.

A. MCL-1 deficiency does not activate apoptosis

Since MCL-1 is an anti-apoptotic protein, I investigated whether apoptosis of myocytes contributed to damage in MCL-1-deficient hearts. Activation of apoptosis was assessed by terminal deoxynucleotidyl transferase UTP nick-end labeling (TUNEL) and immunostaining for cleaved (active) caspase-3 in heart sections at one and two week time points (Figure 24,25). Several apoptotic initiation pathways converge on caspase-3, an effector caspase that initiates the execution phase of apoptosis. During this terminal phase, cleaved-caspase-3 activates endonucleases and proteases that carry out nuclear fragmentation and cytoskeleton disassembly (Taylor *et al.*, 2008; Parrish *et al.*, 2013). Surprisingly, the number of TUNEL positive nuclei and myocytes positive for cleaved caspase-3 was not significantly increased at either time point after deletion of MCL-1. Since low-level apoptosis can still cause extensive damage in terminally differentiated organs such as the heart (Wencker *et al.*, 2003), I employed several additional techniques to rule out apoptotic activation in *Mcl-1*$^{f/f}$*Cre*+ hearts.

To determine whether the loss of MCL-1 activates terminal apoptosis in *Mcl-1*$^{f/f}$*Cre*+ hearts, I measured caspase-3 activity and cleaved-caspase-3 protein levels in cardiac tissue samples. Fluoresecent substrate processing (Figure 26A) and cleaved caspase-3 expression (Figure 26B) were not elevated in *Mcl-1*$^{f/f}$*Cre*+ hearts.

Poly-ADP-ribose-polymerase (PARP) is a nuclear DNA repair protein that is cleaved into characteristic 89 and 24 kDa fragments during apoptosis (Soldani *et al.*, 2001). I did not detect an increase in PARP cleavage in *Mcl-1*$^{f/f}$*Cre*+ heart lysates at one or two week time points (Figure 27A). I also fractionated cardiac lysates to look for evidence of apoptosis inducing factor (AIF) translocation. In response to proapoptotic stimuli, AIF is released from mitochondria and translocates to the nucleus where it causes caspase-independent cell death (Susin *et al.*, 1999). MCL-1-deficient hearts did not exhibit AIF release from mitochondria or increased levels of AIF in the nucleus (Figure 27B). Taken together, these data demonstrate that enhanced apoptosis is not a significant contributor to the cardiac damage observed in MCL-1-deficient hearts.

Cell susceptibility to apoptosis depends on a balance between anti-apoptotic and pro-apoptotic proteins (Korsmeyer *et al.*, 1993). To address the seemingly paradoxical lack of apoptosis in MCL-1 deficient hearts, I quantified other BCL-2 family proteins in cardiac lysates from *Mcl-1*$^{f/f}$ and *Mcl-1*$^{f/f}$*Cre*+ hearts. I found that BCL-2 and BCL-X_L were significantly upregulated upon

deletion of MCL-1 (Figure 28A,B). Overexpression of BCL-2 or BCL-X_L has been shown to rescue MCL-1 deficient myeloid cells from apoptosis (Glaser *et al.*, 2012), and MCL-1 deficient hearts may upregulate these other anti-apoptotic proteins as a compensatory mechanism. Pro-apoptotic BAX was also upregulated in *Mcl-1$^{f/f}$Cre+* hearts after tamoxifen treatment, but the BCL-2/BAX ratio was not altered (Figure 28C). MCL-1 is known to interact with the BH3-only proteins BIM and NOXA, preventing them from activating apoptosis. Translocation of these protiens to mitochondria has been shown to activate MOMP and apoptosis (Han *et al.*, 2007; Tong *et al.*, 2005). Despite the loss of MCL-1, the levels of these proteins at the mitochondria did not increase. Similarly, the loss of MCL-1 did not change the level of the BH3-only protein BNIP3 (Figure 29). In summary, in response to loss of MCL-1, the myocardium upregulates other anti-apoptotic proteins, preserves the BCL-2/BAX balance, and avoids translocation of BH3-only proteins to mitochondria. These changes provide an explanation for the lack of apoptosis in MCL-1 deficient hearts, but they do not account for the loss of myocytes.

B. Loss of MCL-1 in myocytes leads to mitochondrial swelling, permeability transition, and necrosis with LDH release and inflammation

The lack of apoptosis in MCL-1 deficient hearts suggested that myocytes were dying by another mechanism. To elucidate this process, I examined cardiac ultrastructure using transmission electron microscopy (TEM)

images from MCL-1-deficient hearts. Mitochondria in *Mcl-1*$^{f/f}$*Cre*+ myocytes exhibited signs of extensive damage one week after tamoxifen administration including swelling and outer membrane rupture (Figure 30A). Outer membrane rupture indicates that these mitochondria had undergone opening of the mitochondrial permeability transition pore (mPTP), a prominent feature in necrotic cell death. Other signs of necrosis included the presence of cellular debris in the extracellular space from ruptured myocytes and the presence of infiltrating inflammatory cells. In addition to ultrastructural evidence for cardiac injury and myocyte death, circulating lactate dehydrogenase (LDH) activity increased significantly in *Mcl-1*$^{f/f}$*Cre*+ mice (Figure 30B). LDH is a cytosolic enzyme that is released when cells rupture, and it previously served as a clinical biomarker for cardiac injury (Aldous, 2013). Increased circulating LDH indicates that the loss of MCL-1 leads to myocyte rupture. In addition, MCL-1 deficiency led to increased myocardial inflammation. *Mcl-1*$^{f/f}$*Cre*+ hearts exhibited increased CD45+ staining consistent with leukocyte infiltration (Figure 31A) and elevated inflammation markers by qPCR (Figure 31B). These inflammatory cytokines, including TNF-α, IL-6, and TGF-β, are elevated in response to cardiac necrosis during cardiac injury. Although limited inflammation can activate cardioprotective pathways, clear cellular debris, and promote wound healing/stable scar formation, prolonged elevation of these cytokines exacerbates heart failure by inducing hypertrophy, fibrosis, and ventricular dilatation (Gullestad *et al.*, 2012; Frangogiannis, 2012). Taken

together, these findings indicate that myocyte cell death proceeds by necrosis with mPTP opening.

Even unruptured mitochondria in *Mcl-1*$^{f/f}$*Cre*+ hearts appeared fragmented and exhibited extensive swelling and cristae remodeling by TEM. Surprisingly, analysis of mitochondrial fission and fusion proteins in cardiac lysates revealed no changes in MFN1/2, OPA1, FIS1 and DRP-1 levels (Figure 32A,B). Despite extensive mitochondrial fragmentation, I did not detect DRP-1 in the mitochondrial fraction from *Mcl-1*$^{f/f}$*Cre*+ hearts (Figure 32C). Lack of DRP-1 translocation indicates that conventional mitochondrial fission was not activated. Co-immunoprecipitation (COIP) of MCL-1 in cardiac lysates showed that MCL-1 and DRP-1 interact (Figure 33A), and this interaction is enhanced by stress in cardiomyocytes (Figure 33B,C). Thus it is possible that loss of MCL-1 at cardiac mitochondria may impair normal DRP-1 recruitment, leading to aberrant mitochondrial dynamics.

Mitochondrial integrity and permeability transition can be evaluated *in vitro* by subjecting isolated mitochondria to exogenous calcium stress. In the myocardium, mitochondria normally buffer calcium fluxes, and [Ca^{2+}] in the mitochondrial matrix couples respiration with metabolic demand. In contrast, calcium overload in response to stress such as ischemia/reperfusion injury leads to mPTP opening, mitochondrial swelling, and necrosis (Gustafsson & Gottlieb, 2008). Mitochondrial swelling assays (expressed as absorbance at 520nm) confirmed that isolated MCL-1-deficient cardiac mitochondria were

swollen at baseline and exhibited modest calcium-induced swelling compared to wild type cardiac mitochondria (Figure 34). Interestingly, the mPTP inhibitor cyclosporine A initially blocked Ca^{2+}-mediated swelling in MCL-1-deficient mitochondria but after 15 min, it was no longer effective in preventing swelling. These results suggest that MCL-1-deficient mitochondria can swell independently of mPTP opening. Moreover, addition of recombinant MCL-1 to mitochondria isolated from *Mcl-1*$^{f/f}$*Cre+* hearts did not reduce baseline swelling and had no effect on Ca^{2+}-mediated swelling, suggesting that MCL-1 is not a direct regulator of the mPTP (Figure 35).

In addition to baseline swelling, mitochondria from *Mcl-1*$^{f/f}$*Cre+* hearts exhibited impaired respiration and ETC complex activity one week after tamoxifen treatment. Respiration was quantified by measuring oxygen consumption in isolated mitochondria. State 3 respiration refers to functional oxygen consumption during mitochondrial ATP production, state 4 addresses “leak” consumption that takes place when ATP production is blocked/stopped, and FCCP uncoupled respiration provides a measure of maximal respiratory capacity in the absence of a proton gradient. The respiratory control ratio (RCR) measures how tightly oxygen consumption and ATP production are coupled in mitochondria, and healthy mitochondria exhibit higher RCR values. Mitochondria isolated from *Mcl-1*$^{f/f}$*Cre+* hearts had reduced respiration rates compared to *Mcl-1*$^{f/f}$ (Table 2). There was also a significant reduction in the respiratory control ratio between *Mcl-1*$^{f/f}$ and *Mcl-1*$^{f/f}$*Cre+* mitochondria,

confirming that mitochondria from MCL-1-deficient hearts are dysfunctional. Although mitochondrial respiration was significantly reduced in the knockouts, I expected to observe a much more severe decrease in function. However, this modest decrease is most likely due to selection of healthy mitochondria during the isolation process. Most of the damaged mitochondria may be lost during the isolation process and as a result, the defects in respiration are often underestimated.

To complement oxygen consumption data, the enzyme activities of specific ETC complexes were directly measured by monitoring substrate oxidation or reduction by isolated mitochondria with a spectrophotometer. Analysis of the specific enzyme activities confirmed a ~40% reduction in Complex I and a ~50% reduction in Complex II activities in MCL-1-deficient mitochondria (Figure 36). Together, these data indicate that loss of MCL-1 resulted in impairment of mitochondria, opening of the mPTP, and necrotic cell death.

To further investigate the role of mPTP opening and necrosis in *Mcl-1*$^{f/f}$*Cre*+ hearts, I generated *Ppif*$^{-/-}$*Mcl-1*$^{f/f}$*Cre*+ double knockout mice. *Ppif* encodes for cyclophilin D (CypD), which is an essential component of the mPTP (Baines *et al.*, 2005). I hypothesized that antagonizing pore opening would reduce myocyte death and ameliorate the MCL-1 knockout phenotype. Ejection fraction and fractional shortening in *Ppif*$^{-/-}$*Mcl-1*$^{f/f}$*Cre*+ mice were still significantly reduced compared to *Ppif*$^{-/-}$*Mcl-1*$^{f/f}$ mice one week after tamoxifen

treatment (Figure 37A,B). Cardiac function in *Ppif*$^{-/-}$*Mcl-1*$^{f/f}$*Cre*+ mice, however, was significantly better compared to *Mcl-1*$^{f/f}$*Cre*+ mice at one week (EF=69.24±4.98%*, FS=39.57±3.78%** for *Ppif*$^{-/-}$*Mcl-1*$^{f/f}$*Cre*+ vs. EF=47.54±6.27%, FS=24.31±3.68% for *Mcl-1*$^{f/f}$*Cre*+; *,**p<0.05), but the functional differences between these groups were no longer significant at two weeks (EF=61.81±4.82%$^{\#}$, FS=34.53±3.68%$^{\#\#}$ for *Ppif*$^{-/-}$*Mcl-1*$^{f/f}$*Cre*+ vs. EF=47.31±5.57%, FS=24.78±3.33% for *Mcl-1*$^{f/f}$*Cre*+; $^{\#}$,$^{\#\#}$p>0.05). In addition, CypD deletion delayed cardiac dilatation in MCL-1 deficient mice. LVDd did not increase in *Ppif*$^{-/-}$*Mcl-1*$^{f/f}$*Cre*+ hearts until the fourth week after treatment, at which point LVDd increased significantly compared to *Ppif*$^{-/-}$*Mcl-1*$^{f/f}$ hearts (Figure 37B). Double knockout mice also developed cardiac hypertrophy and pulmonary edema (Figure 38A), but had extended survival (up to 40 days, with median survival = 37 days) compared to *Mcl-1*$^{f/f}$*Cre*+ mice (median survival = 16 days) (Figure 38B). Interestingly, LDH activity in blood was not significantly increased one week after initiating tamoxifen treatment (Figure 39). The LDH data indicates that loss of CypD delays activation of cardiac necrosis in MCL-1 deficient hearts. Histological analysis of H&E stained sections revealed myofibrillar disarray similar to what I observed in *Mcl-1*$^{f/f}$*Cre*+ hearts (Figure 40). Consistent with previous reports (Baines *et al.*, 2005), mitochondria from both *Ppif*$^{-/-}$*Mcl-1*$^{f/f}$ *and Ppif*$^{-/-}$*Mcl-1*$^{f/f}$*Cre*+ hearts were resistant to Ca^{2+}-mediated swelling (Figure 41). Similar to *Mcl-1*$^{f/f}$*Cre*+ mitochondria, *Ppif*$^{-/-}$*Mcl-1*$^{f/f}$*Cre*+ mitochondria were already swollen at baseline, indicating that mitochondrial

swelling occurs even in the absence of a functional mPTP. Next, I investigated if lack of a functional mPTP led to activation of apoptosis upon loss of MCL-1. However, MCL-1 deletion in *Ppif*$^{-/-}$*Mcl-1*$^{f/f}$*Cre*+ mice did not lead to an increase in TUNEL positive myocytes, or detectable levels of cleaved caspase-3 in heart sections (Figures 42,43). Thus, lack of a functional mPTP delays but does not rescue development of heart failure upon loss of MCL-1.

Conclusion

These data demonstrate that the loss of MCL-1 in cardiac myocytes does not activate apoptosis. Instead, MCL-1 deficiency leads to mitochondrial permeability transition and swelling, myocyte rupture with LDH release, and cardiac tissue inflammation. These findings are consistent with myocardial necrosis (Kung, *et al.* 2011, de Haan *et al.*, 2013). In MCL-1 deficient hearts, I observed increased BAX levels, which may drive both apoptosis and necrosis (Whelan *et al*., 2012). In the setting of MCL-1 deficiency, however, overexpression of other anti-apoptotic proteins such as BCL-2 may rescue cells from apoptosis (Glaser *et al*., 2012). BCL-2 upregulation in MCL-1 deficient hearts may prevent apoptosis while allowing necrosis to proceed. Deletion of cyclophilin D did not rescue MCL-1 deficient hearts but delays progression to heart failure and reduces cardiac damage markers. These data indicate that mPTP opening contributes to myocyte death and cardiac dysfunction in MCL-1 deficient mice, but other mechanisms are involved.

Acknowledgements

Chapter 4, in part, is a reprint of the material as it appears in Thomas et al., Genes Dev, 2013. The dissertation author was the primary investigator and author of this paper.

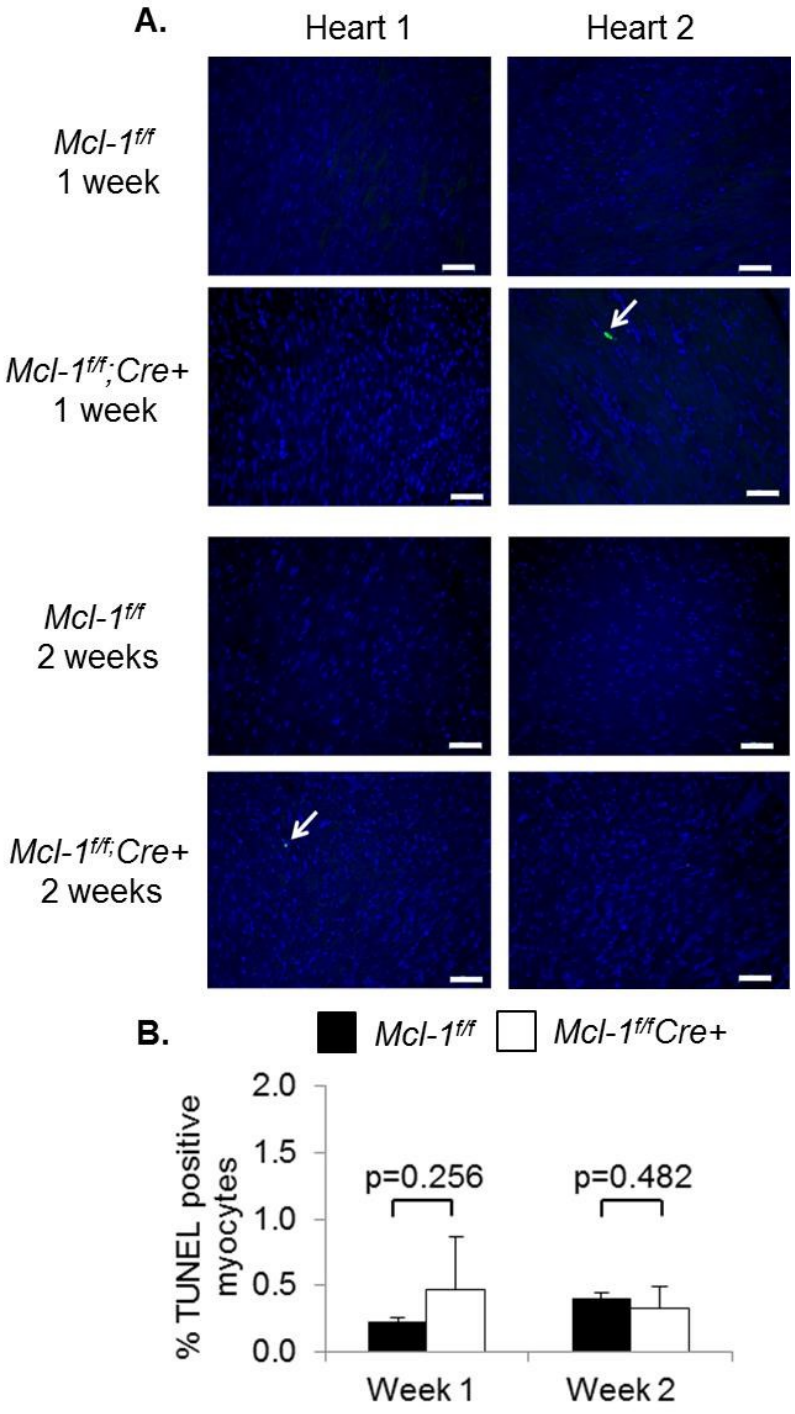

Figure 24: TUNEL staining in *Mcl-1*$^{f/f}$ and *Mcl-1*$^{f/f}$*Cre+* heart sections. Staining shows TUNEL positive cells (green) and nuclei (blue). **A.** Representative images of TUNEL staining from two different hearts at one and two weeks after initiation of tamoxifen injections. Arrows mark TUNEL positive nuclei (scale bar = 50 μm). **B.** Quantitation of TUNEL positive myocytes (n = 3–4).

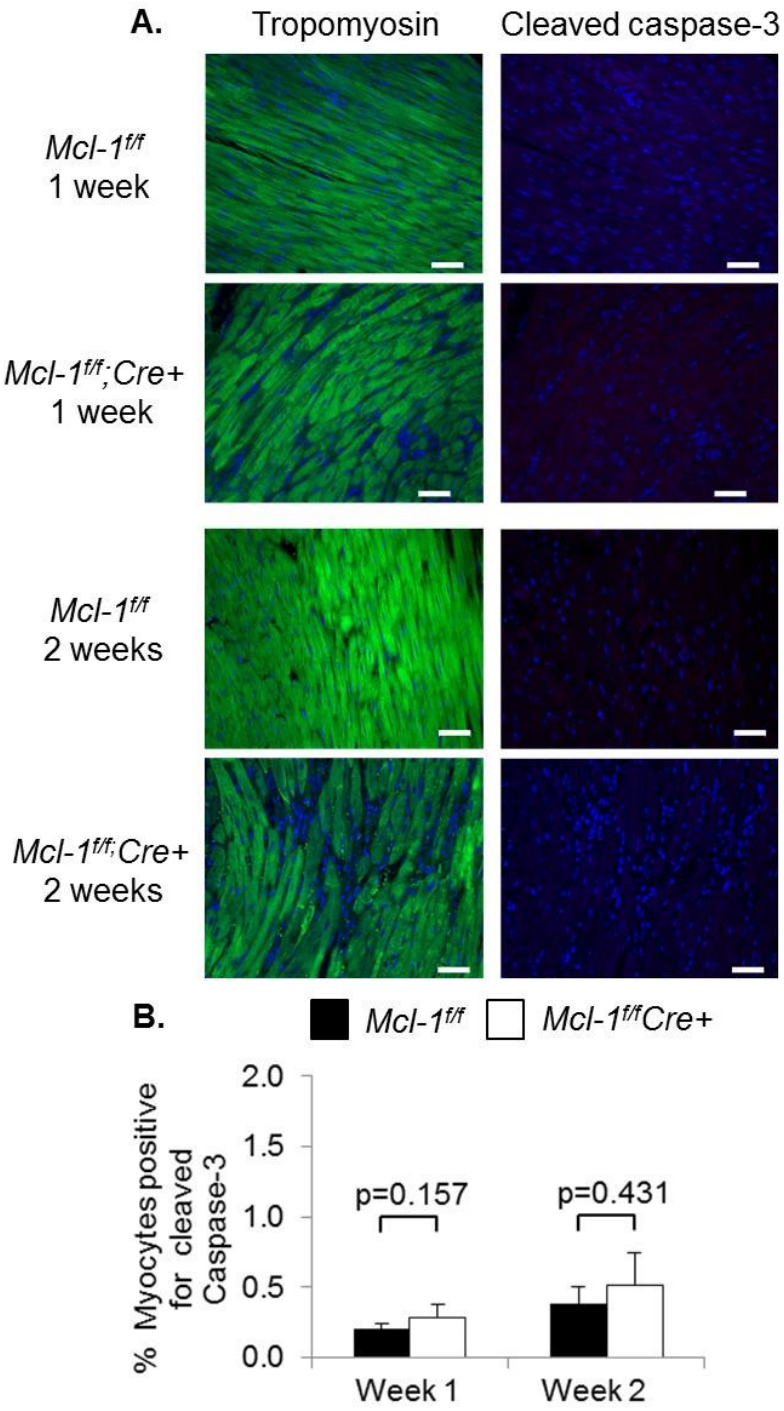

Figure 25: Staining for cleaved caspase-3 in *Mcl-1*$^{f/f}$ and *Mcl-1*$^{f/f}$*Cre+* heart sections. Immunostaining shows tropomyosin (green), cleaved caspase-3 (red), and nuclei (blue). **A.** Representative images of hearts at one and two weeks after initiation of tamoxifen injections (scale bar = 50 μm). **B.** Quantitation of myocytes positive for cleaved caspase-3 (n = 3–4).

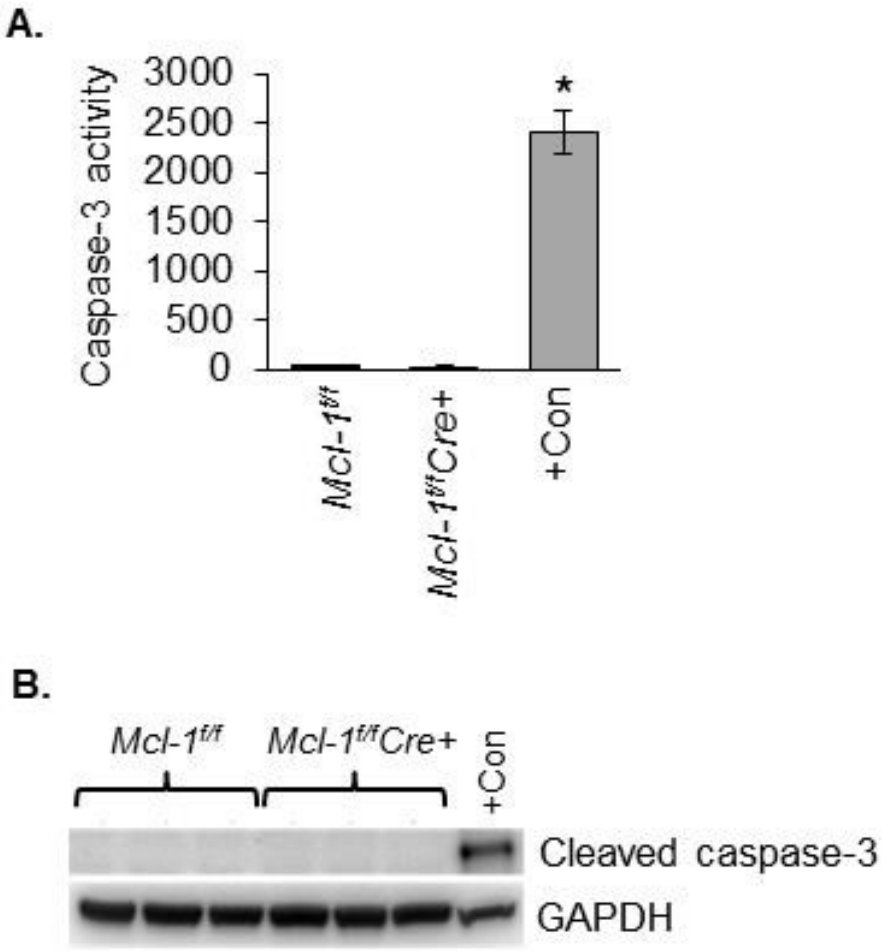

Figure 26: Loss of MCL-1 in myocytes does not activate caspase-3. **A.** Caspase-3 activity assay in heart lysates two weeks after initiating tamoxifen treatment. Positive control consists of HL-60 cells treated with 0.5 mg/mL actinomycin D for 24 hours (n = 3–6, *p<0.001 vs. *Mcl-1$^{f/f}$*). **B.** Representative Western blot for cleaved caspase-3 at two weeks. Positive control consists of HL-1 cells treated with 1 μM staurosporine for eight hours.

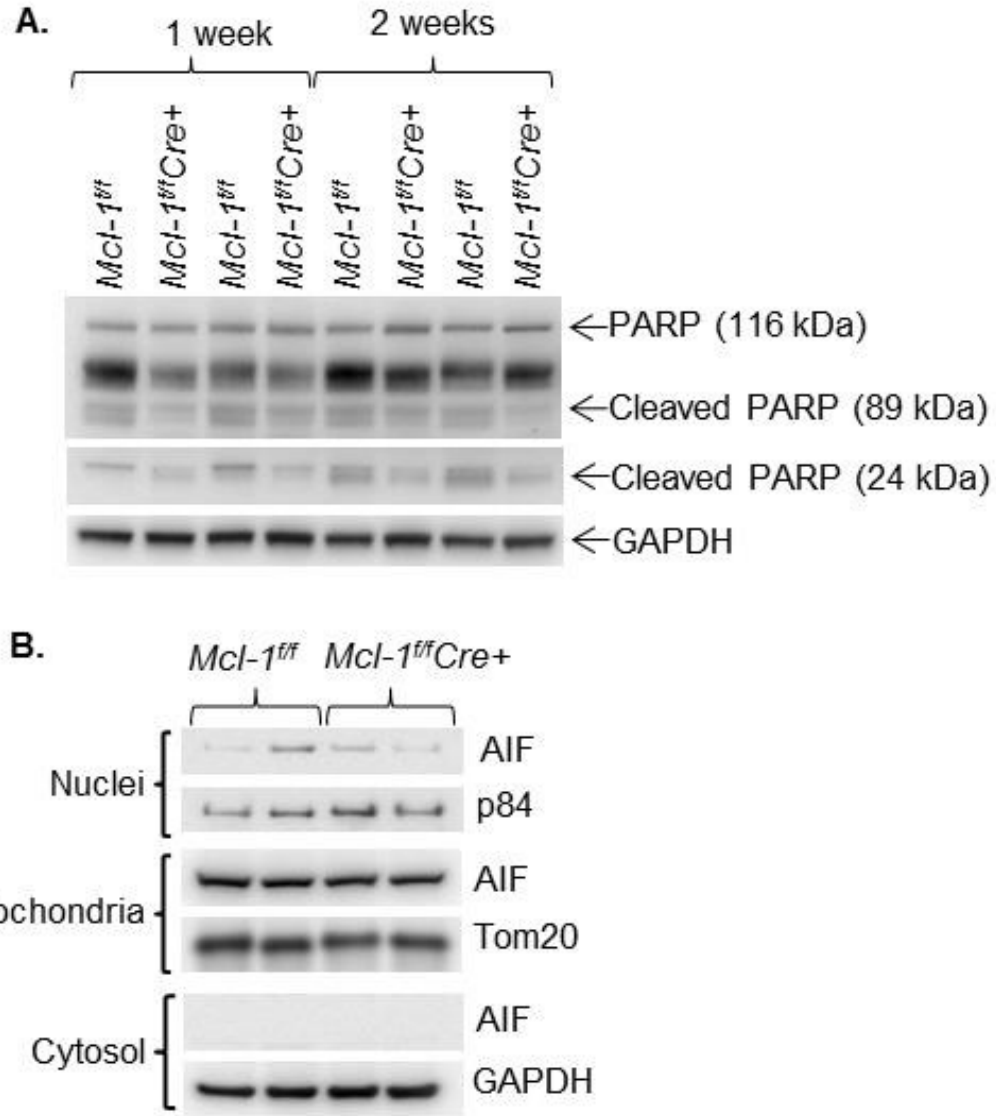

Figure 27: Western blot analysis for apoptotic markers. **A.** Representative Western blot shows that loss of MCL-1 does not activate PARP cleavage. **B.** Western blot analysis of cellular fractionation shows that MCL-1 ablation does not induce AIF translocation to the nucleus two weeks after initiating tamoxifen treatment.

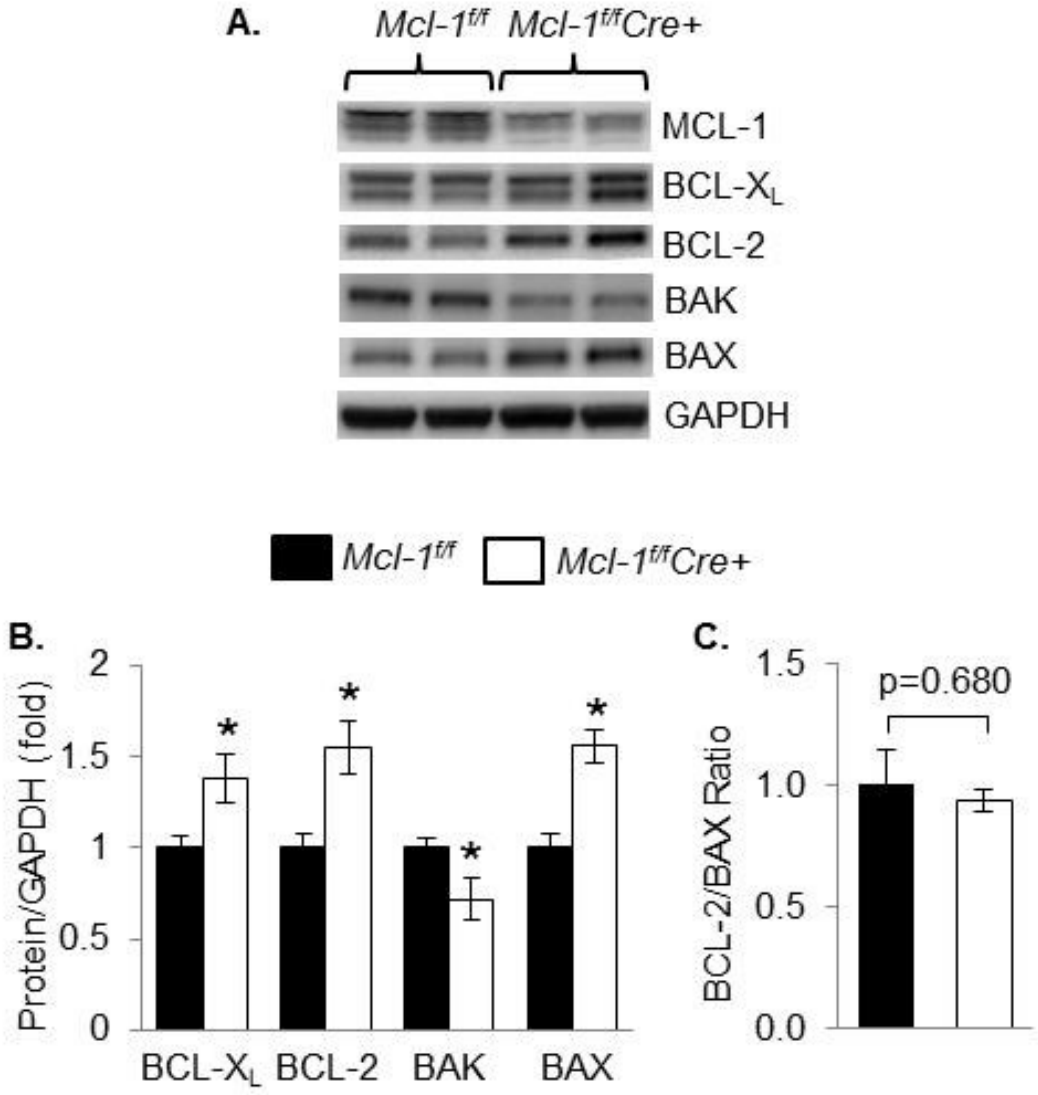

Figure 28: Analysis of BCL-2 family proteins in *Mcl-1$^{f/f}$* and *Mcl-1$^{f/f}$Cre+* hearts. **A.** Representative Western blot shows that loss of MCL-1 leads to upregulation of other anti-apoptotic proteins in cardiac lysates two weeks after initiating tamoxifen treatment. **B.** Quantitation of BCL-2 protein levels (n = 7, *p<0.05 vs. *Mcl-1$^{f/f}$*). **C.** No significant difference in the BCL-2/BAX protein ratio was detected between *Mcl-1$^{f/f}$* and *Mcl-1$^{f/f}$Cre+* hearts by western blot (n = 7).

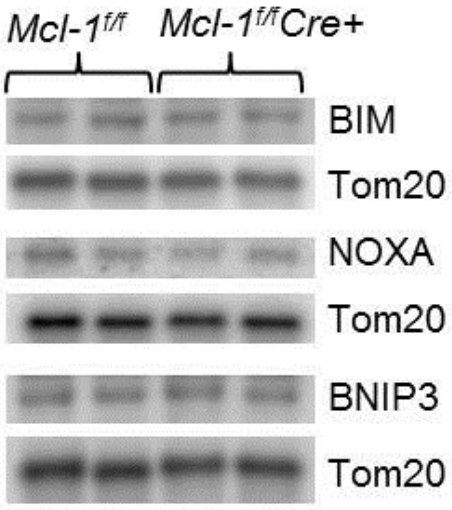

Figure 29: Western blot analysis for BH3-only proteins. Samples consist of mitochondrial fractions from cardiac lysates collected two weeks after initiating tamoxifen treatment. Loss of MCL-1 in cardiac tissue does not alter protein levels of BIM and NOXA, which are binding partners of MCL-1. In addition, MCL-1 deficiency does not change BNIP3 protein levels.

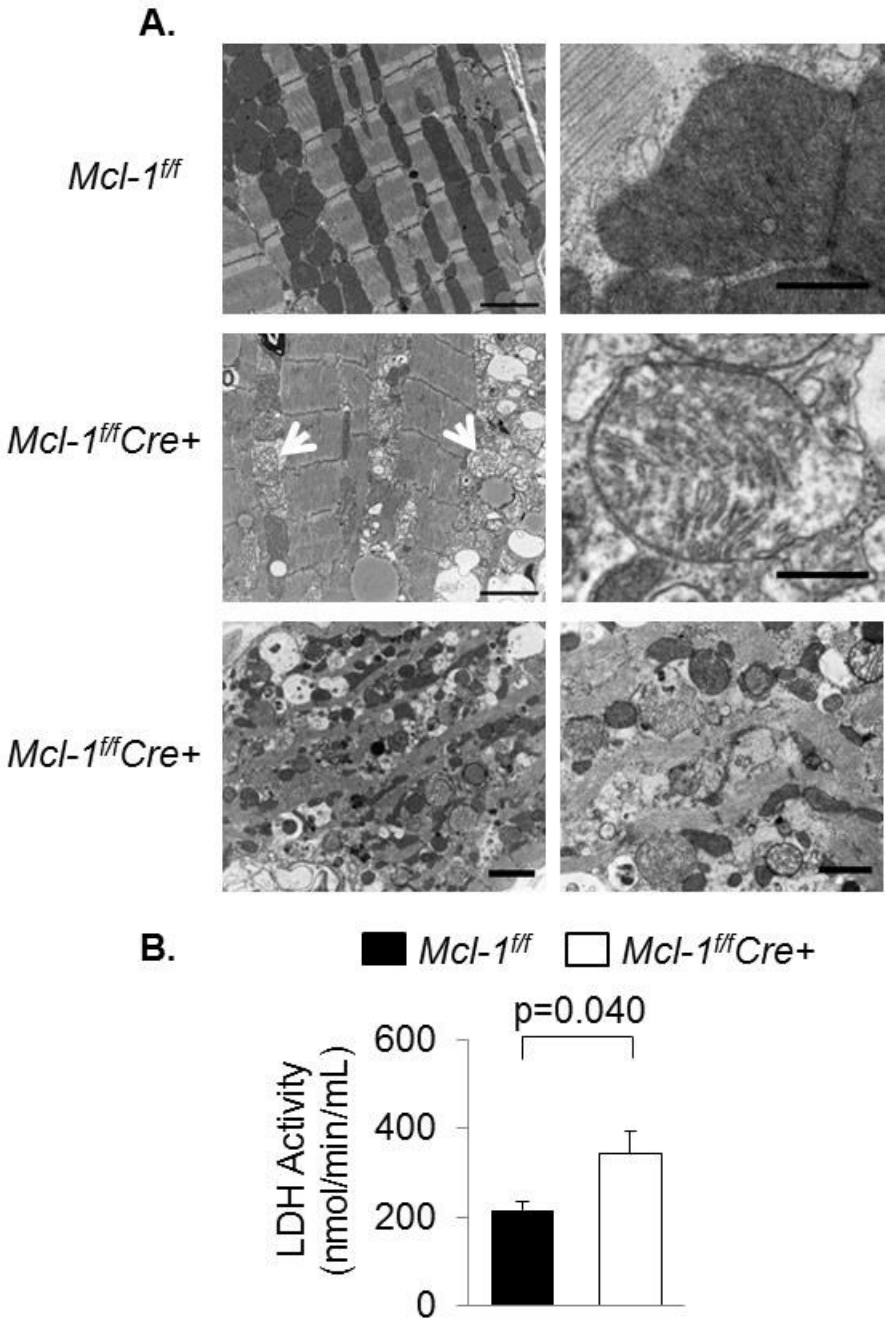

Figure 30: Ablation of MCL-1 leads to degeneration of mitochondria and myocyte rupture. **A.** Ultrastructural images reveal the presence of swollen mitochondria (white arrows) in MCL-1-deficient hearts one week after initiating tamoxifen injections (scale bars: left panels = 2 mm, top and middle right = 0.5 mm; bottom right = 1 mm). **B.** LDH activity in blood at one week (*n* = 5–6). Loss of MCL-1 leads to increased LDH activity in blood samples.

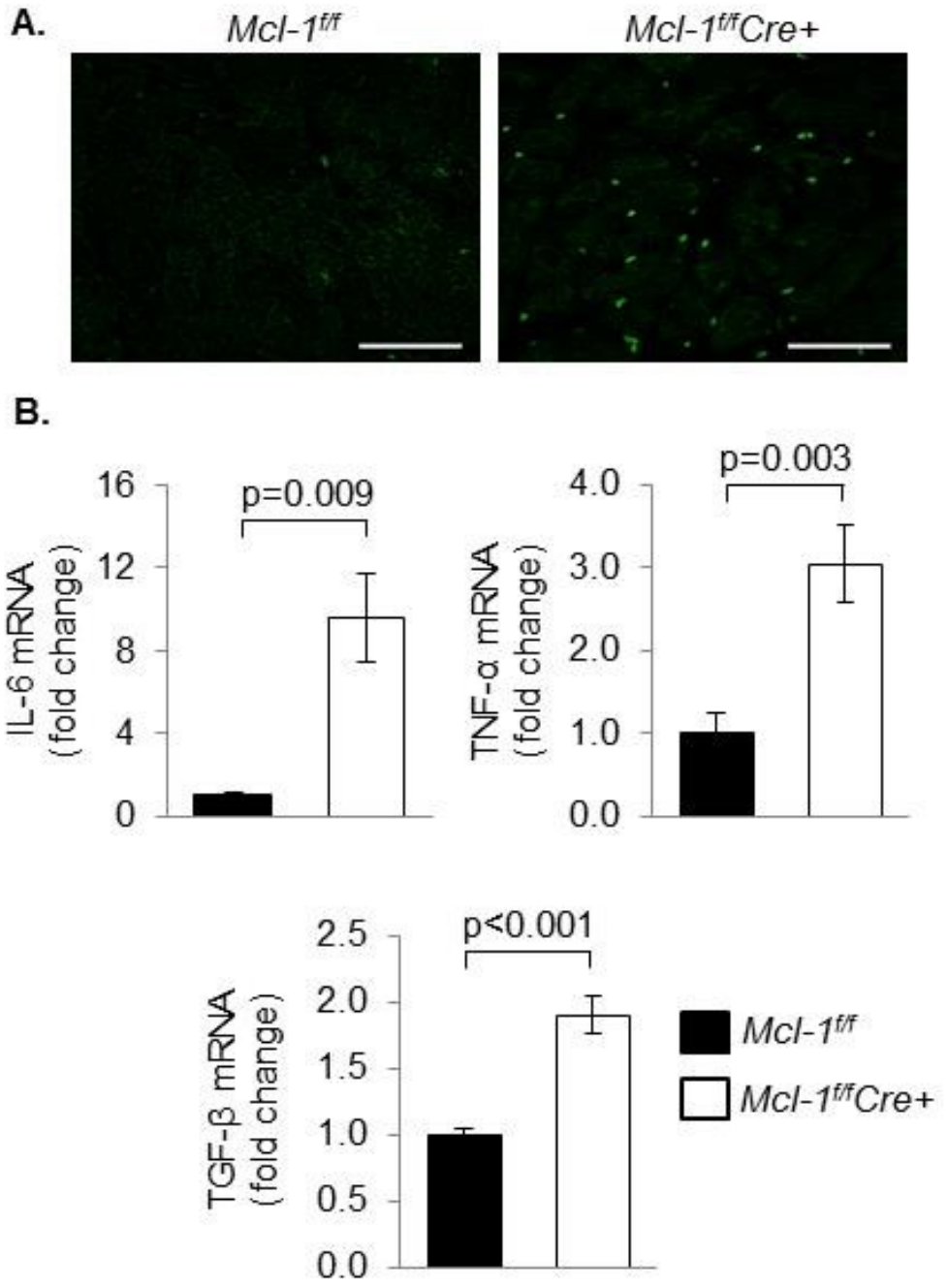

Figure 31: Loss of MCL-1 leads to cardiac inflammation **A.** Representative CD45+ staining in cardiac sections collected two weeks after initiating tamoxifen treatment. Leukocyte infiltration is increased in *Mcl-1$^{f/f}$Cre+* hearts (scale bar = 50 μm). **B.** Analysis of inflammatory markers by qPCR at two weeks (n = 5–8).

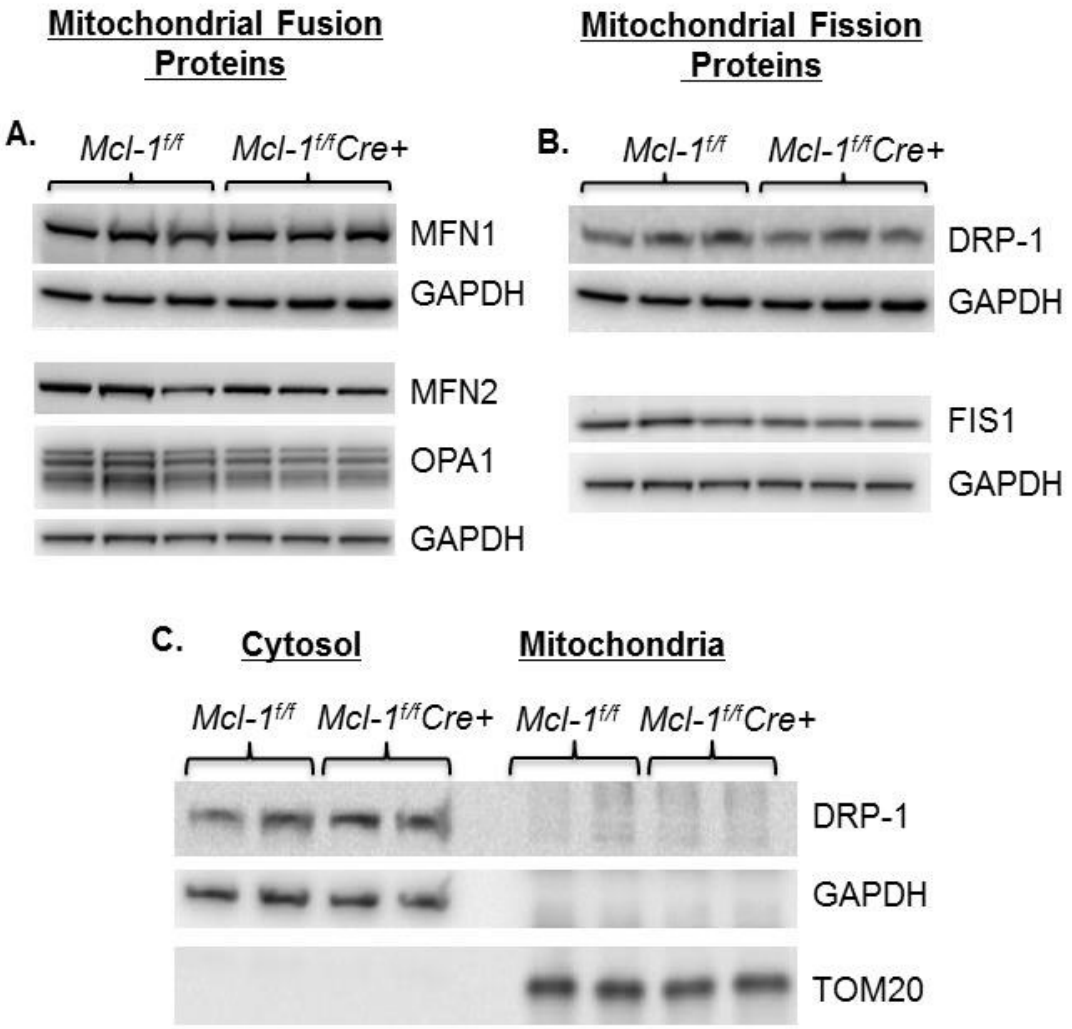

Figure 32: Analysis of mitochondrial fusion and fission proteins in *Mcl-1$^{f/f}$* and *Mcl-1$^{f/f}$Cre*+ hearts. Lysates were prepared from cardiac tissue collected one week after initiating tamoxifen treatment. **A.** Western blot shows no change in mitochondrial fusion protein (MFN1, MFN2, and OPA1) levels. **B.** Western blot shows no change in mitochondrial fission protein (DRP-1 and FIS1) levels. **C.** Western blot analysis of cytosolic and mitochondrial fractions demonstrate that DRP-1 is only detectable in the cytosol.

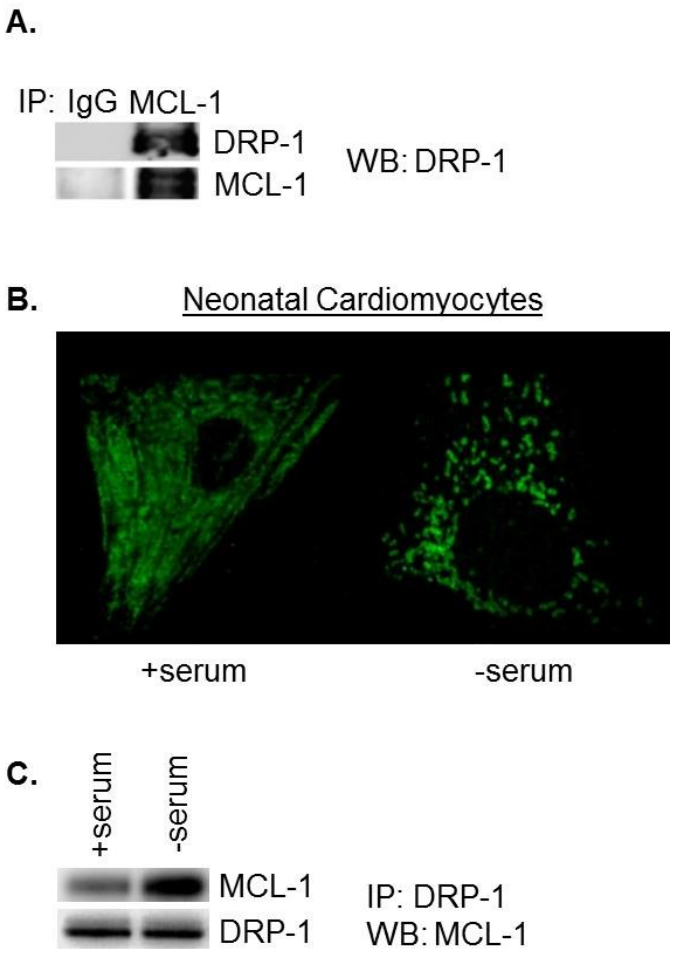

Figure 33: MCL-1 and DRP-1 interact in cardiac myocytes. **A.** Immunoprecipitation of MCL-1 from cardiac lysate reveals that DRP-1 interacts with MCL-1 in the heart. **B.** Serum starvation in neonatal rat cardiac myocytes for 24 hours leads to mitochondrial fission. **C.** COIP between DRP-1 and MCL-1 demonstrates that stress enhances their interaction in neonatal rat cardiac myocytes.

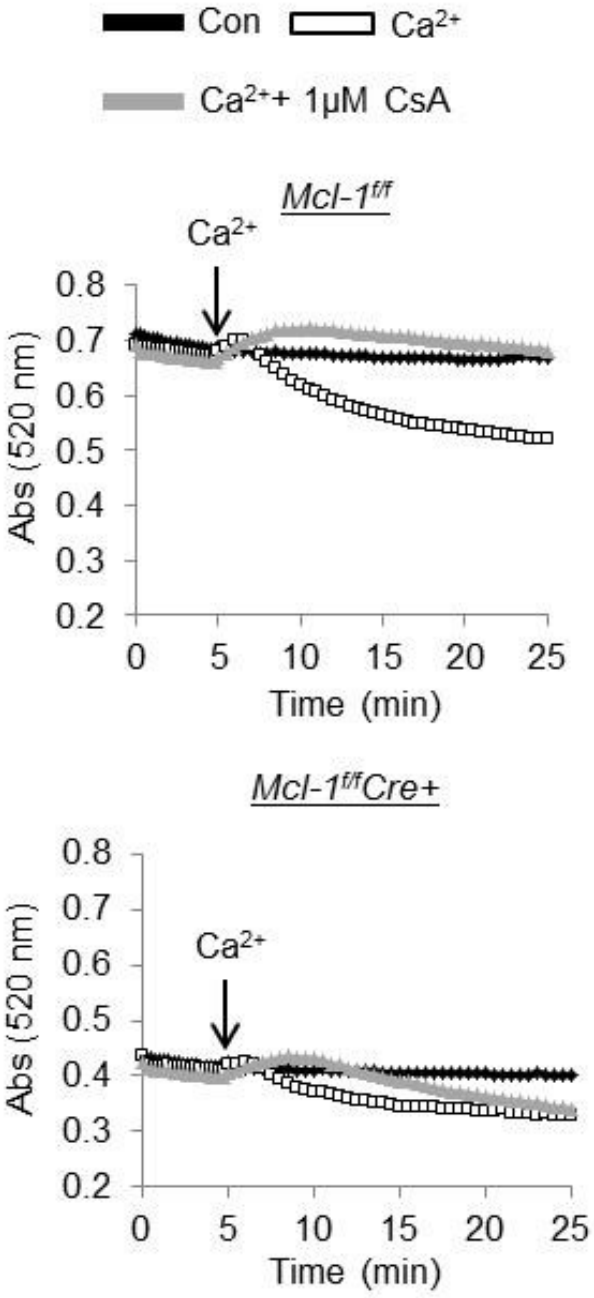

Figure 34: Swelling assay for mitochondria isolated from *Mcl-1$^{f/f}$* and *Mcl-1$^{f/f}$Cre+* hearts. Mitochondria were isolated one week after initiating tamoxifen injections and treated with 250 μM calcium with or without 1 μM CsA. Mitochondria from *Mcl-1$^{f/f}$Cre+* hearts exhibit lower baseline absorbance and swell less in response to calcium. Cyclosporine A treatment prevents swelling in mitochondria from *Mcl-1$^{f/f}$* hearts, but swelling still occurs in mitochondria from *Mcl-1$^{f/f}$Cre+* hearts.

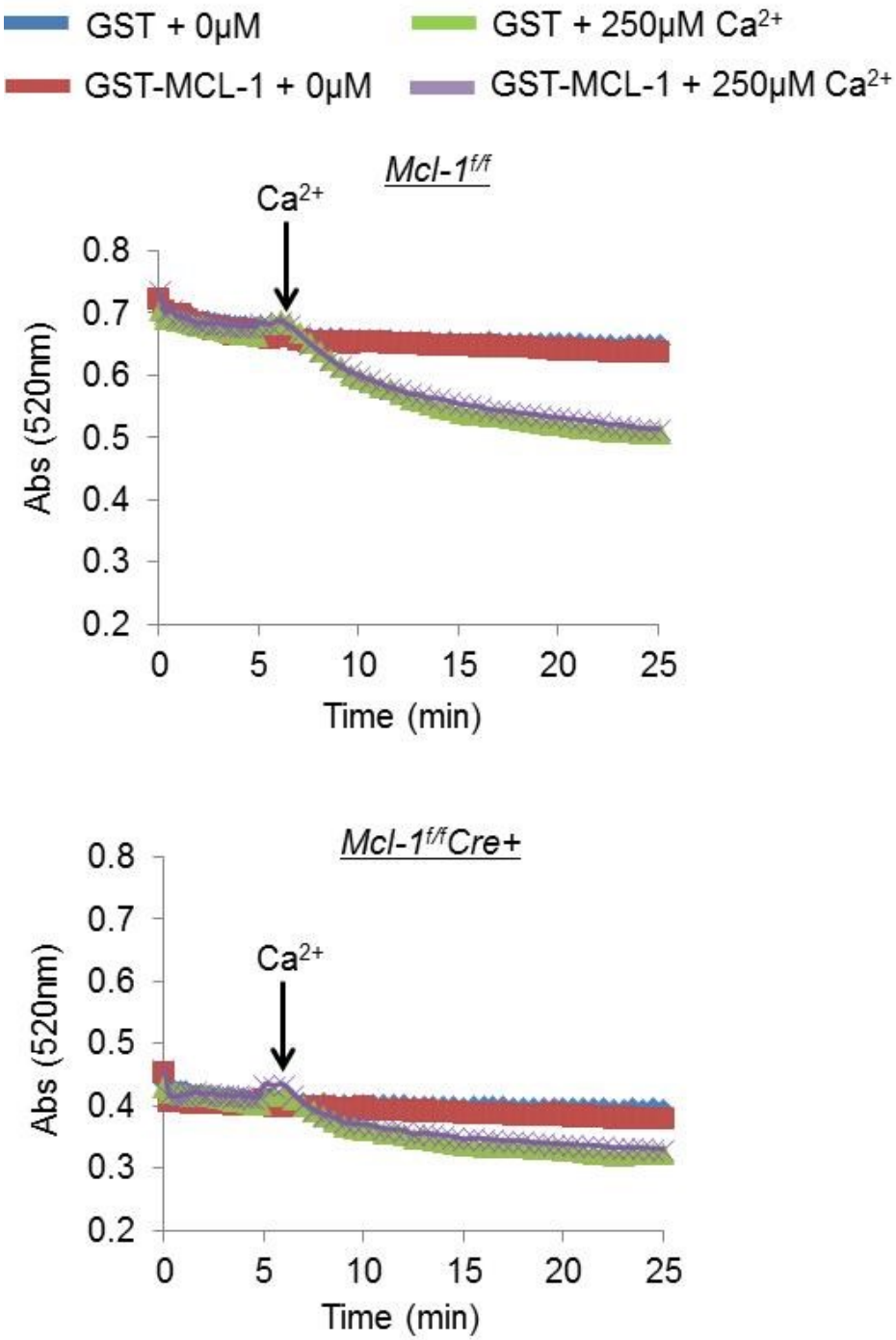

Figure 35: Addition of recombinant MCL-1 does not alter mitochondrial swelling. Prior to the swelling assay, mitochondria were incubated with 1 μg of Glutathione S-Transferase (GST)-tagged recombinant MCL-1. Mitochondria from *Mcl-1$^{f/f}$Cre+* hearts are still swollen at baseline and exhibit limited swelling in response to Ca^{2+} stress.

Table 2: Respiration of mitochondria isolated from *Mcl-1$^{f/f}$* and *Mcl-1$^{f/f}$Cre+* mice. Mitochondria were isolated from cardiac tissue one week after initiating tamoxifen treatment. Rates are nAtoms O/min/mg protein (*p<0.05 vs. Mcl-1$^{f/f}$, n=3-4).

Complex I: Pyruvate/Malate				
Genotype	**State 3**	**State 4**	**FCCP**	**RCR**
Mcl-1$^{f/f}$	268.9±8.8	31.2±2.1	275.5±9.9	8.67±1.16
Mcl-1$^{f/f}$Cre+	247.3±5.5*	48.9±3.4*	240±9.4*	5.07±0.57*
Complex II: Succinate				
Genotype	**State 3**	**State 4**	**FCCP**	**RCR**
Mcl-1$^{f/f}$	428.4±8.1	120.4±4.2	347.9±18.4	3.56±0.23
Mcl-1$^{f/f}$Cre+	332±5.6*	115.4±13.3	287.3±13.3*	2.91±0.18*

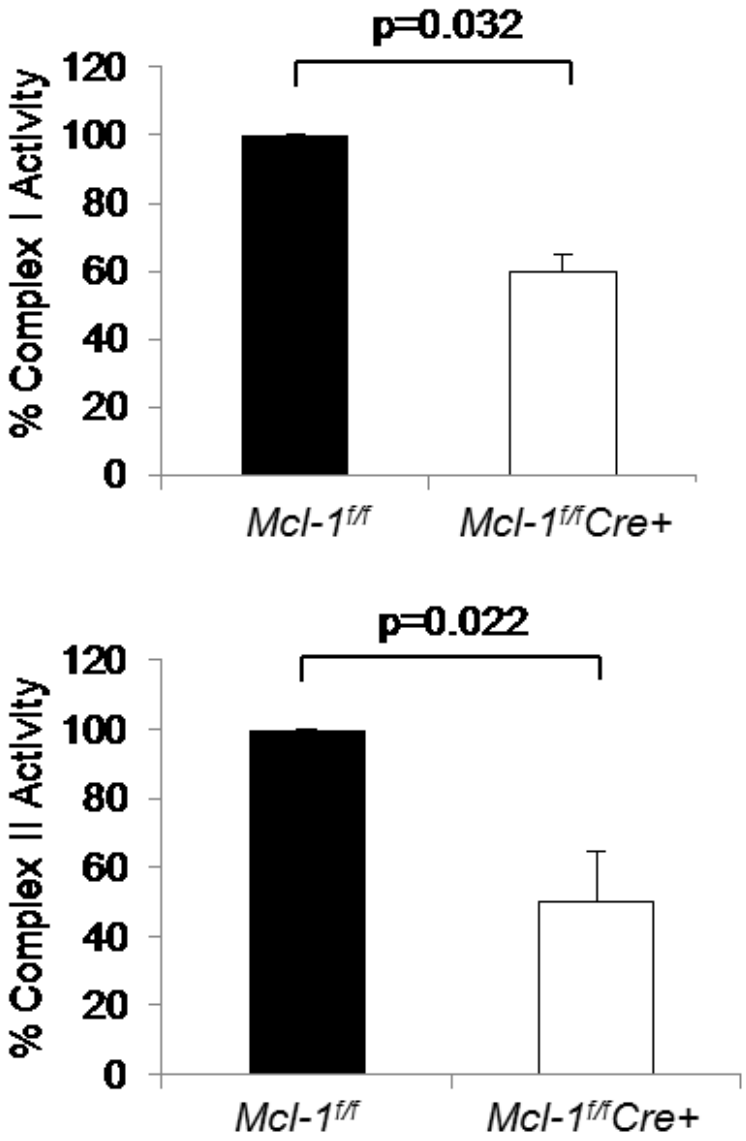

Figure 36: Complex I and complex II activities in isolated mitochondria from *Mcl-1*$^{f/f}$ and *Mcl-1*$^{f/f}$*Cre*+ hearts. Mitochondria were isolated one week after initiating tamoxifen treatment (n = 4).

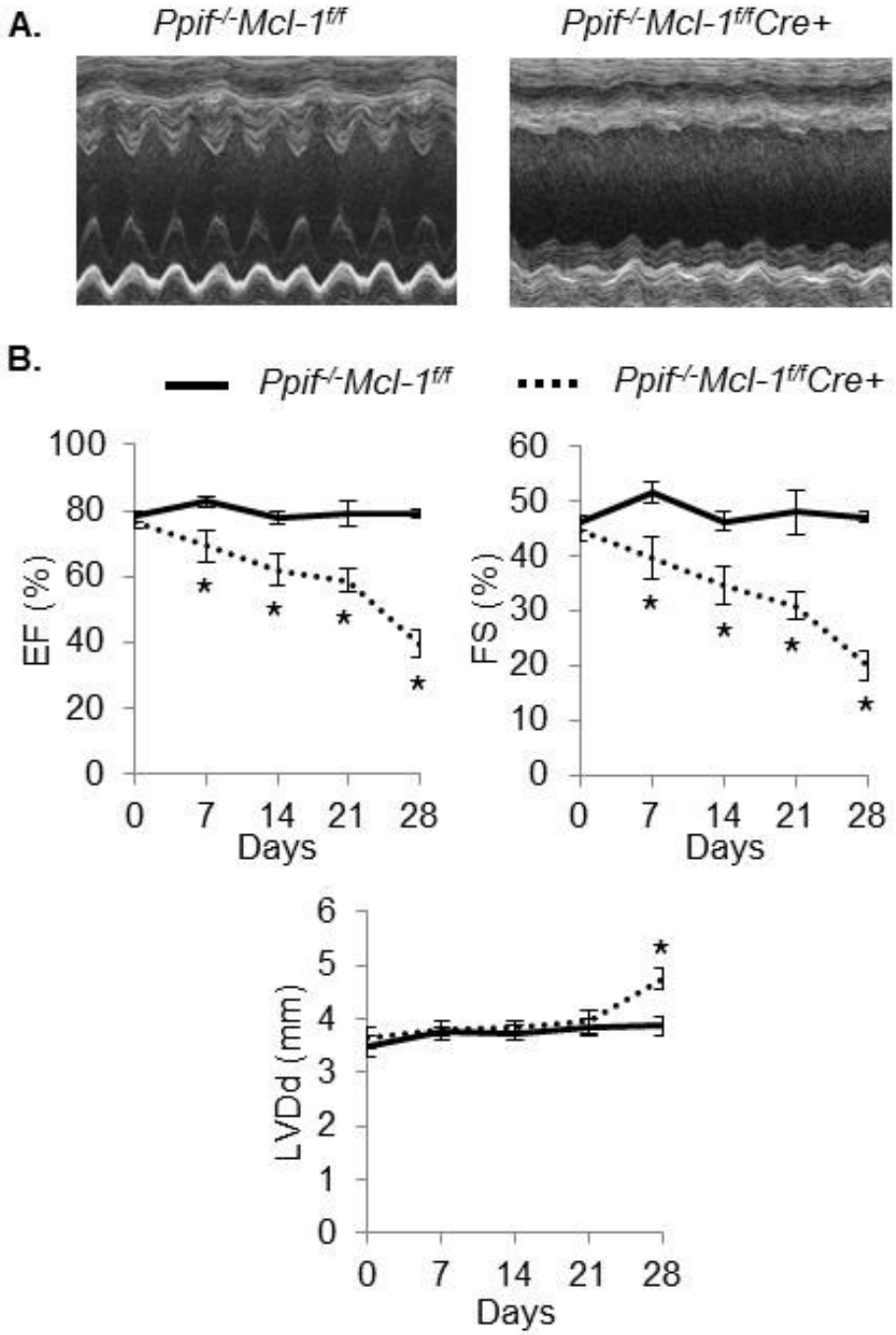

Figure 37: Echocardiography in *Ppif*$^{-/-}$*Mcl-1*$^{f/f}$ and *Ppif*$^{-/-}$*Mcl-1*$^{f/f}$*Cre*+ mice. **A.** Representative M-Mode echocardiograms two weeks after initiating tamoxifen treatment. **B.** Echocadiographic analysis revealed reduced ejection fraction (EF) and fractional shortening (FS) in *Ppif*$^{-/-}$*Mcl-1*$^{f/f}$*Cre*+ mice. Left ventricular diastolic dimension (LVDd) is not significantly increased until four weeks (n = 4–19, *$p<0.05$)

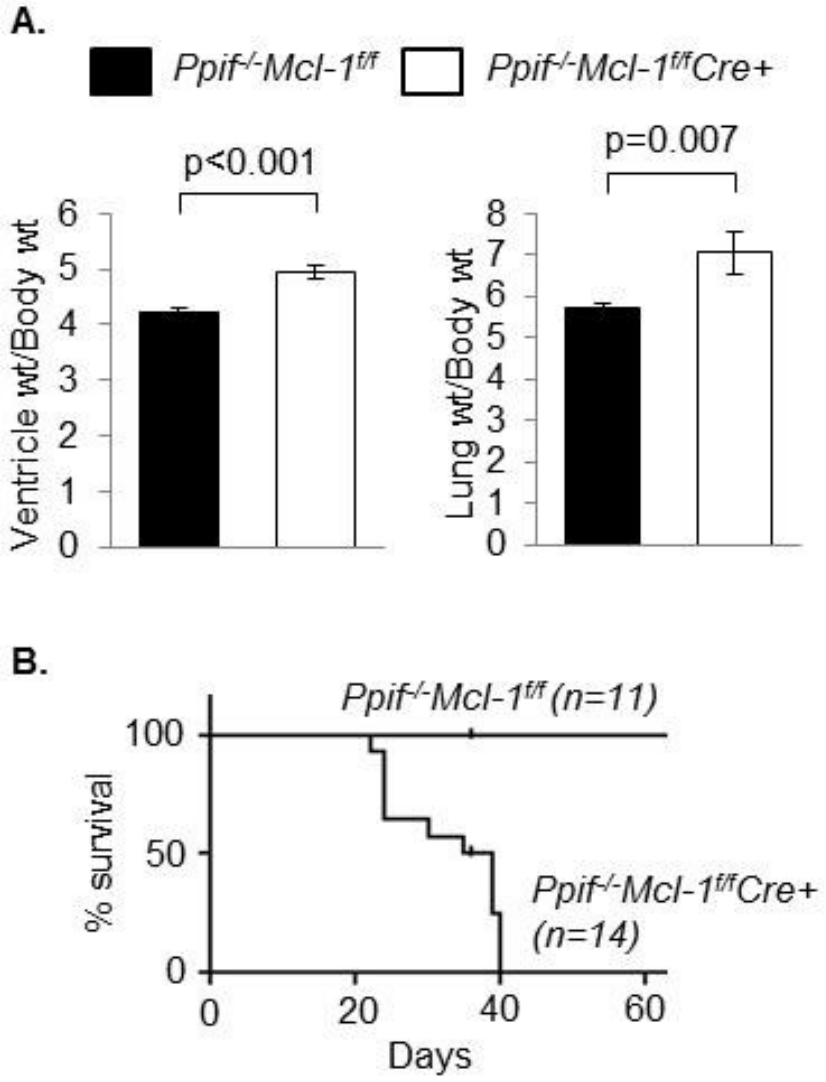

Figure 38: Organ weights and survival curve for *Ppif*$^{-/-}$*Mcl-1*$^{f/f}$ and *Ppif*$^{-/-}$*Mcl-1*$^{f/f}$*Cre+* mice. **A.** Ventricle weight and lung weight to body weight ratios are significantly increased in *Ppif*$^{-/-}$*Mcl-1*$^{f/f}$*Cre+* mice two weeks after initiating tamoxifen treatment (n = 17–21). **B.** Kaplan-Meyer analysis revealed early mortality in *Ppif*$^{-/-}$*Mcl-1*$^{f/f}$*Cre+* mice ($p<0.05$).

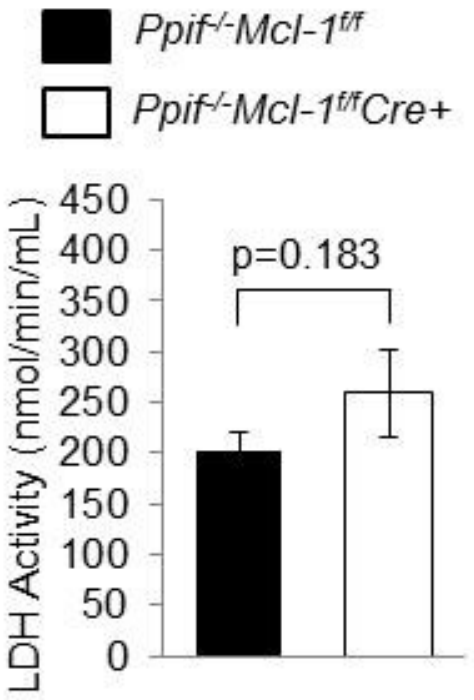

Figure 39: LDH activity in blood from *Ppif*$^{-/-}$*Mcl-1*$^{f/f}$ and *Ppif*$^{-/-}$*Mcl-1*$^{f/f}$*Cre*+ mice. LDH activity was not significantly increased in *Ppif*$^{-/-}$*Mcl-1*$^{f/f}$*Cre*+ mice one week after tamoxifen treatment (n = 5-6).

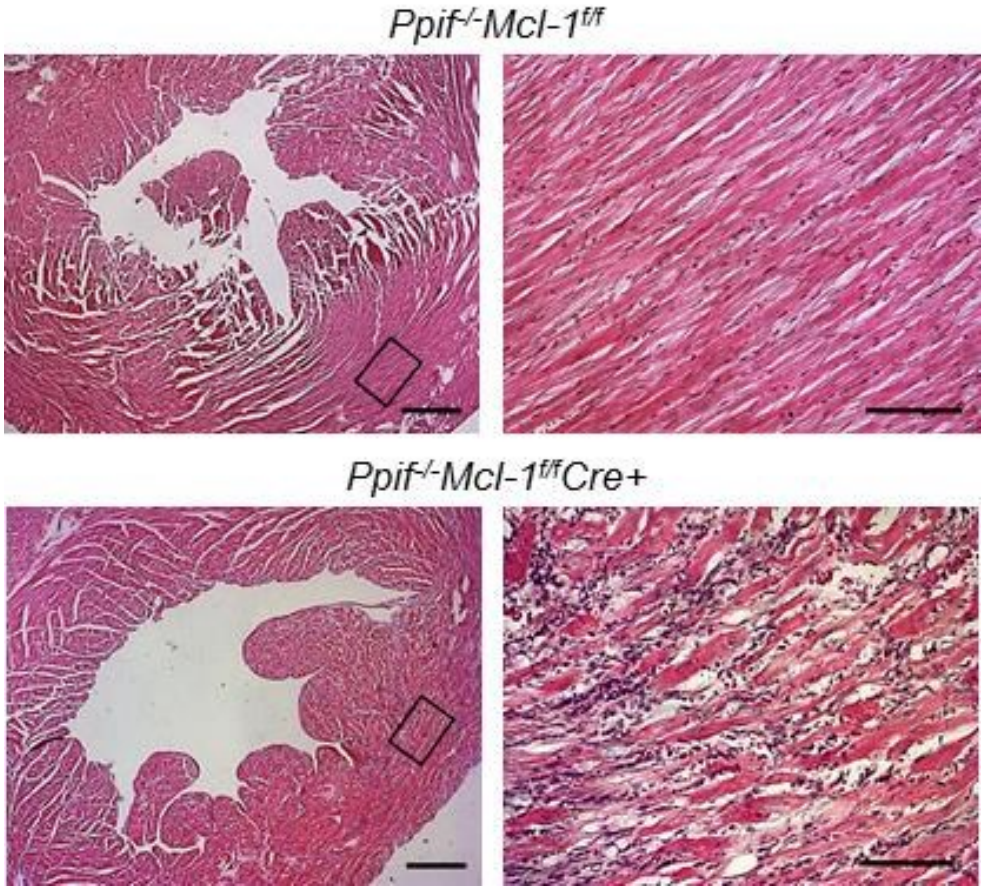

Figure 40: H&E staining in *Ppif*$^{-/-}$*Mcl-1*$^{f/f}$ and *Ppif*$^{-/-}$*Mcl-1*$^{f/f}$*Cre*+ hearts. Representative sections show myocyte disorganization and degeneration in *Ppif*$^{-/-}$*Mcl-1*$^{f/f}$*Cre*+ hearts two weeks after initiating tamoxifen treatment (scale bars: *left* = 500 μm; *right* = 100 μm).

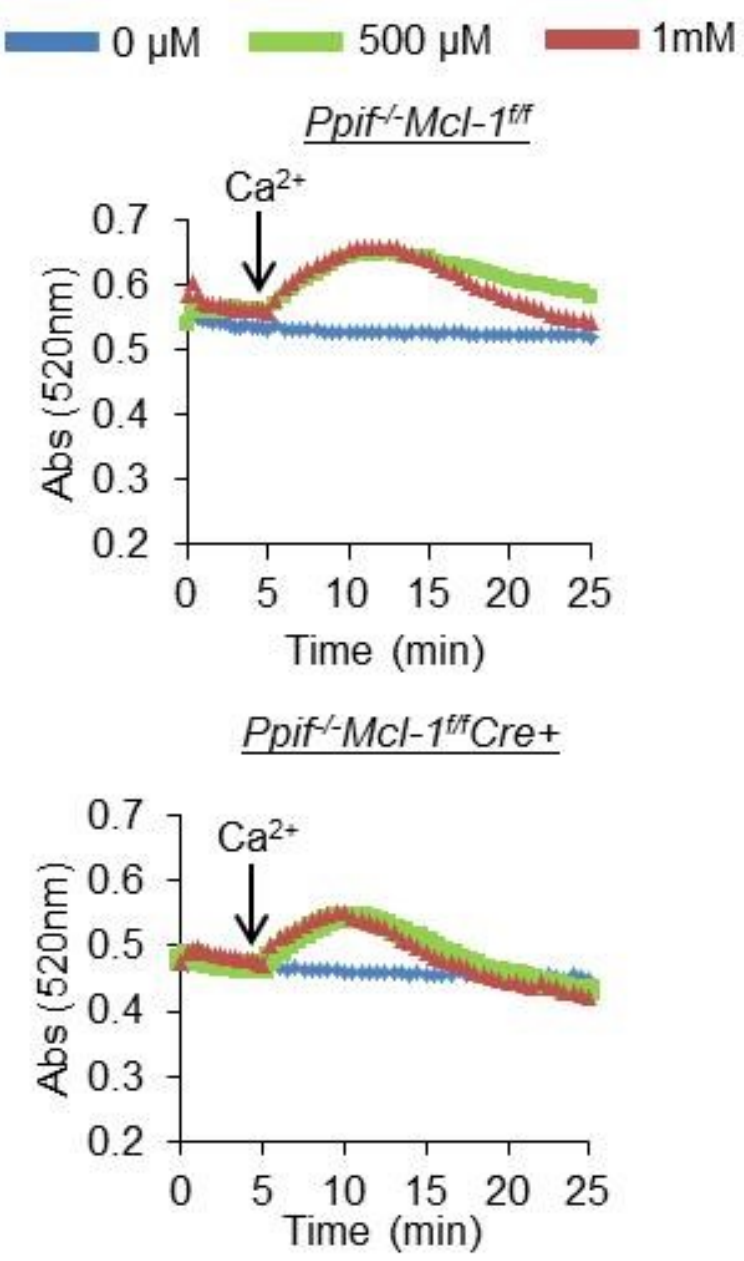

Figure 41: Swelling assay for mitochondria isolated from *Ppif*$^{-/-}$*Mcl-1*$^{f/f}$ and *Ppif*$^{-/-}$*Mcl-1*$^{f/f}$*Cre+* hearts. Mitochondria were isolated one week after initiating tamoxifen treatment. Even mitochondria subjected to high calcium concentrations (0.5 and 1 mM) resist swelling. Regardless, mitochondria from *Ppif*$^{-/-}$*Mcl-1*$^{f/f}$*Cre+* hearts are swollen at baseline relative to mitochondria from *Ppif*$^{-/-}$*Mcl-1*$^{f/f}$ hearts.

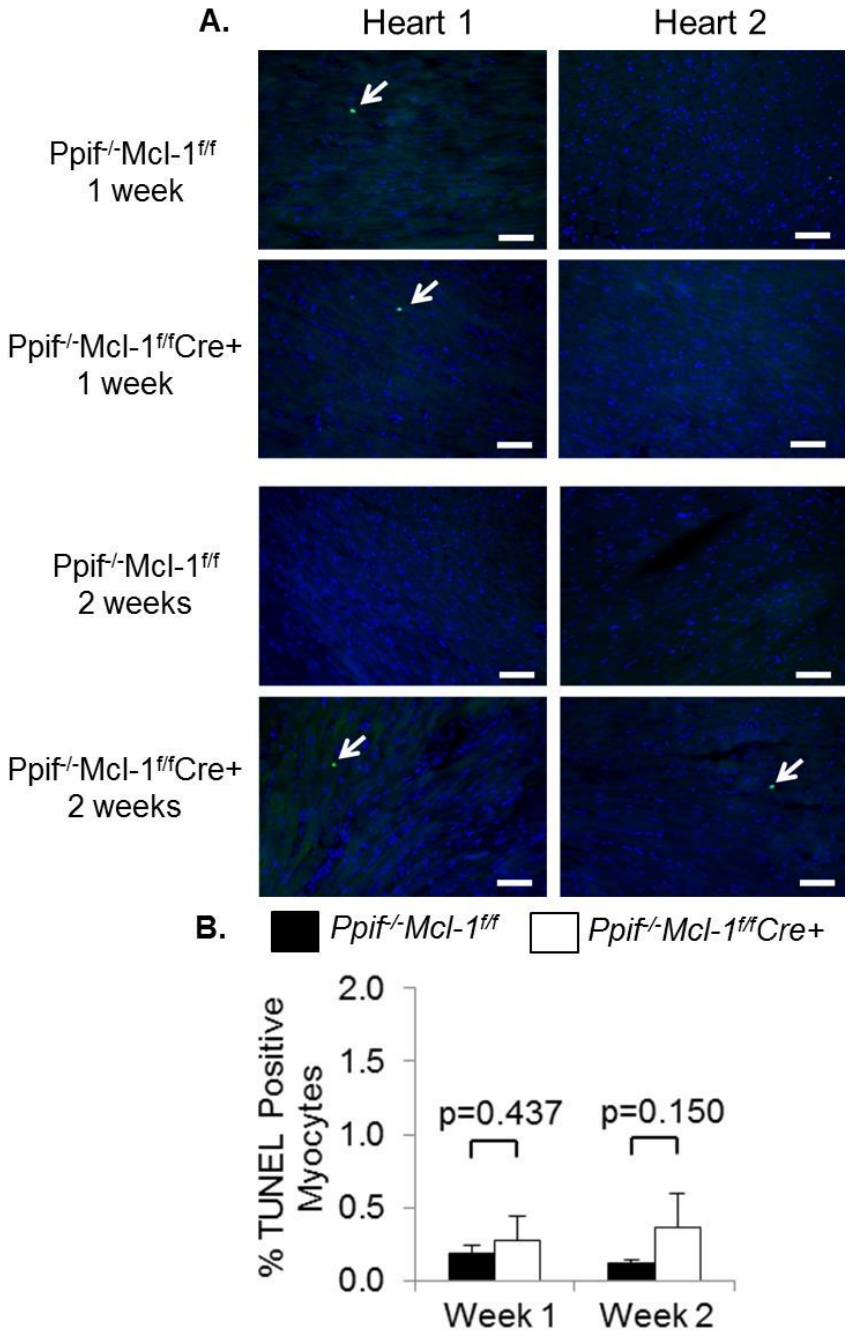

Figure 42: TUNEL staining in *Ppif*$^{-/-}$*Mcl-1*$^{f/f}$ and *Ppif*$^{-/-}$*Mcl-1*$^{f/f}$*Cre+* hearts. **A.** TUNEL (green) and nuclear (blue) staining of heart sections. Representative images of TUNEL staining from two different hearts at one and two weeks after initiation of tamoxifen injections. Arrows mark TUNEL positive nuclei. Scale bar = 50 μm. **B.** Quantitation of TUNEL-positive nuclei in heart sections (n = 3).

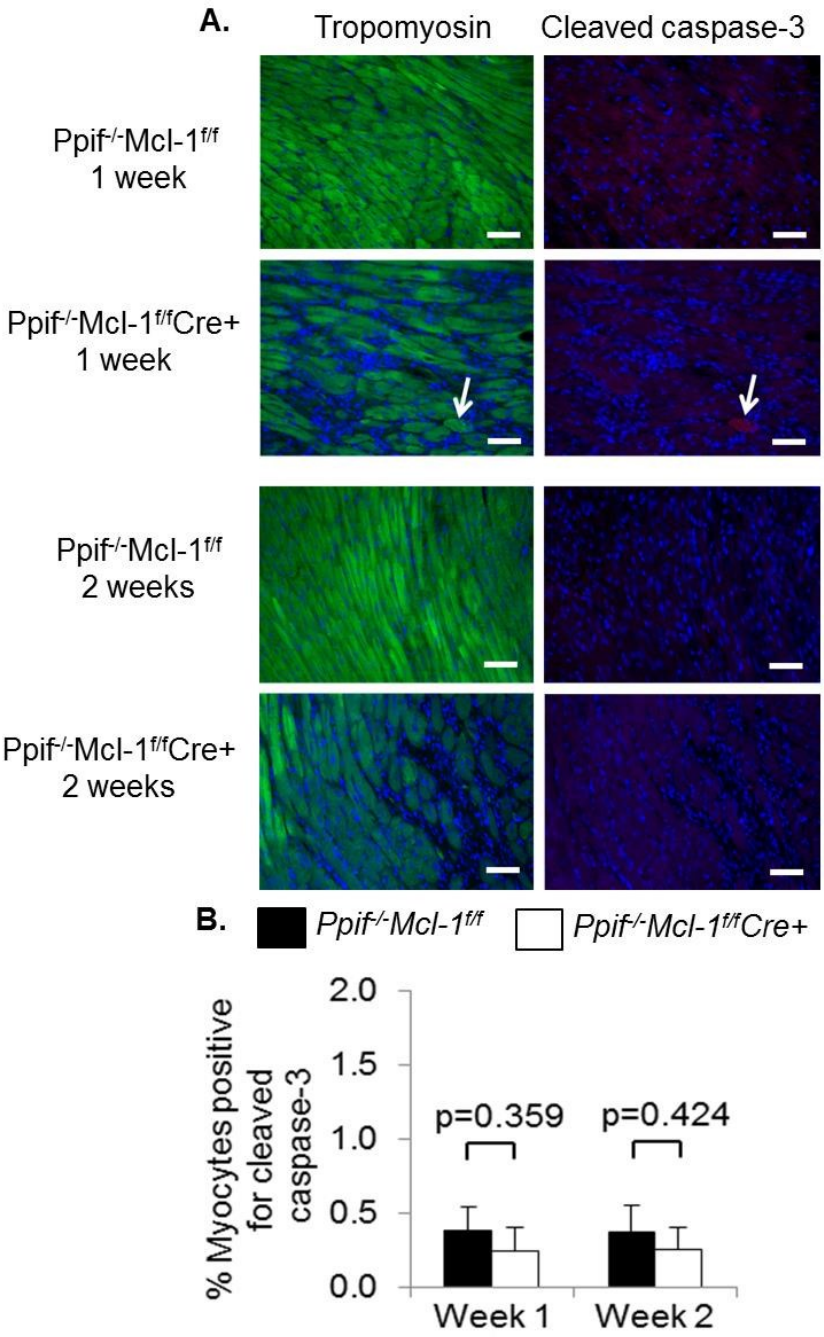

Figure 43: Staining of cleaved caspase-3 in *Ppif$^{-/-}$Mcl-1$^{f/f}$* and *Ppif$^{-/-}$Mcl-1$^{f/f}$Cre+* hearts. **A.** Immunostaining of heart sections for tropomyosin (green), cleaved caspase-3 (red), and nuclei (blue). Representative images of hearts at one and two weeks after initiation of tamoxifen injections. Arrow shows a myocyte positive for cleaved caspase-3 (scale bar = 50 μm). **B.** Quantitation of myocytes positive for cleaved caspase-3 in heart sections (n = 3).

Chapter 5: Loss of MCL-1 leads to impaired autophagy

Introduction

In the last chapter, I described extensive mitochondrial dysfunction, swelling and rupture that result from MCL-1 ablation in the adult heart. The heart normally activates autophagy to clear dysfunctional mitochondria and prevent further damage to cardiac myocytes. The resulting autophagosomes exhibit a characteristic double membrane structure that can be identified in electron micrographs (Mizushima, *et al.,* 2010). Surprisingly, I found no evidence of autophagosome formation in ultrastructural images from MCL-1 deficient hearts. To further investigate this observation, I quantified autophagy markers in *Mcl-1*$^{f/f}$ and *Mcl-1*$^{f/f}$*Cre*+ cardiac tissue. Autophagy is a dynamic process with ongoing synthesis and degradation of autophagic markers such as LC3 and p62. To determine how autophagy is impaired, I conducted autophagy flux experiments *in vivo* that block autophagosome/lysosome fusion (Iwai-Kanai *et al.*, 2008). When this degradation step is blocked, autophagosome accumulation provides an aggregate measure of autophagic activity. In addition, I examined autophagy activation in the heart in response to physiologic stress. The ability to upregulate autophagy is an important survival mechanism for cardiomyocytes (Gustafsson & Gottlieb, 2008). To expand on the mechanism of autophagic impairment in MCL-1 deficiency, I assessed the level of several core autophagic proteins, and explored the

interaction between MCL-1 and Parkin, an E3 ubiquitin ligase responsible for mitophagy. Finally, I examined whether MCL-1 overexpression affects autophagy similarly to the other anti-apoptotic BCL-2 proteins.

A. Autophagy is impaired in MCL-1 deficient hearts under basal and stressed conditions

Although autophagy is normally induced to remove damaged organelles and protein aggregates, no autophagosomes were identified in tamoxifen treated *Mcl-1*$^{f/f}$*Cre*+ hearts by electron microscopy. The lack of autophagy was striking given the extent of myocardial damage and mitochondrial dysfunction in MCL-1-deficient myocytes. To investigate whether autophagy was impaired in MCL-1-deficient hearts, we assessed the levels of LC3II/LC3I and p62 in *Mcl-1*$^{f/f}$ and *Mcl-1*$^{f/f}$*Cre*+ hearts two weeks after tamoxifen administration. The conversion of LC3I to LC3II is indicative of autophagosome formation (Kabeya *et al.*, 2000), whereas the p62 protein is degraded by autophagy and accumulates in cells when autophagic flux is reduced or impaired (Komatsu *et al.*, 2007). We found significantly reduced LC3II/LC3I ratios and accumulation of p62 in *Mcl-1*$^{f/f}$*Cre*+ hearts two weeks after tamoxifen injection (Figure 44A-C). Total LC3 levels were unaffected, indicating that the loss of MCL-1 impaired LC3 processing rather than LC3 expression (Figure 44B).

Since reduced LC3II levels can be caused by decreased autophagosome formation or excessive degradation, we investigated the

effect of MCL-1 deficiency on autophagic flux. One week after initiating tamoxifen injections, *Mcl-1*$^{f/f}$ and *Mcl-1*$^{f/f}$*Cre*+ mice were injected with chloroquine, which inhibits fusion between autophagosomes and lysosomes and causes LC3II to accumulate if autophagosome formation is intact (Iwai-Kanai *et al.*, 2008). Accumulation of LC3II occurred in *Mcl-1*$^{f/f}$ hearts after chloroquine treatment as expected, but no such increase was observed in *Mcl-1*$^{f/f}$*Cre*+ hearts (Figure 45A,B). These results indicate that the loss of MCL-1 compromises autophagsome formation in the heart.

Recent studies have shown that acute exercise causes induction of autophagy in the myocardium (He *et al.*, 2012). To investigate if autophagy could still be induced in MCL-1-deficient hearts, we subjected *Mcl-1*$^{f/f}$ and *Mcl-1*$^{f/f}$*Cre*+ mice to swimming one week after tamoxifen injections. We observed enhanced LC3 processing and p62 degradation in *Mcl-1*$^{f/f}$ hearts but not in *Mcl-1*$^{f/f}$*Cre*+ hearts after up to 120 minutes of swimming (Figure 46A,B,C). Taken together, these results demonstrate that the loss of MCL-1 impairs autophagosome formation in cardiac myocytes. Notably, in contrast to the two week time-point, resting Mcl-1$^{f/f}$Cre+ hearts collected during the swimming study (9 days after initiating tamoxifen injections) did not exhibit reduced LC3II/I ratios (Figure 46B). However, there was still a significant accumulation of p62 at this earlier time point (Figure 46C), suggesting that baseline autophagic flux is still impaired and progressively worsens after loss of MCL-1.

B. MCL-1 ablation disrupts core autophagy proteins and leads to substrate accumulation

Based the observation that autophagosome formation was impaired, I hypothesized that the loss of MCL-1 might alter the expression of critical autophagic proteins. BECLIN-1, ATG5, and LAMP-2 have been shown to play essential roles in phagophore formation, autophagosome elongation, and lysosomal fusion, respectively (Levine & Kroemer, 2008; Boya *et al.*, 2013). By targeting key proteins in each step, I attempted to narrow down which part of the autophagy pathway was affected. Remakably, BECLIN-1 was significantly reduced in MCL-1 deficient hearts (Figure 47A). BECLIN-1 promotes initial formation of the phagophore, and decreased BECLIN-1 expression reduces autophagic flux (Qu *et al.*, 2003). As such, reduced BECLIN-1 levels may contribute to impaired autophagic initiation and flux observed in MCL-1 deficient hearts. I found no significant difference in ATG5 levels (Figure 47B). Although the MCL-1 deficient phenotype recapitulates many of the pathologic signs present in cardiac specific, *Atg5* conditional knockout mice, the effects of MCL-1 deficiency appear to proceed by another mechanism (Nakai *et al.*, 2007). LAMP-2 is important for lysosomal function but also plays a role in chaperone-mediated autophagy of soluble, cytosolic proteins (Bandyopadhyay *et al.*, 2010). Interestingly, LAMP-2 levels were increased in MCL-1-deficient hearts (Figure 47C), suggesting that there might be a compensatory increase in alternative degradation pathways.

Autophagic substrates such as ubiquitinated proteins and lipids typically accumulate in cells when autophagy is impaired (Hara *et al.*, 2006; Sarkar, *et al.*, 2013). Ubiquitin is used to mark proteins and organelles that need to be removed by autophagosomes, and disruption of autophagy leads to accumulation of ubiquitin-containing aggregates (Nakai *et al.*, 2007). I found a significant increase in ubiquitinated proteins in MCL-1 deficient hearts, demonstrating substrate accumulation in the myocardium (Figure 48A,B). Ubiquitinated proteins are also prone to aggregate formation, and these aggregates can have additional cytotoxic effects (Hara *et al.*, 2006).

In addition to clearing organelles and proteins, autophagy also plays a role in mobilization of fatty acids from lipid droplets through a process called lipophagy (Singh, *et al.*, 2009). Disruption of autophagy in disorders such as Niemann-Pick disease leads to toxic lipid accumulation, and stimulating autophagy with rapamycin improves cell viability (Sarkar *et al.*, 2013). In MCL-1 deficient hearts, electron microscopy revealed the presence of numerous, large lipid droplets in tissue sections (Figure 49). Their accumulation suggests that autophagic impairment in MCL-1 deficient hearts is comprehensive, affecting various substrates and metabolic pathways.

C. Loss of MCL-1 leads to reduced PINK1/Parkin activity

I have shown that the loss of MCL-1 compromises mitochondrial integrity and autophagy. The PTEN-induced putative kinase 1 (PINK1)/Parkin

pathway is important in regulating autophagy of dysfunctional mitochondria in myocytes (Kubli & Gustafsson, 2012). To examine if loss of MCL-1 affects mitophagy, I examined the PINK1/Parkin pathway. Although Parkin levels increased in *Mcl-1*$^{f/f}$*Cre+* cytosolic fractions, Parkin was not found on the damaged mitochondria in *Mcl-1*$^{f/f}$*Cre+* hearts (Figure 50). These data suggested that MCL-1 might participate in Parkin recruitment. To investigate this possibility, I used COIP to determine whether MCL-1 directly interacts with Parkin under basal or stress conditions. To mimic mitochondrial damage, I treated cells with FCCP for four hours. This short time point was chosen because Parkin translocation to depolarized mitochondria is rapid (Kubli *et al.,* 2013), and extended FCCP treatment leads to mitophagy which is likely to have degraded the proteins of interest. Although I successfully pulled down MCL-1 in both basal and FCCP treated conditions, I found no association with Parkin under either condition (Figure 51).

While I was conducting these experiments, a proteomics study was published that predicted MCL-1 was a potential substrate for Parkin-mediated ubiquitination and degradation (Sarraf *et al.*, 2013). Indeed, the regulatory region of MCL-1 contains several ubiquitination sites and other ubiquitin ligases have been shown to promote MCL-1 degradation (Thomas *et al.* 2010, Zhong *et al.*, 2005,) To investigate the possibility of Parkin-mediated MCL-1 clearance, I overexpressed MCL-1 in mouse embryonic fibroblasts (MEF) using transient transfection. I then evaluated MCL-1 protein levels in response

to Parkin overexpression with or without mitochondrial stress. If MCL-1 is a Parkin substrate, I hypothesized, then Parkin overexpression should increase MCL-1 degradation. In fact, I found that Parkin overexpression did not alter MCL-1 dynamics under basal conditions or in response to FCCP treatment (Figure 52). To recapitulate these results *in vivo*, I examined MCL-1 levels in wild-type and Parkin-transgenic mice subjected to two weeks of pressure overload induced by trans-aortic constriction (TAC). These mice selectively overexpress Parkin in cardiac myocytes using the α-myosin heavy chain promoter. Pressure overload serves as a chronic cardiac stressor that leads to pathologic hypertrophy and mitochondrial dysfunction (Bugger, *et al.* 2010). No changes in MCL-1 levels were detected in response to Parkin overexpression, TAC, or a combination of these two conditions (Figure 53). Thus, in keeping with my results in MEF's, Parkin levels did not alter MCL-1 protein levels under basal or stressed conditions. These data indicate that MCL-1 is not a substrate for Parkin ubiquitination, nor is MCL-1 directly involved in Parkin recruitment to mitochondria.

To further investigate how MCL-1 ablation disrupts Parkin recruitment, I studied the effects of MCL-1 deficiency on the accumulation of PINK1 at mitochondria. PINK1 normally accumulates on depolarized mitochondria, where it recruits Parkin to mark mitochondria for autophagy. If the PINK1/Parkin pathway operated normally in MCL-1 deficient hearts, extensive mitochondrial damage should elevate PINK1 levels at mitochondria well above

baseline. Instead, I found that PINK1 was significantly reduced at mitochondria in MCL-1-deficient hearts (Figure 54A,B). The loss of MCL-1 may disrupt PINK1 expression, recruitment, or stabilization at mitochondria. Regardless, disrupted PINK dynamics reveals a mechanism by which the loss of MCL-1 also disrupts mitochondrial autophagy. This disruption may allow damaged mitochondria to accumulate, eventually overwhelming cardiac myocytes and triggering necrosis.

Although my data suggest that MCL-1 is required for induction of autophagy in cardiac myocytes, overexpression of MCL-1 has been reported to inhibit autophagy in neurons (Germain *et al.*, 2011). Similarly, anti-apoptotic BCL-2 and BCL-X_L have been shown to inhibit autophagy in mammalian cells (Pattingre *et al.*, 2005; Maiuri *et al.*, 2007). Therefore, we investigated the effect of MCL-1 on induction of autophagy in neonatal rat cardiac myocytes. Interestingly, overexpression of MCL-1 had no effect on the number of GFP-LC3 positive autophagosomes or LC3II/I levels in myocytes after glucose deprivation (Figure 55). These findings suggest that MCL-1 does not function as a negative regulator of autophagy in myocytes. These characteristics distinguish MCL-1 from other anti-apoptotic BCL-2 proteins and suggest a potential unique role for MCL-1 in myocytes.

Conclusion:

In this chapter, I have shown that MCL-1 deficiency impairs cardiac autophagy, alters the expression of critical autophagic proteins, and disrupts the PINK1/Parkin mitophagy pathway. Impaired autophagic flux leads to accumulation of autophagic substrates that may contribute to cytotoxicity. In addition, loss of MCL-1 eliminates the heart's ability to activate autophagy in response to stress. These data indicate degradation of MCL-1 during myocardial injury may compromise survival mechanisms and exacerbate cardiac damage.

Loss of MCL-1 prevents Parkin recruitment to mitochondria, but I found no evidence that these two proteins directly interact. As such, MCL-1 does not appear to function as a Parkin receptor on mitochondria. Despite proteomic models predicting that MCL-1 is Parkin substrate, Parkin overexpression and activation do not alter MCL-1 dynamics. Future studies will be required to elucidate the relationship between MCL-1 and PINK1. Alternatively, MCL-1 deficiency may affect Parkin mediated mitophagy through independent, global effects on the cell.

In cardiomyocytes, MCL-1 acts differently than other anti-apoptotic proteins. Unlike BCL-2 and BCL-X_L, MCL-1 overexpression does not repress autophagy. The subcellular localization of MCL-1 may explain these differences. In 2005, Pattingre *et al.*, demonstrated that BCL-2 at the endoplasmic reticulum inhibits autophagy while mitochondrial targeted BCL-2

does not. Due to high mitochondrial content in cardiomyocytes and robust mitochondrial trafficking of MCL-1, the protein may be unavailable to interact with autophagy proteins in the heart. The interaction between MCL-1 and autophagy machinery will require further characterization

Acknowledgements

Chapter 5, in part, is a reprint of the material as it appears in Thomas et al., Genes Dev, 2013. The dissertation author was the primary investigator and author of this paper.

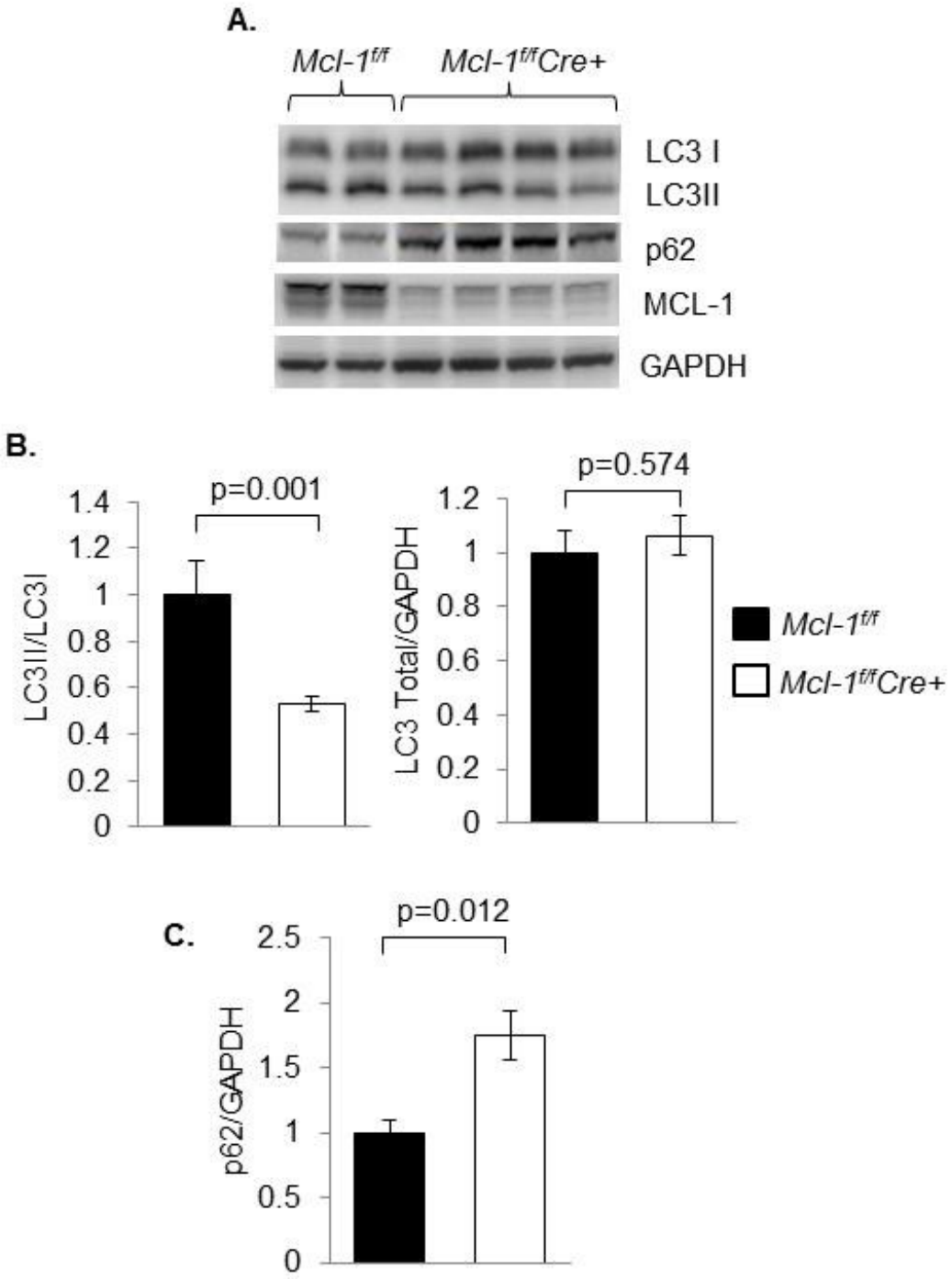

Figure 44: Western analysis of autophagy markers in *Mcl-1$^{f/f}$* and *Mcl-1$^{f/f}$Cre+* hearts. **A.** Representative Western blots of heart lysates prepared two weeks after initiation of tamoxifen administration. **B.** Quantitation analyses of LC3II/I and total LC3 levels **C.** Quantitation analysis of p62 (n = 6–13).

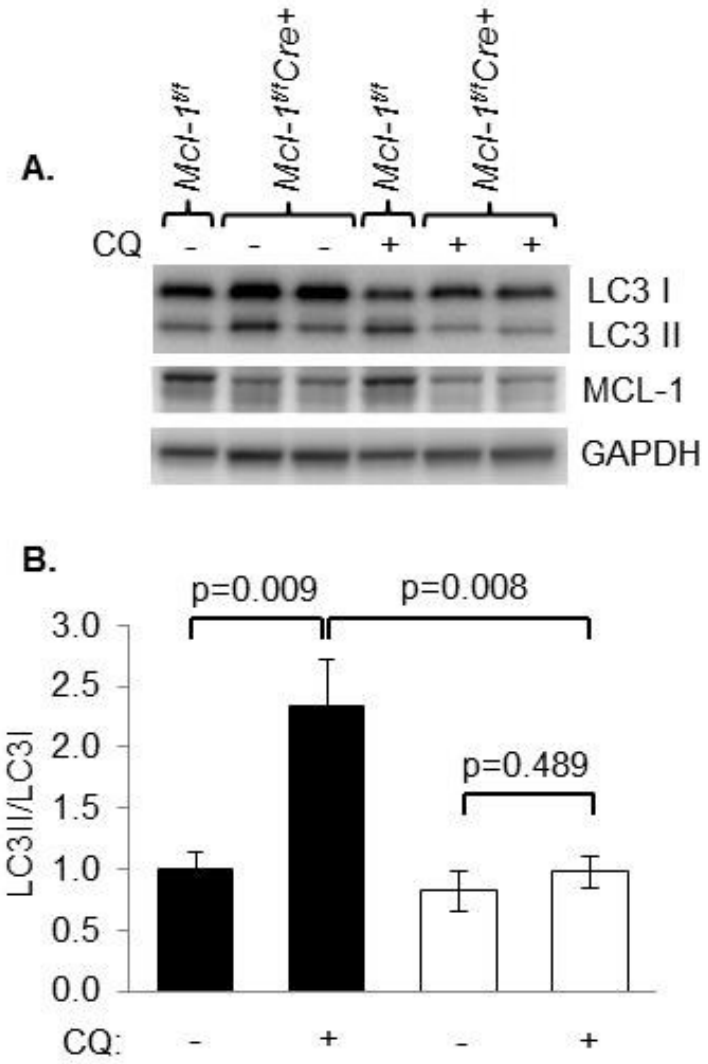

Figure 45: Assessment of autophagic flux *in vivo*. **A.** Representative Western blot for *Mcl-1*$^{f/f}$ and *Mcl-1*$^{f/f}$*Cre*+ hearts collected from vehicle or chloroquine treated mice one week after initiating tamoxifen treatment **B.** Quantitation of LC3II/I levels in chloroquine treated mice shows that MCL-1 ablation leads to reduced LC3II accumulation (n = 4–6).

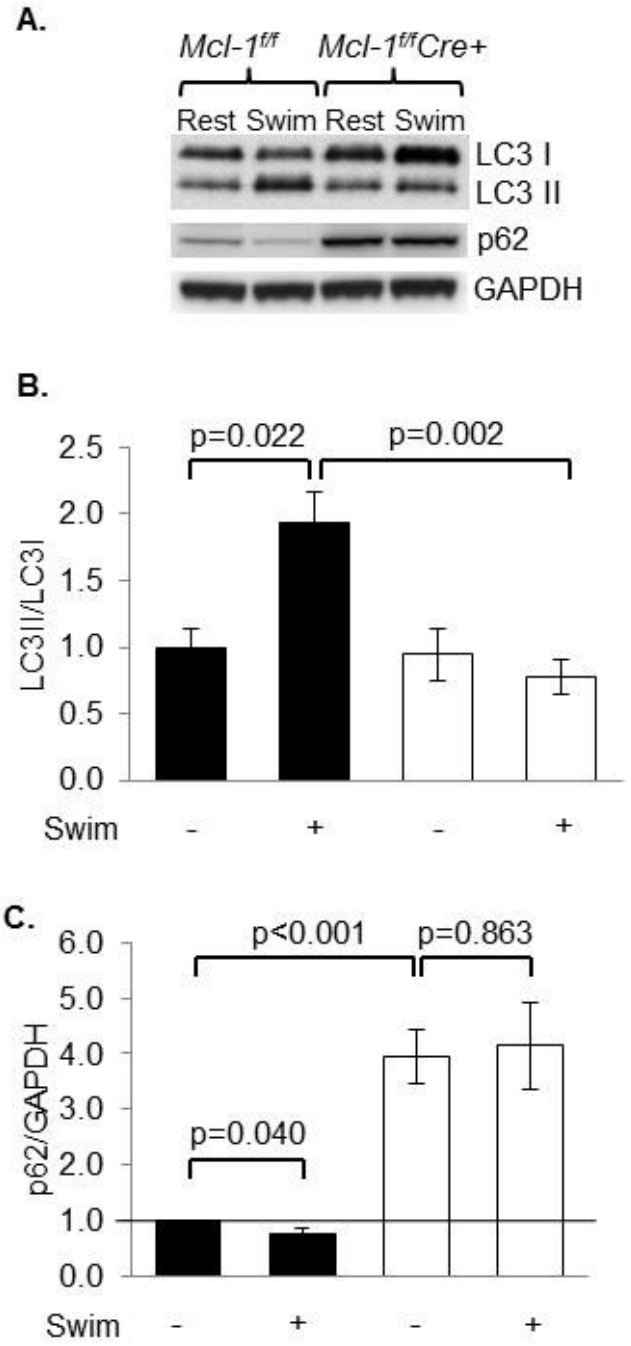

Figure 46: Activation of autophagy in response to exercise. **A.** Representative Western blot of heart lysates after resting or acute swimming. **B.** Quantitation of LC3II/I levels shows that *Mcl-1$^{f/f}$Cre+* mice do not activate LC3 conversion in response to swimming (n = 4–8). **C.** Quantitation of p62 levels reveals baseline accumulation and lack of degradation in response to exercise in *Mcl-1$^{f/f}$Cre+* mice (n = 3–4).

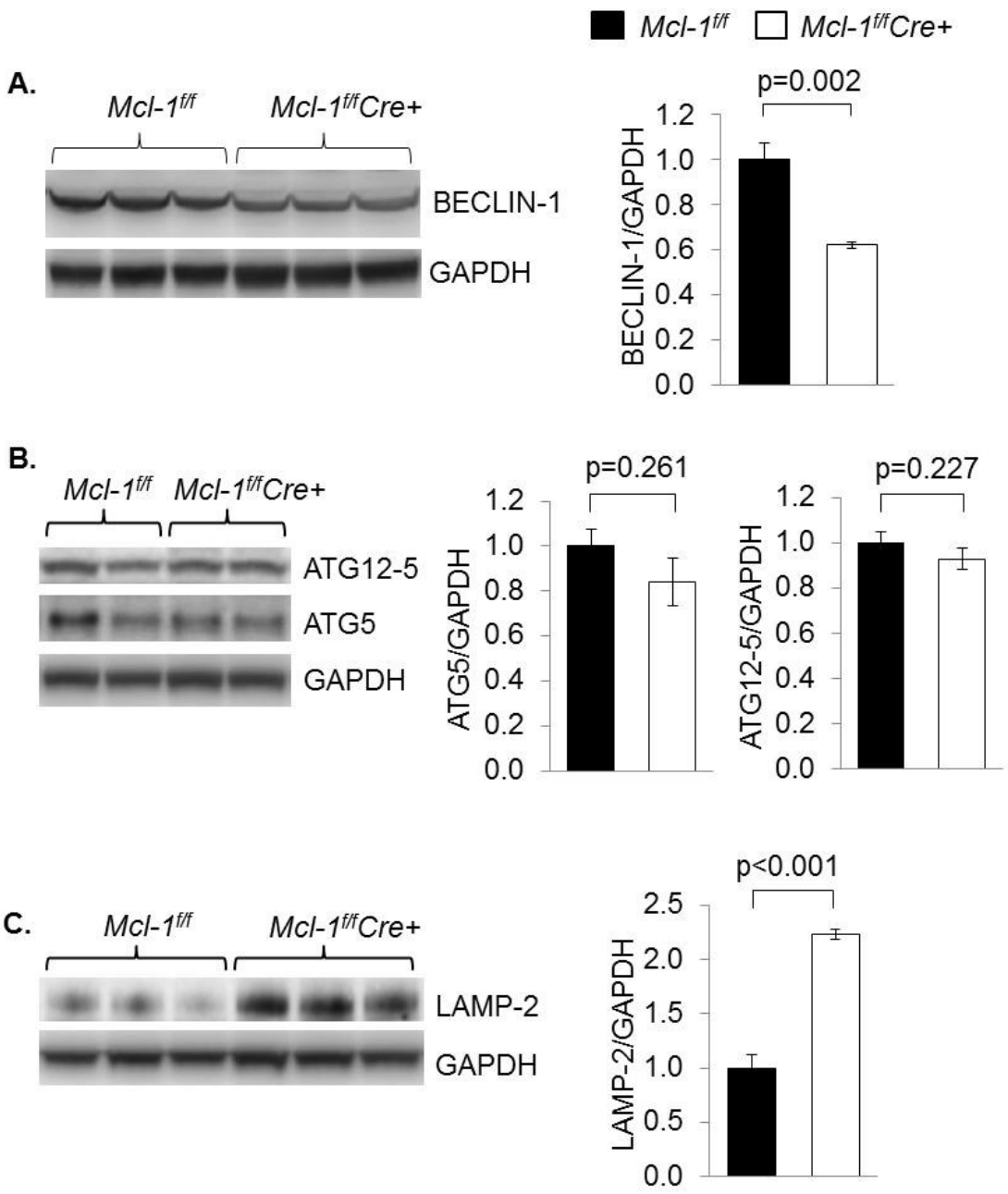

Figure 47: Western analysis of autophagy proteins in *Mcl-1$^{f/f}$* and *Mcl-1$^{f/f}$Cre+* hearts. Lysates were prepared from cardiac tissue collected two weeks after initiating tamoxifen injections. **A.** BECLIN-1 protein levels are reduced in *Mcl-1$^{f/f}$Cre+* hearts (n=4). **B.** MCL-1 ablation does not significantly alter ATG12 or ATG5 levels (n=4). **C.** LAMP-2 levels are significantly elevated in *Mcl-1$^{f/f}$Cre+* hearts (n=4).

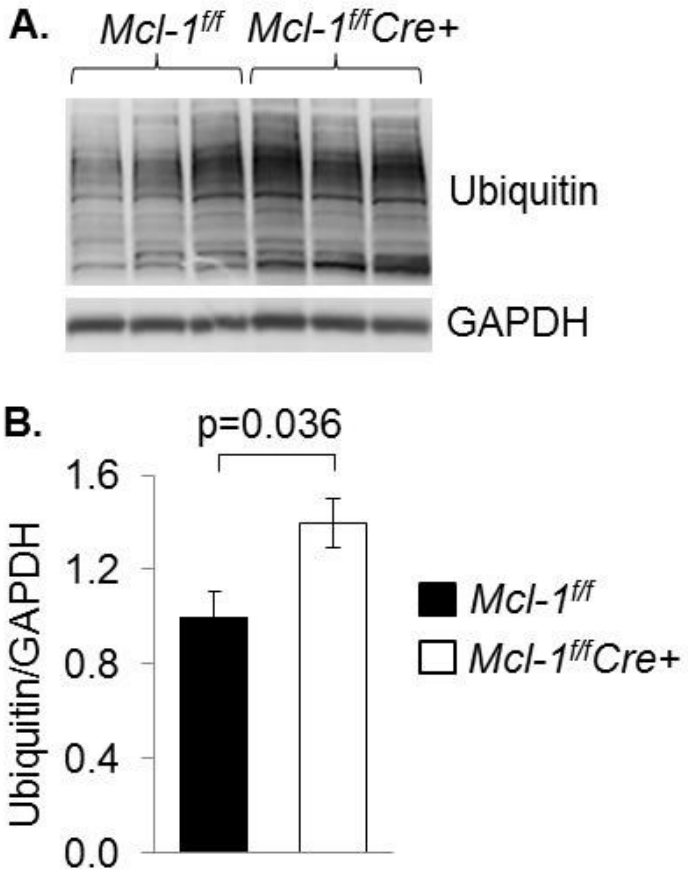

Figure 48: Western analysis of ubiquitin levels in *Mcl-1$^{f/f}$* and *Mcl-1$^{f/f}$Cre+* hearts **A.** Representative Western blot reveals increased protein ubiquitination in *Mcl-1$^{f/f}$Cre+* hearts two weeks after initiating tamoxifen treatment. **B.** Ubiquitination is significantly increased in *Mcl-1$^{f/f}$Cre+* hearts (n = 4).

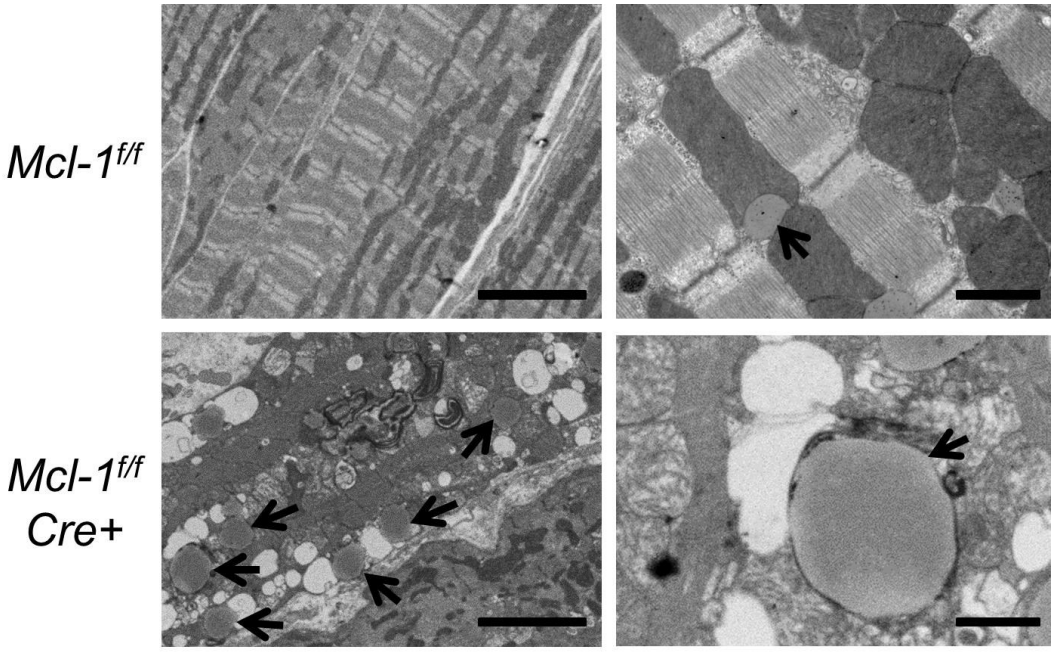

Figure 49: Lipid accumulation in MCL-1 deficient hearts. Lipid droplets are much larger in MCL-1$^{f/f}$Cre+ tissue. Black arrows mark lipid droplets, left scale bar = 5μm, right scale bar = 1μm.

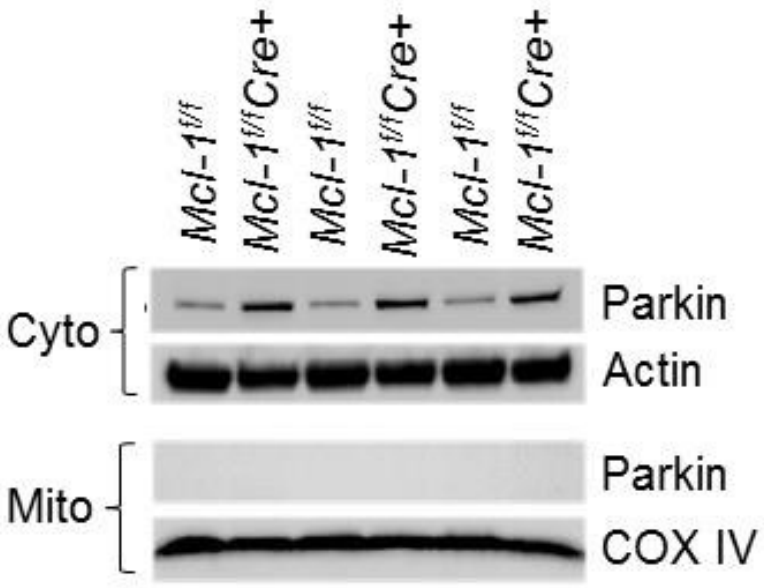

Figure 50: Cellular fractionation for Parkin in *Mcl-1$^{f/f}$* and *Mcl-1$^{f/f}$Cre*+ hearts. Western blot shows that cytosolic Parkin is increased but does not translocate to mitochondria in *Mcl-1$^{f/f}$Cre*+ hearts one week after initiating tamoxifen treatment.

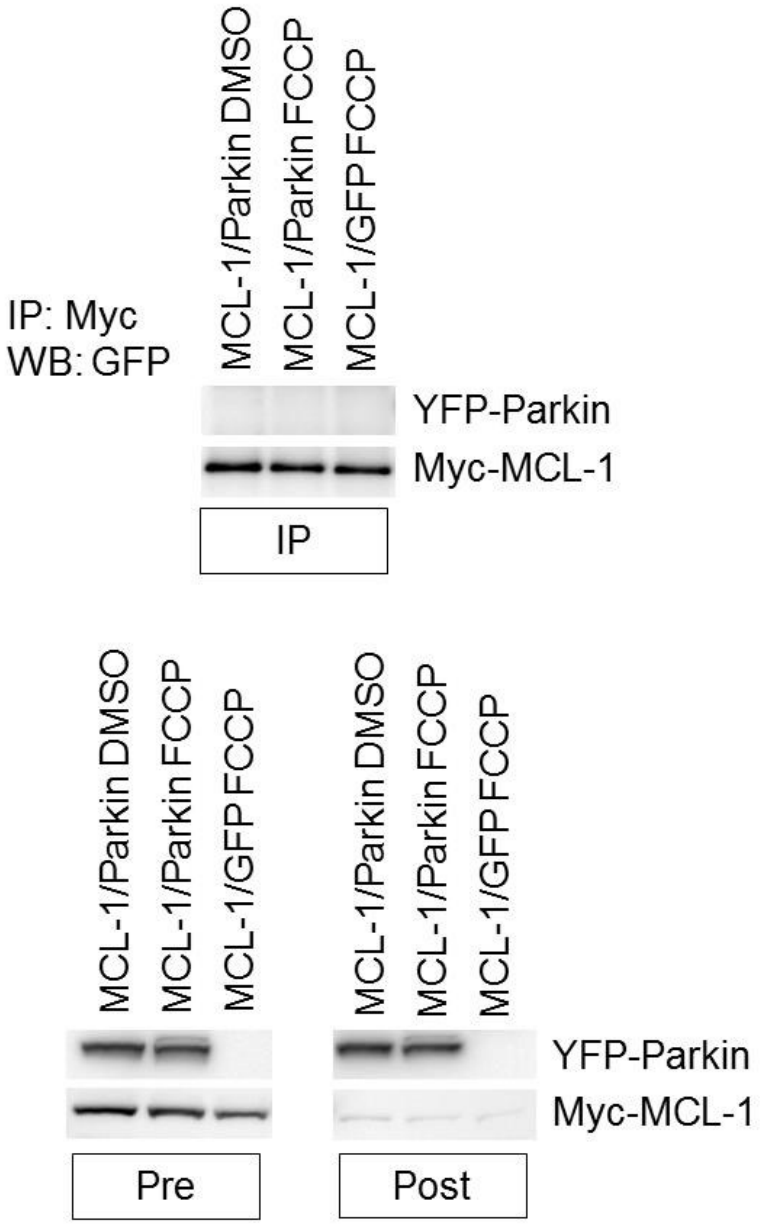

Figure 51: COIP shows no direct interaction between MCL-1 and Parkin under basal or stressed conditions. Myc-MCL-1 and YFP-Parkin were transiently transfected in HeLa cells. Although Myc-MCL-1 immunoprecipitation was successful, no Parkin was pulled down with DMSO or FCCP treatment (10μM for 4hrs).

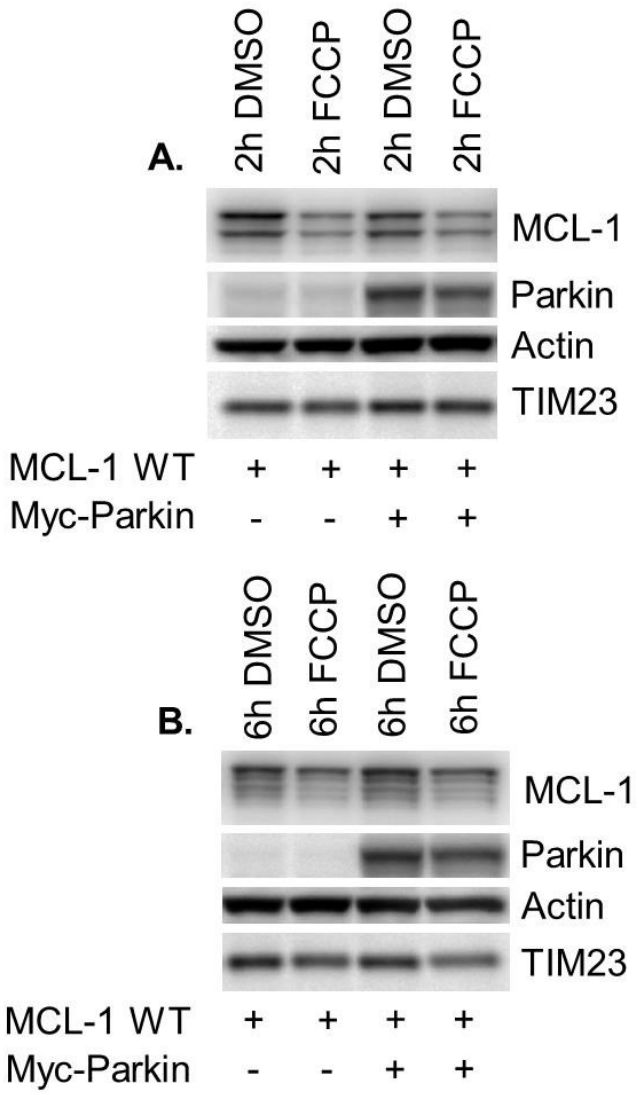

Figure 52: Parkin overexpression does not affect MCL-1 degradation in response to mitochondrial damage. MCL-1 and Parkin were overexpressed in MEFs using transient transfection. **A.** Western for MCL-1 degradation after 10μM FCCP treatment at two hours **B.** Western for MCL-1 degradation after 10μM FCCP treatment at six hours.

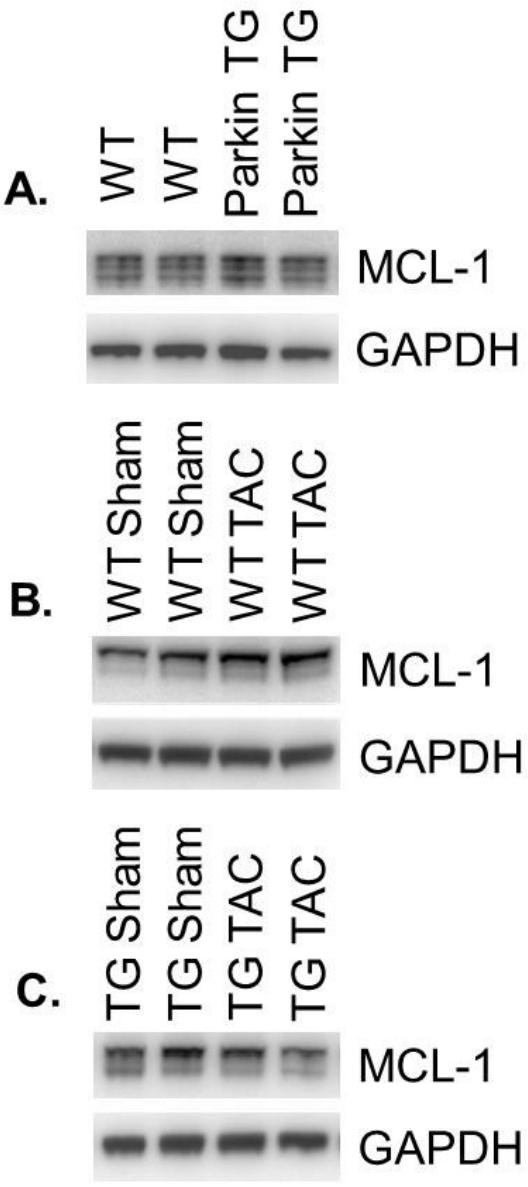

Figure 53: MCL-1 is not degraded by Parkin *in vivo*. **A.** Parkin overexpression in transgenic hearts does not alter MCL-1 levels under basal conditions. **B.** Chronic stress from TAC (2 weeks) does not reduce MCL-1 levels. **C.** Pressure overload in Parkin transgenic hearts (2 weeks) does not lead to increased MCL-1 degradation.

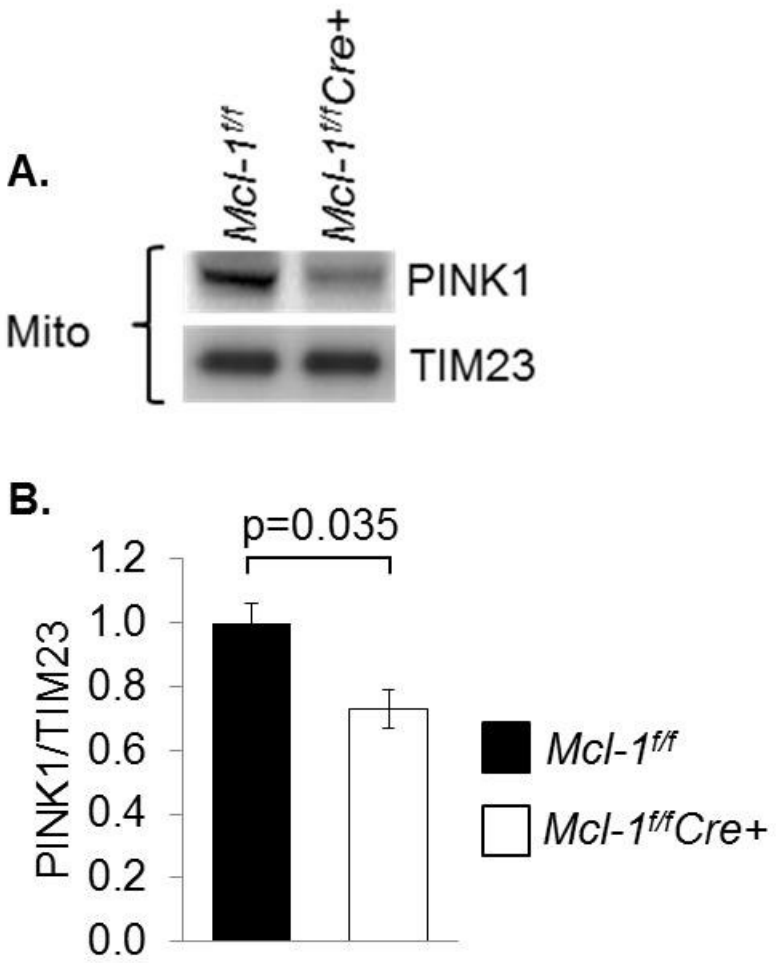

Figure 54: PINK1 levels at mitochondria in *MCL-1$^{f/f}$* and *MCL-1$^{f/f}$Cre+* hearts. **A.** Representative Western blot for PINK1 in the mitochondrial fraction from cardiac lysates one week after initiating tamoxifen treatment. **B.** Quantitation of PINK1 reveals reduced PINK1 protein levels at mitochondria in *MCL-1$^{f/f}$Cre+* hearts (n = 3).

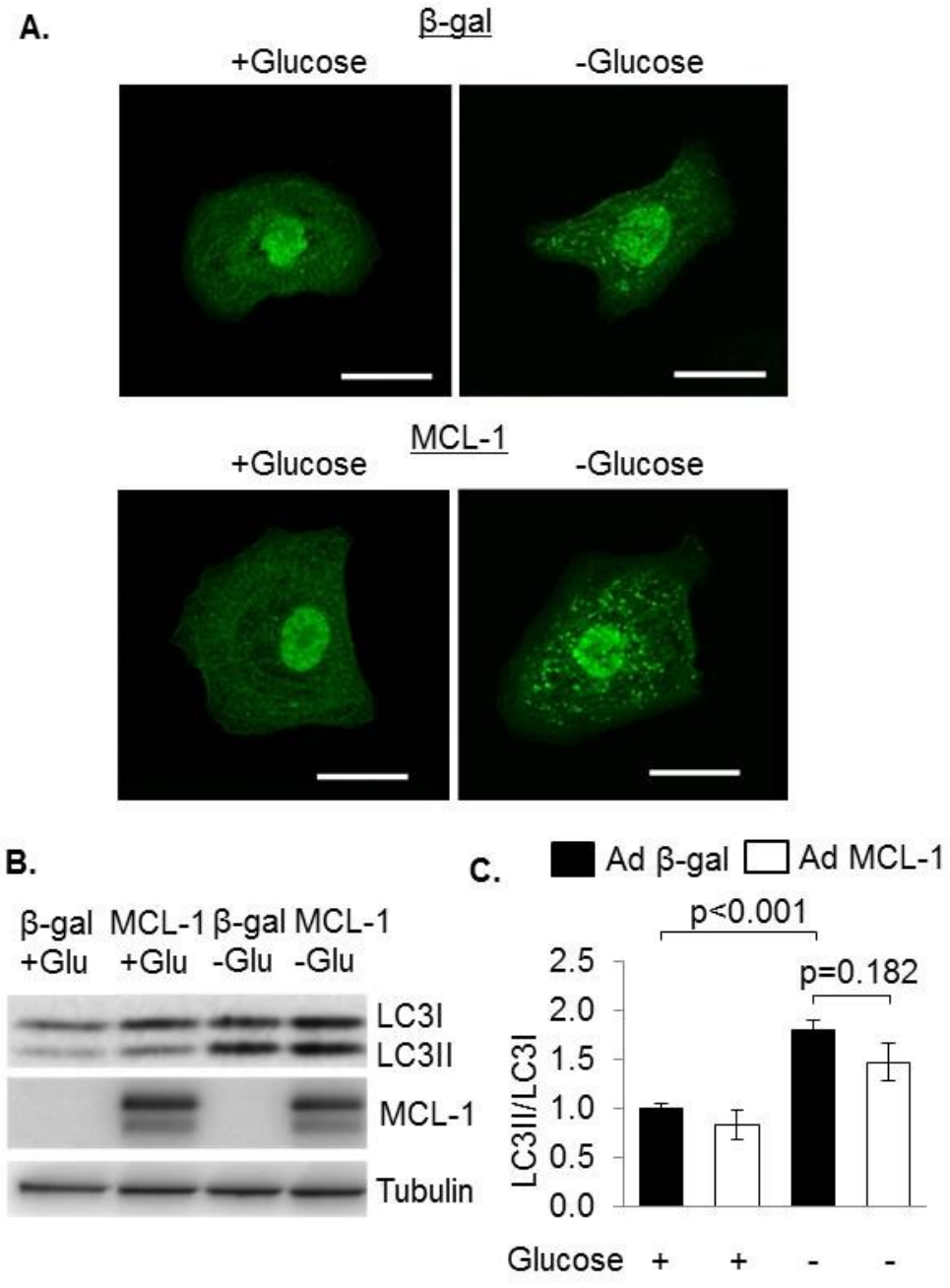

Figure 55: Overexpression of MCL-1 in neonatal cardiac myocytes does not inhibit activation of autophagy. **A.** Representative images of myocytes infected with β-gal or MCL-1 plus GFP-LC3 after six hours of glucose deprivation (scale bar = 20μm). **B.** Western blot for endogenous LC3 in myocytes infected with β-gal or MCL-1 after six hours of glucose (Glu) deprivation. **C.** Quantitation of endogenous LC3II and LC3I levels in neonatal myocytes (n=4).

Chapter 6: Discussion and conclusion

My dissertation research addresses the function of MCL-1 in the heart. This function was previously uncharacterized, and my studies demonstrate that MCL-1 is essential for cardiac homeostasis in adult myocardium. Loss of MCL-1 in cardiac myocytes leads to mitochondrial dysfunction, cardiac necrosis, and rapid development of heart failure. MCL-1 deficiency also disrupts initiation of autophagy under basal conditions and in response to physiological stress. Thus, these findings suggest that in addition to its anti-apoptotic role, MCL-1 is critical in maintaining mitochondrial function and initiating autophagy in cardiac myocytes under normal conditions (Figure 56).

A. MCL-1 expression and processing in cardiac myocytes

My studies show that MCL-1 is highly expressed in normal cardiac tissue. Although the OMM and matrix isoforms of MCL-1 were previously described (Perciavalle *et al.*, 2012), my work is the first to identify these isoforms in the myocardium and demonstrate their differential regulation in response to stress. Myocardial infarction rapidly reduces OMM MCL-1 levels while matrix levels persist. 24 hours after infarction, border zone tissue restores OMM MCL-1 levels and upregulates the matrix isoform. These protein dynamics suggest that MCL-1 is involved in the balance between cell death and survival pathways in vulnerable cardiac myocytes. After cardiac injury, rapid degradation of the anti-apoptotic, OMM isoform may allow apoptosis to

proceed in critically damaged cells. In the meantime, upregulation of the matrix isoform may preserve mitochondrial function in cells that survive this apoptotic window, allowing surviving myocytes to maintain ATP production and recover. The mechanism of this isoform shift remains unclear. OMM MCL-1 may selectively be degraded because it is exposed to cytosolic ubiquitin ligases and caspases while the matrix isoform is protected. Alternatively, MCL-1 on the outer mitochondrial membrane could be selectively imported and cleaved to simultaneously reduce OMM and increase matrix isoforms. Further study will be required to determine which proteins participate in MCL-1 trafficking, and how this process is regulated.

B. MCL-1 ablation leads to mitochondrial dysfunction and necrosis rather than apoptosis

Surprisingly, loss of MCL-1 does not substantially activate apoptosis. Instead, my data suggests that it leads to mitochondrial dysfunction, opening of the mPTP, and subsequent necrotic cell death. Although the anti-apoptotic BCL-2 proteins are well known to regulate the intrinsic pathway of apoptosis, recent studies suggest that this family also plays important roles in other cellular processes including autophagy (Pattingre *et al.*, 2005; Maiuri *et al.*, 2007) and mitochondrial morphology (Berman *et al.*, 2009; Perciavalle *et al.*, 2012). Studies have provided some evidence that MCL-1 has functions beyond regulating apoptosis. For instance, global deletion of MCL-1 results in

peri-implantation embryonic lethality, but *Mcl-1*$^{-/-}$ embryos display normal nuclear architecture and no increase in apoptosis (Rinkenberger *et al.*, 2000). MCL-1 is also important in facilitating mitochondrial fusion and for proper assembly of the F_1F_0-ATP synthase (Perciavalle *et al.*, 2012). Our data show clearly that loss of MCL-1 does not result in massive loss of myocytes due to apoptosis. Instead, loss of MCL-1 leads to mitochondrial swelling and rupturing of the outer mitochondrial membrane. MCL-1 deletion also results in cardiac inflammation, another consequence of necrosis (Frangogiannis, 2012). Cyclophilin D is an important regulator of the mPTP, and mice deficient in CypD are resistant to stresses that promote necrotic cell death (Baines *et al.*, 2005). Interestingly, I found that *Ppif* deletion delays development of cardiac dysfunction and significantly extends survival in MCL-1 deficient mice. These findings suggest that opening of the mPTP and necrotic cell death contribute to the loss of myocytes and development of heart failure, but they are not the underlying cause of the heart failure observed in the MCL-1-deficient mice. Incubation with recombinant MCL-1 has no effect on mitochondrial swelling, indicating that MCL-1 is not a direct regulator of the mPTP. Rather, opening of the mPTP most likely occurs as a consequence of mitochondrial impairment due to MCL-1 deficiency.

Wencker *et al.*, demonstrated that low levels of apoptosis can lead to a lethal cardiomyopathy (Wencker *et al.*, 2003). I have not excluded the possibility that very low levels of apoptosis may contribute to lethality in MCL-

1-deficient mice. However, the lethal cardiac phenotype in MCL-1 knockout mice is exceptionally rapid, indicating that low levels of apoptosis alone are insufficient to produce this phenotype. The absence of significant apoptosis is not surprising since this process is energy dependent. Our data show that loss of MCL-1 leads to defects in mitochondrial respiration which will lead to reduced cellular ATP levels and potentially an inability undergo apoptosis. Interestingly, a companion paper by Wang et al. also reports that loss of MCL-1 leads to rapid development of heart failure, and they discovered that mice lacking BAX/BAK were more resistant to loss of MCL-1 than the CypD knockout mice in our study (Wang *et al.*, 2013). Although the triple BAX/BAK/MCL-1 knockout mice had improved cardiac function and survival, this study also found little evidence of apoptosis upon deletion of MCL-1 in heart tissue (Wang *et al.*, 2013). Thus, the results from our study and the study by Wang *et al.*, suggest the intriguing possibility that BAX/BAK are master regulators of mitochondria-mediated cell death (Thomas *et al.*, 2013; Wang *et al.*, 2013). In fact, a recent study by Whelan *et al.*, found that BAX is an essential regulator of mPTP opening and necrotic cell death in the heart (Whelan *et al.*, 2012). They reported that the BAX/BAK double knockout mice are resistant to both apoptotic and necrotic cell death. These studies confirm that the regulation of cell survival and death by the BCL-2 family proteins is much more complex than initially anticipated. Similarly, previous studies from the Gustafsson lab suggest that BNIP3 induces both apoptosis and necrosis

via BAX/BAK (Kubli *et al.*, 2007; Quinsay *et al.*, 2010). These studies demonstrate that BNIP3 induces permeabilization of the inner mitochondrial membrane as evident by calcein AM release from the matrix in both wild type (WT) and CypD-deficient cells (Quinsay *et al.*, 2010).

C. MCL-1 deficiency leads to impaired autophagy and mitophagy

My dissertation also demonstrates that loss of MCL-1 leads to impaired induction of autophagy. Studies have found that autophagy is essential for homeostasis in the heart under both baseline conditions and in response to stress (Nakai *et al.*, 2007; Matsui *et al.*, 2007; Nishida *et al.*, 2009). Autophagy is also very important in clearing damaged mitochondria in myocytes before they cause harm to the cell (Kubli *et al.*, 2013). Thus, mitochondrial dysfunction combined with inability to clear damaged mitochondria via autophagy as a result of MCL-1 deficiency will quickly be detrimental to the myocyte and accelerate development of heart failure. The finding that MCL-1 deficiency results in impaired autophagy is unexpected since the anti-apoptotic BCL-2 proteins have been reported to inhibit induction of autophagy by sequestering BECLIN-1 (Pattingre *et al.*, 2005; Maiuri *et al.*, 2007). A previous study found that deletion of MCL-1 in cortical neurons led to activation of autophagy (Germain *et al.*, 2011). However, this study found that the levels of other BCL-2 proteins did not change upon loss of MCL-1 in neurons. In contrast, I found a compensatory upregulation of BCL-2 and BCL-

X_L after deletion of MCL-1 in the heart, which could repress autophagy via increased interaction with BECLIN-1. Combined with reduced BECLIN-1 levels in MCL-1 deficient hearts, BCL-2 and BCL-X_L upregulation may reduce autophagosome formation to a level that is insufficient for cardiomyocyte survival. Although the phenotype I observed in MCL-1 deficient hearts resembles the rapid cardiac failure associated with deficient autophagy in ATG5 knockout mice, ATG5 levels were unchanged in *Mcl-1$^{f/f}$Cre*+ hearts (Nakai *et al.,* 2007). Thus, impairment of autophagy is mediated by another mechanism than ATG deficiency in these hearts. Finally, loss of MCL-1 led to upregulation of LAMP-2, which participates in chaperone-mediated autophagy pathways.

The extent of mitochondrial damage in MCL-1 deficient hearts suggests that MCL-1 is required for mitochondrial function. My data shows that MCL-1 deficiency disrupts the PINK1/Parkin pathway. In *Mcl-1$^{f/f}$Cre*+ hearts, Parkin accumulates in the cytosol even though mitochondria are dysfunctional. However, MCL-1 does not appear to interact directly with Parkin by co-immunopreciptation, so it is unlikely to function as a Parkin receptor on mitochondria. Conversely, Parkin overexpression does not alter MCL-1 degradation under basal or stressed conditions, indicating that MCL-1 is not a Parkin substrate. Instead, the loss of MCL-1 appears to disrupt PINK1 accumulation on damaged mitochondria. PINK1 levels should be elevated above baseline in the setting of the mitochondrial damage in *Mcl-1$^{f/f}$Cre*+

hearts, and deficient PINK1 accumulation may explain why Parkin is not recruited to these mitochondria. The resulting loss of mitophagy is likely to exacerbate mitochondrial dysfunction and myocyte death. Additional studies will be needed to determine whether PINK1/Parkin-mediated mitophagy can be activated in *Mcl-1$^{f/f}$Cre+* hearts in response to stress.

In addition to compromising mitophagy, PINK1 dysregulation in MCL-1 deficient hearts may disrupt mitochondrial trafficking and ETC maintenance. PINK1 can phosphorylate MIRO, an atypical Rho GTPase that tethers mitochondria to the tubulin network. Phosphorylation of MIRO1 by PINK1 leads to ubiquitination by Parkin and proteosomal degradation, isolating damaged mitochondria from tubulin transport and the mitochondrial network (Wang et al., 2011). The PINK1/Parkin pathway also regulates selective turnover of specific respiratory chain components (Vincow et al., 2013). Thus, disrupting this pathway may compromise several mitochondrial maintenance mechanisms.

The potential role for MCL-1 in mitophagy is especially interesting in the heart because the process plays a central role in cardiac injury and failure. Cardiovascular disease correlates with energetic and metabolic derangements that severely affect mitochondrial function. These include substrate switching to glyocolytic fuel sources, excess ROS production, lipid accumulation, mitochondrial permeabilization, and deficiencies in mitochondrial coupling (Luk *et al.*, 2012; Aubert *et al.*, 2013; Gustafsson & Gottlieb, 2008; Boudina *et al.*,

2005) In addition, autophagy in the heart declines with age, exacerbating mitochondrial dysfunction and cardiac senescence (Dutta *et al.*, 2012). Novel therapies that maintain mitochondrial integrity and efficiency by facilitating mitophagy have potential to improve clinical outcomes and prevent progression to heart failure. Further study will be required to determine whether MCL-1 expression can be used to promote mitophagy in the heart.

D. Potential pathways for stabilizing MCL-1

Loss of terminally differentiated cardiac myocytes results in a reduced ability to sustain contractile function and can lead to the development of heart failure. Thus, increased understanding of pathways that regulate survival of myocytes is critical for the identification of new therapeutic targets to treat or prevent heart failure. MCL-1 plays an important role in cardiac myocyte survival, and preserving endogenous MCL-1 in the setting of heart disease may represent a novel therapeutic opportunity. Since MCL-1 is a potential oncogene, the protein is a poor candidate for gene therapy. Instead, efforts to preserve MCL-1 expression could target proteins that govern post-translational regulation of MCL-1. MCL-1 ubiquitin ligase E3 (MULE) targets MCL-1 for proteosomal degredation, while USP9X deubiquitinase stabilizes MCL-1 (Zhong et al., 2005; Schwickart et al., 2010). Modulating these regulatory proteins could promote MCL-1 stability, and they may prove to be better drug targets than MCL-1 itself.

A second regulatory pathway involves the chaperone protein HSP70. HSP70 is involved in protein trafficking to mitochondria and HSP70 overexpression has been shown to prevent MCL-1 degradation in the setting of stress (Young *et al.,* 2003). Specifically, HSP70 prevents MCL-1 ubiquitination by MULE and promotes continued MCL-1 synthesis (Stankiewicz *et al.,* 2009; Liu *et al.,* 1992). HSP70 also participates in transport and assembly of mitochondrial matrix protiens (Kang et al., 1990), and may play a role in the matrix accumulation of MCL-1 after myocardial infarction. Activating HSP70 in the setting of cardiac injury may protect mitochondria by preserving the expression of MCL-1 and other mitochondrial protiens. HSP70 also interacts with co-chaperones such as BAG3 that stabilize MCL-1 (Boiani *et al.,* 2013) providing additional potential targets for intervention.

Finally, recent work by Ekholm-Reed *et al.,* demonstrates that Parkin actually degrades a multisubunit ubiquitin ligase named Fbw7β in neurons, leading to MCL-1 stabilization and enhanced cell survival in the setting of oxidative stress (Ekholm-Reed *et al.,* 2013*).* If a similar pathway operates in the heart, then Parkin upregulation in the cytosol may have resulted from the heart's attempt to preserve declining MCL-1 levels. This study also corroborates my finding that crosstalk between Parkin and MCL-1 proceed through protein intermediates rather than direct interaction.

E. Potential cardiac toxicity of chemotherapeutic MCL-1 antagonists

A number of BCL-2 family protein inhibitors have entered clinical trials for the treatment of leukemia, lymphoma, and solid tumors (Azmi *et al.*, 2011). Some of these specifically target MCL-1 in an effort to counter its anti-apoptotic effects (Dash *et al.*, 2011). Unfortunately, our study suggests that antagonizing MCL-1 may lead to significant cardiotoxicity. Indeed my studies demonstrate that targeting MCL-1 may rapidly lead myocardial dysfunction. By compromising both autophagy and mitochondrial function, MCL-1 inhibitors are likely to affect the cells' energy supply. Although these effects on mitochondria may potentiate chemotherapeutic cytotoxicity, the Warburg effect reduces dependence on mitochondrial respiration in many malignancies by upregulating glycolytic machinery (Bensinger & Christofk, 2012). In contrast, cardiac myocytes rely on mitochondria for ATP to maintain contraction and exhibit the greatest mitochondrial density of any tissue in the body, making the heart especially vulnerable to antagonists that target MCL-1. The story of double-edged chemotherapeutics with cardiotoxicity is familiar from our experience with anthracyclines such as doxorubicin. Despite this concern, BCL-2 family inhibitors may become useful chemotherapeutics. Chemotherapeutic proteosome inhibitors such as Bortezomib exhibit pronounced drug toxicity that can be moderated using transient dosing and recovery periods (Hainsworth, *et al.,* 2008). In order to evaluate the effects of partial MCL-1 reduction in the myocardium, I monitored cardiac function in

tamoxifen-treated mice that were heterozygous for the floxed-MCL-1 allele. I found that partial MCL-1 ablation in the heart produces transient cardiac dysfunction that improves with time. These results suggest that temporary, reversible MCL-1 blockade may be therapeutically viable. Further characterization of MCL-1 in the heart, however, will be required to employ MCL-1 antagonists safely.

F. Future Studies

My current findings recommend a number of future studies that would extend the scope and impact of the work presented here. This dissertation implicates a number of potential protein binding partners for MCL-1 in the heart. MCL-1 appears to interact with DRP-1, but the significance of this interaction has not been characterized. After MCL-1 deletion, DRP-1 is not recruited to mitochondria despite mitochondrial dysfunction. Fission is necessary for mitochondrial pruning by mitophagy, and compromised DRP-1 function may contribute to mitochondrial disorganization in MCL-1 deficient hearts. MCL-1 may also interact with PINK1 to promote PINK1 accumulation on dysfunctional mitochondria. Although MCL-1 deficient hearts exhibit mitochondrial impairment with paradoxically reduced PINK1 levels, a specific relationship linking MCL-1 and PINK1 has not been clarified. Finally, BH domain binding partners of MCL-1 have been extensively characterized, but no studies have comprehensively addressed MCL-1 interactions with other

protein families. My data demonstrates that MCL-1 deletion alters the expression of BECLIN-1 and LAMP-2 and reduces autophagic flux in the heart. MCL-1 may interact with other autophagic proteins, and new binding partners may potentially be identified in cardiac myocytes using MCL-1 immunoprecipitation followed by mass spectrometry to analyze associated protein complexes.

Having identified outer mitochondrial membrane and matrix isoforms of MCL-1 across murine tissues including myocardium, future efforts should address the function of each isoform in myocytes. Monitoring the dynamics of endogenous MCL-1 *in vitro* provides an opportunity to accessibly study individual isoform dynamics in response to apoptotic (i.e. staurosporine), necrotic (i.e. peroxide), autophagic (i.e. starvation), mitochondrial (i.e. FCCP), and ischemic (I/R) stressors. In addition, genetic constructs have been developed that can be used to overexpress outer mitochondrial and matrix MCL-1 isoforms individually (Perciavalle *et al.,* 2012). Studies that establish how the individual isoforms affect mitochondrial morphology, mitochondrial autophagy/clearance, and cell survival in cardiac myocytes are likely to provide important new insights into the functions of MCL-1 in the heart.

G. Summary

My results demonstrate that the loss of MCL-1 leads to rapid mitochondrial dysfunction, impaired autophagy, and heart failure in the

absence of stress. To my knowledge, this is the first study that selectively deletes an anti-apoptotic BCL-2 family protein in the heart, and explores the function of MCL-1 in that organ. My dissertation also suggests that therapies that preserve endogenous MCL-1 have therapeutic potential for cardiovascular disease. Finally, chemotherapeutics that target MCL-1 must be carefully designed to avoid cardiotoxicity.

Acknowledgments

Chapter 6, in part, is a reprint of the material as it appears in Thomas *et al.*, Circ J, 2013, Thomas *et al.*, Autophagy 2013, and Thomas et al., Genes Dev, 2013. The dissertation author was the primary investigator and author of these papers.

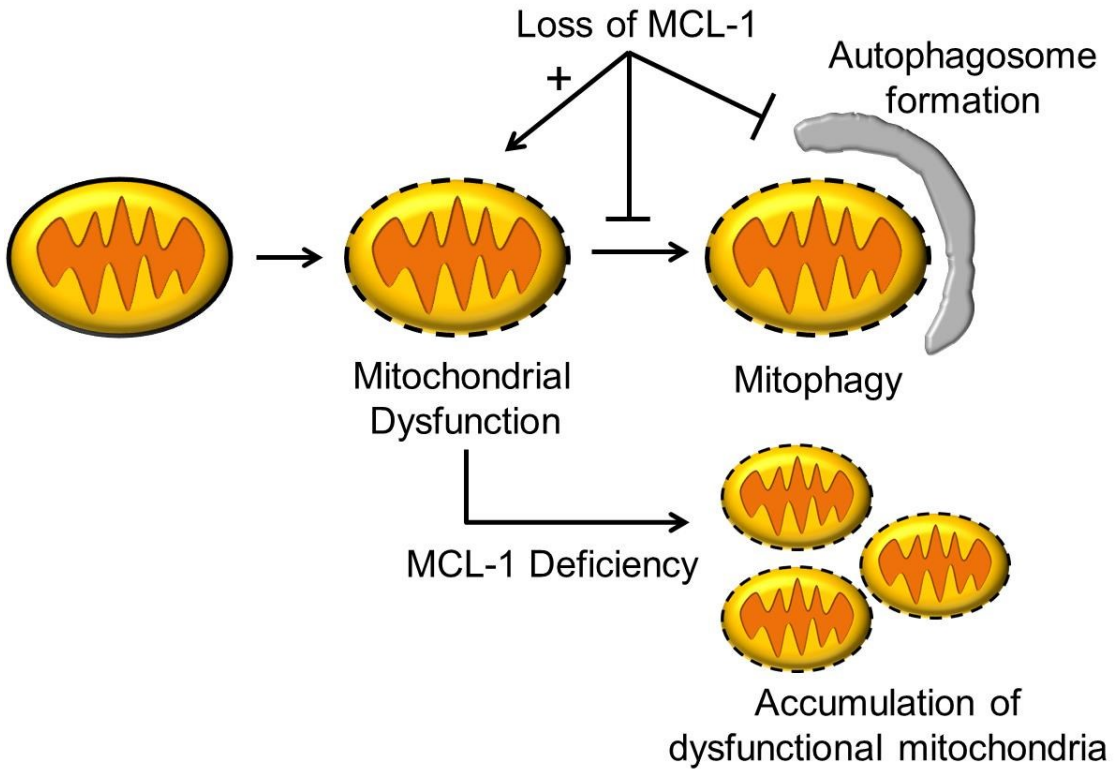

Figure 56: Model for detrimental effects of MCL-1 deficiency. Mitochondrial integrity and clearance are both compromised, exacerbating mitochondrial dysfunction.

References

Aldous SJ. Cardiac biomarkers in acute myocardial infarction. Int J Cardiol. 2013 Apr 15;164(3):282-94.

Aubert G, Vega RB, Kelly DP. Perturbations in the gene regulatory pathways controlling mitochondrial energy production in the failing heart. Biochim Biophys Acta. 2013 Apr;1833(4):840-7.

Azmi AS, Wang Z, Philip PA, Mohammad RM, Sarkar FH. Emerging Bcl-2 inhibitors for the treatment of cancer. Expert Opin Emerg Drugs. 2011 Mar;16(1):59-70.

Baines CP, Kaiser RA, Purcell NH, Blair NS, Osinska H, Hambleton MA, Brunskill EW, Sayen MR, Gottlieb RA, Dorn GW, Robbins J, Molkentin JD. Loss of cyclophilin D reveals a critical role for mitochondrial permeability transition in cell death. Nature. (2005) Mar 31;434(7033): 658-62.

Bandyopadhyay U, Sridhar S, Kaushik S, Kiffin R, Cuervo AM. Identification of regulators of chaperone-mediated autophagy. Mol Cell. 2010 Aug 27;39(4):535-47.

Bensinger SJ, Christofk HR. New aspects of the Warburg effect in cancer cell biology. Semin Cell Dev Biol. 2012 Jun;23(4):352-61.

Berman SB, Chen YB, Qi B, McCaffery JM, Rucker EB 3rd, Goebbels S, Nave KA, Arnold BA, Jonas EA, Pineda FJ, Hardwick JM. Bcl-x L increases mitochondrial fission, fusion, and biomass in neurons. J Cell Biol. 2009 Mar 9;184(5):707-19.

Beroukhim R, Mermel CH, Porter D, Wei G, Raychaudhuri S, Donovan J, Barretina J, Boehm JS, Dobson J, Urashima M, Mc Henry KT, Pinchback RM, Ligon AH, Cho YJ, Haery L, Greulich H, Reich M, Winckler W, Lawrence MS, Weir BA, Tanaka KE, Chiang DY, Bass AJ, Loo A, Hoffman C, Prensner J, Liefeld T, Gao Q, Yecies D, Signoretti S, Maher E, Kaye FJ, Sasaki H, Tepper JE, Fletcher JA, Tabernero J, Baselga J, Tsao MS, Demichelis F, Rubin MA, Janne PA, Daly MJ, Nucera C, Levine RL, Ebert BL, Gabriel S, Rustgi AK, Antonescu CR, Ladanyi M, Letai A, Garraway LA, Loda M, Beer DG, True LD, Okamoto A, Pomeroy SL, Singer S, Golub TR, Lander ES, Getz G, Sellers WR, Meyerson M. The landscape of somatic copy-number alteration across human cancers. Nature. 2010 Feb 18;463(7283):899-905.

Boiani M, Daniel C, Liu X, Hogarty MD, Marnett LJ. The stress protein BAG3 stabilizes Mcl-1 protein and promotes survival of cancer cells and resistance to antagonist ABT-737. J Biol Chem. 2013 Mar 8;288(10):6980-90.

Boise LH, González-García M, Postema CE, Ding L, Lindsten T, Turka LA, Mao X, Nuñez G, Thompson CB. bcl-x, a bcl-2-related gene that functions as a dominant regulator of apoptotic cell death. Cell. 1993 Aug 27;74(4):597-608.

Boudina S, Sena S, O'Neill BT, Tathireddy P, Young ME, Abel ED. Reduced mitochondrial oxidative capacity and increased mitochondrial uncoupling impair myocardial energetics in obesity. Circulation. 2005 Oct 25;112(17):2686-95.

Boya P, Reggiori F, Codogno P. Emerging regulation and functions of autophagy. Nat Cell Biol. 2013 Jul;15(7):713-20.

Bugger H, Schwarzer M, Chen D, Schrepper A, Amorim PA, Schoepe M, Nguyen TD, Mohr FW, Khalimonchuk O, Weimer BC, Doenst T. Proteomic remodelling of mitochondrial oxidative pathways in pressure overload-induced heart failure. Cardiovasc Res. 2010 Jan 15;85(2):376-84.

Carreira RS, Lee Y, Ghochani M, Gustafsson ÅB, Gottlieb RA. Cyclophilin D is required for mitochondrial removal by autophagy in cardiac cells. Autophagy. 2010 May;6(4):462-72.

Chatterjee K, Zhang J, Honbo N, Karliner JS. Doxorubicin cardiomyopathy. Cardiology. 2010;115(2):155-62.

Chen Y, Dorn GW 2nd. PINK1-phosphorylated mitofusin 2 is a Parkin receptor for culling damaged mitochondria. Science. 2013 Apr 26;340(6131):471-5.

Chen Z, Chua CC, Ho YS, Hamdy RC, Chua BH. Overexpression of Bcl-2 attenuates apoptosis and protects against myocardial I/R injury in transgenic mice. Am J Physiol Heart Circ Physiol. 2001 May;280(5):H2313-20.

Chen-Levy Z, Nourse J, Cleary ML. The bcl-2 candidate proto-oncogene product is a 24-kilodalton integral-membrane protein highly expressed in lymphoid cell lines and lymphomas carrying the t(14;18) translocation. Mol Cell Biol. 1989 Feb;9(2):701-10.

Chomczynski P, Sacchi N. Single-step method of RNA isolation by acid guanidinium thiocyanate-phenol-chloroform extraction. Anal Biochem. 1987 Apr;162(1):156-9.

Czerski L, Nuñez G. Apoptosome formation and caspase activation: is it different in the heart? Journal of Molecular and Cellular Cardiology (2004) 37(3): 643-652

Dash R, Azab B, Quinn BA, Shen X, Wang XY, Das SK, Rahmani M, Wei J, Hedvat M, Dent P, Dmitriev IP, Curiel DT, Grant S, Wu B, Stebbins JL, Pellecchia M, Reed JC, Sarkar D, Fisher PB. Apogossypol derivative BI-97C1 (Sabutoclax) targeting Mcl-1 sensitizes prostate cancer cells to mda-7/IL-24-mediated toxicity. Proc Natl Acad Sci. 2011 108(21):8785-8790.

D'Agostino RB Sr, Vasan RS, Pencina MJ, Wolf PA, Cobain M, Massaro JM, Kannel WB.General cardiovascular risk profile for use in primary care: the Framingham Heart Study. Circulation. 2008 Feb 12;117(6):743-53.

de Haan JJ, Smeets MB, Pasterkamp G, Arslan F. Danger Signals in the Initiation of the Inflammatory Response after Myocardial Infarction. Mediators Inflamm. 2013;2013:206039.

Del Re DP, Miyamoto S, Brown JH. RhoA/Rho kinase up-regulate Bax to activate a mitochondrial death pathway and induce cardiomyocyte apoptosis. J Biol Chem. 2007 Mar 16;282(11):8069-78.

Diwan A, Krenz M, Syed FM, Wansapura J, Ren X, Koesters AG, Li H, Kirshenbaum LA, Hahn HS, Robbins J, Jones WK, Dorn GW. 2007 Inhibition of ischemic cardiomyocyte apoptosis through targeted ablation of Bnip3 restrains postinfarction remodeling in mice. *J Clin Invest* **117**:2825-2833.

Dorn GW 2nd. Mitochondrial pruning by Nix and BNip3: an essential function for cardiac-expressed death factors. J Cardiovasc Transl Res. 2010 Aug;3(4):374-83.

Dorn II GW. Mitochondrial dynamism and cardiac fate. Circ J. 2013 May 24;77(6):1370-9.

Dutta D, Calvani R, Bernabei R, Leeuwenburgh C, Marzetti E. Contribution of impaired mitochondrial autophagy to cardiac aging: mechanisms and therapeutic opportunities. Circ Res. 2012 Apr 13;110(8):1125-38.

Ekholm-Reed S, Goldberg MS, Schlossmacher MG, Reed SI.Parkin-dependent degradation of the F-box protein Fbw7β promotes neuronal survival in response to oxidative stress by stabilizing Mcl-1. Mol Cell Biol. 2013 Sep;33(18):3627-43.

Elgendy M, Sheridan C, Brumatti G, Martin SJ. Oncogenic Ras-Induced Expression of Noxa and Beclin-1Promotes Autophagic Cell Death and Limits Clonogenic Survival. Mol Cell. 2011 Apr 8;42(1): 23-35.

Elrod JW, Molkentin JD. Physiologic functions of cyclophilin D and the mitochondrial permeability transition pore. Circ J. 2013;77(5):1111-22.

Foo RS, Mani K, Kitsis RN. Death begets failure in the heart. J Clin Invest. 2005 Mar;115(3):565-71.

Frangogiannis NG. Regulation of the inflammatory response in cardiac repair. Circ Res. 2012 Jan 6;110(1):159-73.

Frazier AE, Thorburn DR. Biochemical analyses of the electron transport chain complexes by spectrophotometry. Methods Mol Biol. 2012;837:49-62.

Geisler S, Holmström KM, Skujat D, Fiesel FC, Rothfuss OC, Kahle PJ, Springer W. PINK1/Parkin-mediated mitophagy is dependent on VDAC1 and p62/SQSTM1. Nat Cell Biol. 2010 Feb;12(2):119-31.

Germain M, Nguyen AP, Le Grand JN, Arbour N, Vanderluit JL, Park DS, Opferman JT, Slack RS. MCL-1 is a stress sensor that regulates autophagy in a developmentally regulated manner. EMBO J. 2011 Jan 19;30(2):395-407.

Glaser SP, Lee EF, Trounson E, Bouillet P, Wei A, Fairlie WD, Izon DJ, Zuber J, Rappaport AR, Herold MJ, Alexander WS, Lowe SW, Robb L, Strasser A. Anti-apoptotic Mcl-1 is essential for the development and sustained growth of acute myeloid leukemia. Genes Dev. 2012 Jan 15;26(2):120-5.

Go AS, Mozaffarian D, Roger VL, Benjamin EJ, Berry JD, Borden WB, Bravata DM, Dai S, Ford ES, Fox CS, Franco S, Fullerton HJ, Gillespie C, Hailpern SM, Heit JA, Howard VJ, Huffman MD, Kissela BM, Kittner SJ, Lackland DT, Lichtman JH, Lisabeth LD, Magid D, Marcus GM, Marelli A, Matchar DB, McGuire DK, Mohler ER, Moy CS, Mussolino ME, Nichol G, Paynter NP, Schreiner PJ, Sorlie PD, Stein J, Turan TN, Virani SS, Wong ND, Woo D, Turner MB; American Heart Association Statistics Committee and Stroke Statistics Subcommittee. Executive summary: heart disease and stroke statistics--2013 update: a report from the American Heart Association. Circulation. 2013 Jan 1;127(1):143-52.

Goff DJ, Recart AC, Sadarangani A, Chun HJ, Barrett CL, Krajewska M, Leu H, Low-Marchelli J, Ma W, Shih AY, Wei J, Zhai D, Geron I, Pu M, Bao L, Chuang R, Balaian L, Gotlib J, Minden M, Martinelli G, Rusert J, Dao KH, Shazand K, Wentworth P, Smith KM, Jamieson CA, Morris SR, Messer K,

Goldstein LS, Hudson TJ, Marra M, Frazer KA, Pellecchia M, Reed JC, Jamieson CH. A Pan-BCL2 inhibitor renders bone-marrow-resident human leukemia stem cells sensitive to tyrosine kinase inhibition. Cell Stem Cell. 2013 Mar 7;12(3):316-28.

Gomes LC, Di Benedetto G, Scorrano L. During autophagy mitochondria elongate, are spared from degradation and sustain cell viability. Nat Cell Biol. 2011 May;13(5):589-98.

Grover GJ, Atwal KS, Sleph PG, Wang FL, Monshizadegan H, Monticello T, Green DW. Excessive ATP hydrolysis in ischemic myocardium by mitochondrial F1F0-ATPase: effect of selective pharmacological inhibition of mitochondrial ATPase hydrolase activity. Am J Physiol Heart Circ Physiol. 2004 Oct;287(4):H1747-55.

Gullestad L, Ueland T, Vinge LE, Finsen A, Yndestad A, Aukrust P. Inflammatory cytokines in heart failure: mediators and markers. Cardiology. 2012;122(1):23-35.

Gupta MP. Factors controlling cardiac myosin-isoform shift during hypertrophy and heart failure. J Mol Cell Cardiol. 2007 Oct;43(4):388-403.

Gustafsson AB, Gottlieb RA. Bcl-2 family members and apoptosis, taken to heart. Am J Physiol Cell Physiol. 2007 Jan;292(1):C45-51.

Gustafsson AB, Gottlieb RA. Heart mitochondria: gates of life and death. Cardiovasc Res. 2008 Jan 15;77(2):334-43.

Gustafsson AB, Gottlieb RA. Recycle or die: the role of autophagy in cardioprotection. J Mol Cell Cardiol. 2008 Apr;44(4):654-61.

Hainsworth JD, Spigel DR, Barton J, Farley C, Schreeder M, Hon J, Greco FA. Weekly treatment with bortezomib for patients with recurrent or refractory multiple myeloma: a phase 2 trial of the Minnie Pearl Cancer Research Network. Cancer. 2008 Aug 15;113(4):765-71.

Hamacher-Brady A, Brady NR, Logue SE, Sayen MR, Jinno M, Kirshenbaum LA, Gottlieb RA, Gustafsson AB. Response to myocardial ischemia/ reperfusion injury involves Bnip3 and autophagy. Cell Death Differ. 2007 Jan;14(1):146-57.

Han J, Goldstein LA, Hou W, Rabinowich H. Functional linkage between NOXA and Bim in mitochondrial apoptotic events. J Biol Chem. 2007 Jun 1;282(22):16223-31.

Hanna RA, Quinsay MN, Orogo AM, Giang K, Rikka S, Gustafsson ÅB. Microtubule-associated protein 1 light chain 3 (LC3) interacts with Bnip3 protein to selectively remove endoplasmic reticulum and mitochondria via autophagy. J Biol Chem. 2012 Jun 1;287(23):19094-104.

Hara T, Nakamura K, Matsui M, Yamamoto A, Nakahara Y, Suzuki-Migishima R, Yokoyama M, Mishima K, Saito I, Okano H, Mizushima N. Suppression of basal autophagy in neural cells causes neurodegenerative disease in mice. Nature. 2006 Jun 15;441(7095):885-9.

He C, Bassik MC, Moresi V, Sun K, Wei Y, Zou Z, An Z, Loh J, Fisher J, Sun Q, Korsmeyer S, Packer M, May HI, Hill JA, Virgin HW, Gilpin C, Xiao G, Bassel-Duby R, Scherer PE, Levine B. Exercise-induced BCL2-regulated autophagy is required for muscle glucose homeostasis. Nature. 2012 Jan 18;481(7382):511-5.

Hoshino A, Matoba S, Iwai-Kanai E, Nakamura H, Kimata M, Nakaoka M, Katamura M, Okawa Y, Ariyoshi M, Mita Y, Ikeda K, Ueyama T, Okigaki M, Matsubara H. p53-TIGAR axis attenuates mitophagy to exacerbate cardiac damage after ischemia. J Mol Cell Cardiol. 2012 Jan;52(1):175-84.

Huang CR, Yang-Yen HF. The fast-mobility isoform of mouse Mcl-1 is a mitochondrial matrix-localized protein with attenuated anti-apoptotic activity. FEBS Lett. 2010 Aug 4;584(15):3323-30.

Huang J, Ito Y, Morikawa M, Uchida H, Kobune M, Sasaki K, Abe T, Hamada H. Bcl-xL gene transfer protects the heart against ischemia/reperfusion injury. Biochem Biophys Res Commun. 2003 Nov 7;311(1):64-70.

Hutchins MU, Veenhuis M, Klionsky DJ. Peroxisome degradation in Saccharomyces cerevisiae is dependent on machinery of macroautophagy and the Cvt pathway. J Cell Sci. 1999 Nov;112 (Pt 22):4079-87.

Imahashi K, Schneider MD, Steenbergen C, Murphy E. Transgenic expression of Bcl-2 modulates energy metabolism, prevents cytosolic acidification during ischemia, and reduces ischemia/reperfusion injury. Circ Res. 2004 Oct 1;95(7):734-41.

Iwai-Kanai E, Yuan H, Huang C, Sayen MR, Perry-Garza CN, Kim L, Gottlieb RA. A method to measure cardiac autophagic flux in vivo. Autophagy. 2008 Apr;4(3):322-9.

Jin SM, Youle RJ. The accumulation of misfolded proteins in the mitochondrial matrix is sensed by PINK1 to induce PARK2/Parkin-mediated mitophagy of polarized mitochondria. Autophagy. 2013 Nov 1;9(11):1750-7.
Kabeya Y, Mizushima N, Ueno T, Yamamoto A, Kirisako T, Noda T, Kominami E, Ohsumi Y, Yoshimori T. LC3, a mammalian homologue of yeast Apg8p, is localized in autophagosome membranes after processing. EMBO J. 2000 Nov 1;19(21):5720-8.

Kang MH, Reynolds CP. Bcl-2 inhibitors: targeting mitochondrial apoptotic pathways in cancer therapy. Clin Cancer Res. 2009 Feb 15;15(4):1126-32.

Kang PJ, Ostermann J, Shilling J, Neupert W, Craig EA, Pfanner N. Requirement for hsp70 in the mitochondrial matrix for translocation and folding of precursor proteins. Nature. 1990 Nov 8;348(6297):137-43.

Kiefer MC, Brauer MJ, Powers VC, Wu JJ, Umansky SR, Tomei LD, Barr PJ. Modulation of apoptosis by the widely distributed Bcl-2 homologue Bak. Nature. 1995 Apr 20;374(6524):736-9.

Kim Y, Park J, Kim S, Song S, Kwon SK, Lee SH, et, al. PINK1 controls mitochondrial localization of Parkin through direct phosphorylation. Biochem Biophys Res Commun. 2008 Dec 19;377(3):975-80.

Kirshenbaum LA, de Moissac D. The bcl-2 gene product prevents programmed cell death of ventricular myocytes. Circulation. 1997 Sep 2;96(5):1580-5.

Kitada T, Asakawa S, Hattori N, Matsumine H, Yamamura Y, Minoshima S, Yokochi M, Mizuno Y, Shimizu N. Mutations in the parkin gene cause autosomal recessive juvenile parkinsonism. Nature. 1998 Apr 9;392(6676):605-8.

Koitabashi N, Bedja D, Zaiman AL, Pinto YM, Zhang M, Gabrielson KL, Takimoto E, Kass DA. Avoidance of transient cardiomyopathy in cardiomyocyte-targeted tamoxifen-induced MerCreMer gene deletion models. Circ Res. 2009 Jul 2;105(1):12-5.

Komatsu M, Waguri S, Koike M, Sou YS, Ueno T, Hara T, Mizushima N, Iwata J, Ezaki J, Murata S, Hamazaki J, Nishito Y, Iemura S, Natsume T, Yanagawa T, Uwayama J, Warabi E, Yoshida H, Ishii T, Kobayashi A, Yamamoto M, Yue Z, Uchiyama Y, Kominami E, Tanaka K. Homeostatic levels of p62 control cytoplasmic inclusion body formation in autophagy-deficient mice. Cell. 2007 Dec 14;131(6):1149-63.

Korsmeyer SJ, Shutter JR, Veis DJ, Merry DE, Oltvai ZN. Bcl-2/Bax: a rheostat that regulates an anti-oxidant pathway and cell death. Semin Cancer Biol. 1993 Dec;4(6):327-32.

Kozopas KM, Yang T, Buchan HL, Zhou P, Craig RW. MCL1, a gene expressed in programmed myeloid cell differentiation, has sequence similarity to BCL2. Proc Natl Acad Sci U S A. 1993 Apr 15;90(8):3516-20.

Kraft C, Deplazes A, Sohrmann M, Peter M. Mature ribosomes are selectively degraded upon starvation by an autophagy pathway requiring the Ubp3p/Bre5p ubiquitin protease. Nat Cell Biol. 2008 May;10(5):602-10.

Krajewski S, Bodrug S, Krajewska M, Shabaik A, Gascoyne R, Berean K, Reed JC. Immunohistochemical analysis of Mcl-1 protein in human tissues. Differential regulation of Mcl-1 and Bcl-2 protein production suggests a unique role for Mcl-1 in control of programmed cell death in vivo. Am J Pathol. 1995 Jun;146(6):1309-19.

Kubli DA, Ycaza JE, Gustafsson AB. Bnip3 mediates mitochondrial dysfunction and cell death through Bax and Bak. Biochem J. 2007 Aug 1;405(3):407-15.

Kubli DA, Gustafsson ÅB. Mitochondria and mitophagy: the yin and yang of cell death control. Circ Res. 2012 Oct 12;111(9):1208-21.

Kubli DA, Zhang X, Lee Y, Hanna RA, Quinsay MN, Nguyen CK, Jimenez R, Petrosyan S, Murphy AN, Gustafsson AB. Parkin protein deficiency exacerbates cardiac injury and reduces survival following myocardial infarction. J Biol Chem. 2013 Jan 11;288(2):915-26.

Kung G, Konstantinidis K, Kitsis RN. Programmed necrosis, not apoptosis, in the heart. Circ Res. 2011 Apr 15;108(8):1017-36.

Levine B, Kroemer G. Autophagy in the pathogenesis of disease. Cell. 2008 Jan 11;132(1):27-42.

Lin X, Morgan-Lappe S, Huang X, Li L, Zakula DM, Vernetti LA, Fesik SW, Shen Y. 'Seed' analysis of off-target siRNAs reveals an essential role of Mcl-1 in resistance to the small-molecule Bcl-2/Bcl-XL inhibitor ABT-737. Oncogene. 2007 Jun 7;26(27):3972-9.

Lip GY, Gibbs CR. Does heart failure confer a hypercoagulable state? Virchow's triad revisited. J Am Coll Cardiol. 1999 Apr;33(5):1424-6.

Liu RY, Li X, Li L, Li GC. Expression of human hsp70 in rat fibroblasts enhances cell survival and facilitates recovery from translational and transcriptional inhibition following heat shock. Cancer Res. 1992 Jul 1;52(13):3667-73.
Lu Y, Rolland SG, Conradt B. A molecular switch that governs mitochondrial fusion and fission mediated by the BCL2-like protein CED-9 of Caenorhabditis elegans. Proc Natl Acad Sci U S A. 2011 Oct 11;108(41):E813-22.

Luk TH, Dai YL, Siu CW, Yiu KH, Li SW, Fong B, Wong WK, Tam S, Tse HF. Association of lower habitual physical activity level with mitochondrial and endothelial dysfunction in patients with stable coronary artery disease. Circ J. 2012;76(11):2572-8.

Maiuri MC, Le Toumelin G, Criollo A, Rain JC, Gautier F, Juin P, Tasdemir E, Pierron G, Troulinaki K, Tavernarakis N, Hickman JA, Geneste O, Kroemer G. Functional and physical interaction between Bcl-X(L) and a BH3-like domain in Beclin-1. EMBO J. 2007 May 16;26(10):2527-39.

Mani K. Programmed cell death in cardiac myocytes: strategies to maximize post-ischemic salvage. Heart Fail Rev. 2008 Jun;13(2):193-209.

Matsuda N, Sato S, Shiba K, Okatsu K, Saisho K, Gautier CA, Sou YS, Saiki S, Kawajiri S, Sato F, Kimura M, Komatsu M, Hattori N, Tanaka K. PINK1 stabilized by mitochondrial depolarization recruits Parkin to damaged mitochondria and activates latent Parkin for mitophagy. J Cell Biol. 2010 Apr 19;189(2):211-21.

Matsui Y, Takagi H, Qu X, Abdellatif M, Sakoda H, Asano T, Levine B, Sadoshima J. Distinct roles of autophagy in the heart during ischemia and reperfusion: roles of AMP-activated protein kinase and Beclin 1 in mediating autophagy.Circ Res. 2007 Mar 30;100(6):914-22.

McDonnell TJ, Deane N, Platt FM, Nunez G, Jaeger U, McKearn JP, Korsmeyer SJ. bcl-2-immunoglobulin transgenic mice demonstrate extended B cell survival and follicular lymphoproliferation. Cell. 1989 Apr 7;57(1):79-88.

Mizushima N, Levine B, Cuervo AM, Klionsky DJ. Autophagy fights disease through cellular self-digestion. Nature. 2008 Feb 28;451(7182):1069-75

Mizushima N, Yoshimori T, Levine B. Methods in mammalian autophagy research. Cell. 2010 Feb 5;140(3):313-26.

Motoyama N, Wang F, Roth KA, Sawa H, Nakayama K, Nakayama K, Negishi I, Senju S, Zhang Q, Fujii S, Loh D. Massive cell death of immature

hematopoietic cells and neurons in Bcl-x-deficient mice. Science. 1995 Mar 10;267(5203):1506-10.

Nakai A, Yamaguchi O, Takeda T, Higuchi Y, Hikoso S, Taniike M, Omiya S, Mizote I, Matsumura Y, Asahi M, Nishida K, Hori M, Mizushima N, Otsu K. The role of autophagy in cardiomyocytes in the basal state and in response to hemodynamic stress. Nat Med. 2007 May;13(5): 619-24.

Nakayama H, Chen X, Baines CP, Klevitsky R, Zhang X, Zhang H, Jaleel N, Chua BH, Hewett TE, Robbins J, Houser SR, Molkentin JD. Ca2+- and mitochondrial-dependent cardiomyocyte necrosis as a primary mediator of heart failure. J Clin Invest. 2007 Sep;117(9): 2431-44.

Narendra DP, Jin SM, Tanaka A, Suen DF, Gautier CA, Shen J, Cookson MR, Youle RJ. PINK1 is selectively stabilized on impaired mitochondria to activate Parkin. PLoS Biol. 2010 Jan 26;8(1):e1000298.

Nguyen M, Marcellus RC, Roulston A, Watson M, Serfass L, Murthy Madiraju SR, Goulet D, Viallet J, Bélec L, Billot X, Acoca S, Purisima E, Wiegmans A, Cluse L, Johnstone RW, Beauparlant P, Shore GC. Small molecule obatoclax (GX15-070) antagonizes MCL-1 and overcomes MCL-1-mediated resistance to apoptosis. Proc Natl Acad Sci U S A. 2007 Dec 4;104(49):19512-7.

Nishino I, Fu J, Tanji K, Yamada T, Shimojo S, Koori T, Mora M, Riggs JE, Oh SJ, Koga Y, Sue CM, Yamamoto A, Murakami N, Shanske S, Byrne E, Bonilla E, Nonaka I, DiMauro S, Hirano M. Primary LAMP-2 deficiency causes X-linked vacuolar cardiomyopathy and myopathy (Danon disease). Nature. 2000 Aug 24;406(6798):906-10.

Oka T, Hikoso S, Yamaguchi O, Taneike M, Takeda T, Tamai T, Oyabu J, Murakawa T, Nakayama H, Nishida K, Akira S, Yamamoto A, Komuro I, Otsu K. Mitochondrial DNA that escapes from autophagy causes inflammation and heart failure. Nature. 2012 May 10;485(7397):251-5.

Oltvai ZN, Milliman CL, Korsmeyer SJ. Bcl-2 heterodimerizes in vivo with a conserved homolog, Bax, that accelerates programmed cell death. Cell. 1993 Aug 27;74(4):609-19.

Opferman JT, Letai A, Beard C, Sorcinelli MD, Ong CC, Korsmeyer SJ. Development and maintenance of B and T lymphocytes requires antiapoptotic MCL-1. Nature. 2003 Dec 11;426(6967):671-6.

Pankiv S, Clausen TH, Lamark T, Brech A, Bruun JA, Outzen H, Øvervatn A, Bjørkøy G, Johansen T. p62/SQSTM1 binds directly to Atg8/LC3 to facilitate

degradation of ubiquitinated protein aggregates by autophagy. J Biol Chem. 2007 Aug 17;282(33):24131-45.

Parrish AB, Freel CD, Kornbluth S. Cellular mechanisms controlling caspase activation and function. Cold Spring Harb Perspect Biol. 2013 Jun 1;5(6).

Pattingre S, Tassa A, Qu X, Garuti R, Liang XH, Mizushima N, Packer M, Schneider MD, Levine B. Bcl-2 antiapoptotic proteins inhibit Beclin 1-dependent autophagy. Cell. 2005 Sep 23;122(6):927-39.

Perciavalle RM, Stewart DP, Koss B, Lynch J, Milasta S, Bathina M, Temirov J, Cleland MM, Pelletier S, Schuetz JD, Youle RJ, Green DR, Opferman JT. Anti-apoptotic MCL-1 localizes to the mitochondrial matrix and couples mitochondrial fusion to respiration. Nat Cell Biol. 2012 Apr 29;14(6):575-83.

Qu X, Yu J, Bhagat G, Furuya N, Hibshoosh H, Troxel A, Rosen J, Eskelinen EL, Mizushima N, Ohsumi Y, Cattoretti G, Levine B. Promotion of tumorigenesis by heterozygous disruption of the beclin 1 autophagy gene. J Clin Invest. 2003 Dec;112(12):1809-20.

Quinsay MN, Lee Y, Rikka S, Sayen MR, Molkentin JD, Gottlieb RA, Gustafsson AB. Bnip3 mediates permeabilization of mitochondria and release of cytochrome c via a novel mechanism. J Mol Cell Cardiol. 2010 Jun;48(6):1146-56.

Quinsay MN, Thomas RL, Lee Y, Gustafsson AB. Bnip3-mediated mitochondrial autophagy is independent of the mitochondrial permeability transition pore. Autophagy. 2010 Oct;6(7):855-62.

Raichlin E, Chandrasekaran K, Kremers WK, Frantz RP, Clavell AL, Pereira NL, Rodeheffer RJ, Daly RC, McGregor CG, Edwards BS, Kushwaha SS. Sirolimus as primary immunosuppressant reduces left ventricular mass and improves diastolic function of the cardiac allograft. Transplantation. 2008 Nov 27;86(10):1395-400.

Rinkenberger JL, Horning S, Klocke B, Roth K, Korsmeyer SJ. Mcl-1 deficiency results in peri-implantation embryonic lethality. Genes Dev. 2000 Jan 1;14(1):23-7.

Sarkar S, Carroll B, Buganim Y, Maetzel D, Ng AH, Cassady JP, Cohen MA, Chakraborty S, Wang H, Spooner E, Ploegh H, Gsponer J, Korolchuk VI, Jaenisch R. Impaired autophagy in the lipid-storage disorder niemann-pick type c1 disease. Cell Rep. 2013 Dec 12;5(5):1302-15.

Sarraf SA, Raman M, Guarani-Pereira V, Sowa ME, Huttlin EL, Gygi SP, Harper JW. Landscape of the PARKIN-dependent ubiquitylome in response to mitochondrial depolarization. Nature. 2013 Apr 18;496(7445):372-6.

Sayen MR, Gustafsson AB, Sussman MA, Molkentin JD, Gottlieb RA. Calcineurin transgenic mice have mitochondrial dysfunction and elevated superoxide production. Am J Physiol Cell Physiol. 2003 Feb;284(2):C562-70.

Schmittgen TD, Livak KJ. Analyzing real-time PCR data by the comparative C(T) method. Nat Protoc. 2008;3(6):1101-8.

Schwickart M, Huang X, Lill JR, Liu J, Ferrando R, French DM, Maecker H, O'Rourke K, Bazan F, Eastham-Anderson J, Yue P, Dornan D, Huang DC, Dixit VM. Deubiquitinase USP9X stabilizes MCL1 and promotes tumour cell survival. Nature. 2010 Jan 7;463(7277):103-7.

Sciarretta S, Zhai P, Volpe M, Sadoshima J. Pharmacological modulation of autophagy during cardiac stress. J Cardiovasc Pharmacol. 2012 Sep;60(3):235-41.

Shin JH, Ko HS, Kang H, Lee Y, Lee YI, Pletinkova O, Troconso JC, Dawson VL, Dawson TM. PARIS (ZNF746) repression of PGC-1α contributes to neurodegeneration in Parkinson's disease. Cell. 2011 Mar 4;144(5):689-702.

Singh R, Kaushik S, Wang Y, Xiang Y, Novak I, Komatsu M, Tanaka K, Cuervo AM, Czaja MJ. Autophagy regulates lipid metabolism. Nature. 2009 Apr 30;458(7242):1131-5.

Sohal DS, Nghiem M, Crackower MA, Witt SA, Kimball TR, Tymitz KM, Penninger JM, Molkentin JD. Temporally regulated and tissue-specific gene manipulations in the adult and embryonic heart using a tamoxifen-inducible Cre protein. Circ Res. 2001 Jul 6;89(1):20-5.

Soldani C, Lazzè MC, Bottone MG, Tognon G, Biggiogera M, Pellicciari CE, Scovassi AI.Poly(ADP-ribose) polymerase cleavage during apoptosis: when and where? Exp Cell Res. 2001 Oct 1;269(2):193-201.

Stankiewicz AR, Livingstone AM, Mohseni N, Mosser DD. Regulation of heat-induced apoptosis by Mcl-1 degradation and its inhibition by Hsp70. Cell Death Differ. 2009 Apr;16(4):638-47. doi: 10.1038/cdd.2008.189. Epub 2009 Jan 16.

Sun Y, Vashisht AA, Tchieu J, Wohlschlegel JA, Dreier L. Voltage-dependent anion channels (VDACs) recruit Parkin to defective mitochondria to promote mitochondrial autophagy. J Biol Chem. 2012 Nov 23;287(48):40652-60.

Susin SA, Lorenzo HK, Zmzami N, Marzo I, Snow BE, Brothers GM, Mangion J, Jacotot E, Constantini P, Loeffler M, et al. 1999. *Nature* **397**: 441-446.
Taylor RC, Cullen SP, Martin SJ. Apoptosis: controlled demolition at the cellular level. Nat Rev Mol Cell Biol. 2008 Mar;9(3):231-41.

Terada M, Nobori K, Munehisa Y, Kakizaki M, Ohba T, Takahashi Y, Koyama T, Terata Y, Ishida M, Iino K, Kosaka T, Watanabe H, Hasegawa H, Ito H. Double transgenic mice crossed GFP-LC3 transgenic mice with alphaMyHC-mCherry-LC3 transgenic mice are a new and useful tool to examine the role of autophagy in the heart. Circ J. 2010 Jan;74(1):203-6.

Thomas LW, Lam C, Edwards SW. Mcl-1; the molecular regulation of protein function. FEBS Lett. 2010 Jul 16;584(14):2981-9.

Thomas RL, Gustafsson AB. MCL1 is critical for mitochondrial function and autophagy in the heart. Autophagy. 2013 Nov 1;9(11):1902-3.

Thomas RL, Gustafsson AB. Mitochondrial autophagy--an essential quality control mechanism for myocardial homeostasis. Circ J. 2013;77(10):2449-54.

Thomas RL, Roberts DJ, Kubli DA, Lee Y, Quinsay MN, Owens JB, Fischer KM, Sussman MA, Miyamoto S, Gustafsson ÅB. Loss of MCL-1 leads to impaired autophagy and rapid development of heart failure. Genes Dev. 2013 Jun 15;27(12):1365-1377.

Tong T, Ji J, Jin S, Li X, Fan W, Song Y, Wang M, Liu Z, Wu M, Zhan Q. Gadd45a expression induces Bim dissociation from the cytoskeleton and translocation to mitochondria. Mol Cell Biol. 2005 Jun;25(11):4488-500.

Toraason M, Luken ME, Breitenstein M, Krueger JA, Biagini RE. Comparative toxicity of allylamine and acrolein in cultured myocytes and fibroblasts from neonatal rat heart. Toxicology. 1989 May 31;56(1):107-17.

Tsujimoto Y, Finger LR, Yunis J, Nowell PC, Croce CM. Cloning of the chromosome breakpoint of neoplastic B cells with the t(14;18) chromosome translocation. Science. 1984 Nov 30;226(4678):1097-9.

Twig G, Elorza A, Molina AJ, Mohamed H, Wikstrom JD, Walzer G, Stiles L, Haigh SE, Katz S, Las G, Alroy J, Wu M, Py BF, Yuan J, Deeney JT, Corkey

BE, Shirihai OS. Fission and selective fusion govern mitochondrial segregation and elimination by autophagy. EMBO J. 2008 Jan 23;27(2):433-46.

Vaux DL, Cory S, Adams JM. Bcl-2 gene promotes haemopoietic cell survival and cooperates with c-myc to immortalize pre-B cells. Nature. 1988 Sep 29;335(6189):440-2.

Veis DJ, Sorenson CM, Shutter JR, Korsmeyer SJ. Bcl-2-deficient mice demonstrate fulminant lymphoid apoptosis, polycystic kidneys, and hypopigmented hair. Cell. 1993 Oct 22;75(2):229-40.

Vincow ES, Merrihew G, Thomas RE, Shulman NJ, Beyer RP, MacCoss MJ, Pallanck LJ. The PINK1-Parkin pathway promotes both mitophagy and selective respiratory chain turnover in vivo. Proc Natl Acad Sci U S A. 2013 Apr 16;110(16):6400-5.

Vliegen HW, van der Laarse A, Cornelisse CJ, Eulderink F. Myocardial changes in pressure overload-induced left ventricular hypertrophy. A study on tissue composition, polyploidization and multinucleation. Eur Heart J. 1991 Apr;12(4):488-94.

Volkmann N, Marassi FM, Newmeyer DD, Hanein D. The rheostat in the membrane: BCL-2 family proteins and apoptosis. Cell Death Differ. 2013 Oct 25. doi: 10.1038/cdd.2013.153. [Epub ahead of print]

Wang X, Bathina M, Lynch J, Koss B, Calabrese C, Frase S, Schuetz JD, Rehg JE, Opferman JT. Deletion of MCL-1 causes lethal cardiac failure and mitochondrial dysfunction. Genes Dev. 2013 Jun 15;27(12):1351-64.

Wang X, Winter D, Ashrafi G, Schlehe J, Wong YL, Selkoe D, Rice S, Steen J, LaVoie MJ, Schwarz TL. PINK1 and Parkin target Miro for phosphorylation and degradation to arrest mitochondrial motility. Cell. 2011 Nov 11;147(4):893-906.

Wei G, Margolin AA, Haery L, Brown E, Cucolo L, Julian B, Shehata S, Kung AL, Beroukhim R, Golub TR. Chemical genomics identifies small-molecule MCL1 repressors and BCL-xL as a predictor of MCL1 dependency. Cancer Cell. 2012 Apr 17;21(4):547-62.

Wei J, Stebbins JL, Kitada S, Dash R, Placzek W, Rega MF, Wu B, Cellitti J, Zhai D, Yang L, Dahl R, Fisher PB, Reed JC, Pellecchia M. BI-97C1, an optically pure Apogossypol derivative as pan-active inhibitor of antiapoptotic B-cell lymphoma/leukemia-2 (Bcl-2) family proteins. J Med Chem. 2010 May 27;53(10):4166-76.

Wencker D, Chandra M, Nguyen K, Miao W, Garantziotis S, Factor SM, Shirani J, Armstrong RC, Kitsis RN. A mechanistic role for cardiac myocyte apoptosis in heart failure. J Clin Invest. 2003 May;111(10):1497-504.

Weng C, Li Y, Xu D, Shi Y, Tang H. Specific cleavage of Mcl-1 by caspase-3 in tumor necrosis factor-related apoptosis-inducing ligand (TRAIL)-induced apoptosis in Jurkat leukemia T cells. J Biol Chem. 2005 Mar 18;280(11):10491-500.

Whelan RS, Konstantinidis K, Wei AC, Chen Y, Reyna DE, Jha S, Yang Y, Calvert JW, Lindsten T, Thompson CB, Crow MT, Gavathiotis E, Dorn GW 2nd, O'Rourke B, Kitsis RN. Bax regulates primary necrosis through mitochondrial dynamics. Proc Natl Acad Sci U S A. 2012 Apr 24;109(17):6566-71.

Wu CF, Bishopric NH, Pratt RE. Atrial natriuretic peptide induces apoptosis in neonatal rat cardiac myocytes. J Biol Chem. 1997 Jun 6;272(23):14860-6.

Wuillème-Toumi S, Robillard N, Gomez P, Moreau P, Le Gouill S, Avet-Loiseau H, Harousseau JL, Amiot M, Bataille R. Mcl-1 is overexpressed in multiple myeloma and associated with relapse and shorter survival. Leukemia. 2005 Jul;19(7):1248-52.

Xiang SY, Vanhoutte D, Del Re DP, Purcell NH, Ling H, Banerjee I, Bossuyt J, Lang RA, Zheng Y, Matkovich SJ, Miyamoto S, Molkentin JD, Dorn GW 2nd, Brown JH. RhoA protects the mouse heart against ischemia/reperfusion injury. J Clin Invest. 2011 Aug;121(8):3269-76.

Xiong H, Wang D, Chen L, Choo YS, Ma H, Tang C, Xia K, Jiang W, Ronai Z, Zhuang X, Zhang Z.Parkin, PINK1, and DJ-1 form a ubiquitin E3 ligase complex promoting unfolded protein degradation. J Clin Invest. 2009 Mar;119(3):650-60.

Yang XP, Liu YH, Rhaleb NE, Kurihara N, Kim HE, Carretero OA. Echocardiographic assessment of cardiac function in conscious and anesthetized mice. Am J Physiol. 1999 Nov;277(5 Pt 2):H1967-74.

Yecies D, Carlson NE, Deng J, Letai A. Acquired resistance to ABT-737 in lymphoma cells that up-regulate MCL-1 and BFL-1. Blood. 2010 Apr 22;115(16):3304-13.

Young JC, Hoogenraad NJ, Hartl FU. Molecular chaperones Hsp90 and Hsp70 deliver preproteins to the mitochondrial import receptor Tom70. Cell. 2003 Jan 10;112(1):41-50.

Zhong Q, Gao W, Du F, Wang X. Mule/ARF-BP1, a BH3-only E3 ubiquitin ligase, catalyzes the polyubiquitination of Mcl-1 and regulates apoptosis. Cell. 2005 Jul 1;121(7):1085-95.

Zhou P, Qian L, Kozopas KM, Craig RW. Mcl-1, a Bcl-2 family member, delays the death of hematopoietic cells under a variety of apoptosis-inducing conditions. Blood. 1997 Jan 15;89(2):630-43.

Zhu L, Yu Y, Chua BH, Ho YS, Kuo TH. Regulation of sodium-calcium exchange and mitochondrial energetics by Bcl-2 in the heart of transgenic mice. J Mol Cell Cardiol. 2001 Dec;33(12):2135-44.

Zhu H, Tannous P, Johnstone JL, Kong Y, Shelton JM, Richardson JA, Le V, Levine B, Rothermel BA, Hill JA. Cardiac autophagy is a maladaptive response to hemodynamic stress. J Clin Invest. 2007 Jul;117(7):1782-93.

Zungu M, Schisler J, Willis MS. All the little pieces. -Regulation of mitochondrial fusion and fission by ubiquitin and small ubiquitin-like modifer and their potential relevance in the heart.-. Circ J. 2011;75(11):2513-21.